

Constructing and analysing off-shore hydrogen system designs powered by wind farms in the North Sea

A multi-sink multi-source network optimisation approach

D.H.J. (David) van Tongeren



The cover photo was shot by [Doherty \(2018\)](#).

CONSTRUCTING AND ANALYSING OFFSHORE
HYDROGEN SYSTEM DESIGNS POWERED BY WIND
FARMS IN THE NORTH SEA — A MULTI-SINK
MULTI-SOURCE NETWORK OPTIMISATION
APPROACH

A thesis submitted to the Delft University of Technology in partial
fulfillment of the requirements for the degree of

Master of Science
in Complex Systems Engineering and Management
Track: Energy Systems

by

D.H.J. (David) van Tongeren
Student ID: 5411572

August 2022

D.H.J. (David) van Tongeren: *Constructing and analysing offshore hydrogen system designs powered by wind farms in the North Sea — A multi-sink multi-source network optimisation approach* (2022)



Faculty of Technology, Policy and Management
Delft University of Technology

Thesis committee: Dr. A.F. (Aad) Correljé, TU Delft, chair
Dr. ir. P.W. (Petra) Heijnen, TU Delft, first supervisor
Dr. A.F. (Aad) Correljé, TU Delft, second supervisor
Dr. ir. R. (Rutger) van Bergem, TU Delft, external supervisor
Dr. ir. A. (Alberto) Nocentini, TU Delft, external supervisor

ACKNOWLEDGEMENTS

Dear reader,

The report before you is my master's thesis. A project I have been working on for the past half year. This thesis is the final work of my Master in Complex Systems Engineering and Management. It concludes the educational and joyful two years I had at the Technical University of Delft. My thesis and my experience at the TU Delft would not have been the same without the following people to whom I would like to express my gratitude:

First, I would like to thank Petra Heijnen, my first supervisor. I really enjoyed our weekly meetings. Your excellent feedback and quick responses certainly helped me along. And aside from on an academic level, you also taught me how to cope with my thesis on a personal level, which I found truly invaluable. Second, I would like to thank Aad Correljé, my second supervisor. Your good critique pushed me into a more multidisciplinary and broad view on my subject. This elevated my work. Third, I would like to thank Rutger van Bergem. Your guidance was great. And you especially helped me with your economic expertise. And finally, Alberto Nocentini, my fourth supervisor. I really enjoyed working with you, and I can not wait to become colleagues.

Furthermore, I would like to thank my family and friends for supporting me and with whom I had to pleasure to be with during my master's programme. In particular my girlfriend Annemarijn, you really helped me to keep up the good spirit during my master's programme and especially during my thesis. You also forced me to have the necessary fun (with you) during this period. Thank you for that. Next, I would like to thank my great (study) friends Joost, Paulette, Kieron, Roos, and Stijn. It was a pleasure working as a group with all of you and having the deserved drinks after exam periods. I would also like to thank Steffan from the University of Utrecht. It was heaps of fun to discuss our similar work with each other over the past months.

Finally, a big thanks to my "make the thesis more readable" crew: Anton (a good neighbour is better than a far friend), Emese (with her colourful comments), and my mother (fulfilling the role of a grandmother).

This thesis finalizes my master's at the TU Delft. I learned a lot and enjoyed doing the research. But, if I could do it again... I would do it in a different season, due to climate change.

David van Tongeren

EXECUTIVE SUMMARY

To provoke the needed energy transition, European Union (EU) countries initiated significant offshore wind energy investments in the North Sea. However, there also exist adverse aspects to the use of higher renewable electricity levels:

- renewable energy sources, such as offshore wind energy, may threaten the security of our energy system, since they are characterised by a high variability, and limited predictability and controllability;
- the effectiveness with respect to decreasing greenhouse gas emissions is limited, because electrification can be not applied within all sectors, such as heavy industry and heavy duty transport;
- a large increase in offshore wind capacity requires moving further offshore. This results in relatively high costs because of the energy losses within the (longer) electricity cables.

One way of coping with these challenges, is by producing hydrogen offshore, by means of wind energy, and transporting it to shore by for example repurposing the existing offshore natural gas infrastructure. Such an offshore hydrogen system located in the North Sea might sound favorable; however, the feasibility of such a system on this scale is yet to be determined.

In this thesis the possibility is investigated to design a future proof offshore hydrogen system. Such a system would consist of (current as well as new) wind farms, electrolyzers to produce hydrogen by using (a part of) the electricity generated by the wind farms, and an infrastructure to bring the hydrogen to shore. Given the EU investment plans in offshore wind energy, a phasing period is used from 2030, 2040, to 2050. This research is done by:

- deriving multiple hydrogen system designs by for example optimising the transmission infrastructure;
- analysing the supply potential of these system designs.

The results show that a cost-competitive hydrogen system in the North Sea can be realized. The proposed system design has a Levelised Cost Of Hydrogen (LCOH) of 2,08 EUR/kg and a positive Net Present Value (NPV) for the most relevant pricing scenarios. This LCOH is relatively low compared to other researches, which are mostly between 2 and 3,5 EUR/kg.

An interesting result concerns including refurbished pipelines of the existing offshore gas infrastructure. When using only new pipelines, the transmission infrastructure costs increase with 36%. Furthermore, the results show that it is more cost-efficient to downscale electrolyser capacities than to use the peak of the available electricity to determine the capacity of the electrolyzers. Additionally, the productivity of the wind farms can increase up to even 220% by using the different electricity surplus for hydrogen production.

Based on this research, recommendations can be given:

- National governments should formulate policy on whether or when gas extraction in the North Sea should stop. Thereupon, the (energy) transmission system operators should scope their plans towards transporting offshore hydrogen to onshore, as well as start planning the onshore hydrogen backbone.
- The EU should decide whether to build one interconnected system in the North Sea, or multiple isolated (per country) hydrogen systems. Based on this decision, it is important to start shaping rules and standards for hydrogen trade, as well as determining regulatory regimes to support offshore hydrogen production.
- Further research should be done on the electrolyser costs and efficiencies, as well as the different types of electrolyser locations; on the possibilities of hydrogen storage; and, to include (regional) hydrogen demand values.

CONTENTS

1	INTRODUCTION	1
1.1	Offshore Wind Energy	1
1.2	Offshore Hydrogen Systems	2
1.3	Thesis Scope	3
2	RESEARCH FORMULATION	5
2.1	State-of-the-Art Review	5
2.1.1	Hydrogen Systems	5
2.1.2	Network Optimisation Models	7
2.2	Research Objective	8
2.3	Report Structure	10
3	RESEARCH METHODOLOGY	11
3.1	Scenario set-up	11
3.2	Wind Farm and Electrolyser Locations	14
3.2.1	Wind Farms	14
3.2.2	Electrolysers	19
3.3	Electricity Potential	20
3.3.1	Electricity Supply Potential for Hydrogen — Electricity-driven	21
3.3.2	Electricity Supply Potential for Hydrogen — Hydrogen-driven	23
3.4	Network Optimisation Model	24
3.4.1	Geometric Graph Theory	25
3.4.2	Network Optimisation Model	27
3.4.3	Model Adaption	29
3.5	Economic Assessment	31
3.5.1	Levelised Cost of Hydrogen	32
3.5.2	Net Present Value	32
3.5.3	Additional Remarks	33
4	DATA PREPARATION	35
4.1	Electrolysers	35
4.1.1	Electrolyser Hub	35
4.1.2	In-Turbine Electrolysers	35
4.2	Natura2000 Areas	36
4.3	Existing Transmission Infrastructure and Onshore Entry Points	37
4.3.1	Existing Connections	37
4.3.2	Onshore Entry Points	39
4.4	Techno-Economic Data	40
5	RESULTS	43
5.1	Electrolyser locations	43
5.2	Maximum Electricity Potential for Hydrogen Production	44
5.2.1	Electricity Supply Potential for Hydrogen 2030	44
5.2.2	Electricity Supply Potential for Hydrogen 2040	45
5.2.3	Electricity Supply Potential for Hydrogen 2050	46
5.3	Network and Economic Assessment	47

5.3.1	Scenario 2030 (A30B1 and A30B2)	47
5.3.2	Scenario 2040 (A40B1 and A40B2)	50
5.3.3	Scenario 2050 (A50B1 and A50B2)	53
5.3.4	Analysis of the system as a whole (2030–2040–2050)	55
5.4	Sensitivity Analysis	59
5.4.1	Parameter Overview	59
5.4.2	Sensitivity Analysis Results	61
6	CONCLUSION	64
6.1	Feasibility	64
6.2	Optimal Design	64
7	DISCUSSION AND RECOMMENDATIONS	66
7.1	Discussion	66
7.1.1	Transmission Infrastructure	66
7.1.2	Onshore Entry Points	67
7.1.3	Electrolysers	68
7.1.4	Economic Assessment	69
7.1.5	Interconnection between Countries	70
7.1.6	Effect of Storage	70
7.1.7	Utilising the Surplus	71
7.1.8	Regulatory Framework	71
7.2	Recommendations	72
A	OFFSHORE WIND FARM CHARACTERISTICS	85
B	NATURAL GAS INFRASTRUCTURE CHARACTERISTICS	88
C	TECHNO-ECONOMIC DATA	92
C.1	Offshore Wind Energy	92
C.2	Transmission Infrastructure	93
C.3	Electrolyser	94
D	ELECTROLYSERS	96

LIST OF FIGURES

Figure 1.1	System demarcation within the North Sea	3
Figure 3.1	Scenarios used.	12
Figure 3.2	Methodology flowchart.	13
Figure 3.3	Bathymetry of the North Sea (De Hauwere, n.d.).	15
Figure 3.4	Average wind speeds in the North Sea during winter (left panel) and summer (right panel) (Bonaduce et al., 2019).	15
Figure 3.5	Showing the significant wave height (a + b) and the mean wave period (c + d) during winter (left panels) and summer (right panels) (Bonaduce et al., 2019).	16
Figure 3.6	Map of the wind farms locations presented by EMOD-net (2021).	18
Figure 3.7	A depiction of the locations of the offshore sub stations of wind farms NLD ₁₀ , NLD ₁₁ , NLD ₁₂ , NLD ₁₃ , NLD ₂₂ . Derived from (4C Offshore, n.d.)	20
Figure 3.8	Stacked energy chart of an arbitrary case indicating the available wind surplus within a month.	23
Figure 3.9	Distance threshold between the two operational modes.	24
Figure 3.10	Two simple graphs.	25
Figure 3.11	A simple directed graph.	26
Figure 3.12	A connected and a disconnected graph	26
Figure 3.13	A simple graph with a tree topology.	26
Figure 3.14	Example of a minimum spanning tree, minimum-cost spanning tree, and Steiner tree output with obstacles (grey polygons) by the Network Optimisation Model (NOM) (Heijnen, 2022).	28
Figure 3.15	Comparison of a final network topology without (left) and with (right) existing connections by the NOM (Heijnen, 2022).	29
Figure 3.16	Visualisation of the super sink.	30
Figure 3.17	Estimation of future demand-supply curves for hydrogen.	33
Figure 4.1	Map of the Natura2000 sites within the system of interest, derived from European Environment Agency (2022).	36
Figure 4.2	Changes between the starting and final data-set of the pipelines.	38
Figure 4.3	Sinks with the associated gas pipelines. The entry point with a "*" is not taken into account as it only transports gas over the Wadden Sea.	40
Figure 4.4	Estimation of the electricity prices in the EU over the upcoming years (Schmitt, 2022).	42

Figure 5.1	Build-up electrolyser hubs and compressor stations for 2030, 2040, to 2050. The nodes which are marked by a green circle are the compressor stations of the H ₂ -in-Turbine wind farms.	44
Figure 5.2	Electricity potential for the electricity-driven operational mode derived by the Energy Transition Model (ETM) and the Electricity Merit Order Model (EMOM) for 2030.	45
Figure 5.3	Results of the electricity potential for the electricity-driven operational mode derived by the ETM and the EMOM for 2040.	46
Figure 5.4	Electricity potential for the electricity-driven operational mode derived by the ETM and the EMOM for 2050.	47
Figure 5.5	Network optimisation in 2030 for scenario A30B1 (interconnected).	48
Figure 5.6	Network optimisation in 2030 for scenario A30B2 (isolated).	48
Figure 5.7	LCOH values evaluated of different organisations for 2020 (Braun & Hesel, 2020).	49
Figure 5.8	box plot (a) and the probability density function (b) of the electricity potential for the electricity-driven electrolyzers in 2030.	50
Figure 5.9	Network optimisation in 2040 for scenario A40B1 (interconnected).	51
Figure 5.10	Network optimisation in 2040 for scenario A40B2 (isolated).	51
Figure 5.11	The H ₂ -in-Turbine wind farm lay-out in Germany 2040.	52
Figure 5.12	box plot (a) and the probability density function (b) of the electricity potential for the electricity-driven electrolyzers in 2040.	53
Figure 5.13	Network optimisation results visualisation in 2050 for scenario A50B1 (interconnected).	54
Figure 5.14	Network optimisation results visualisation in 2050 for scenario A50B2 (isolated).	54
Figure 5.15	box plot (a) and the probability density function (b) of the electricity potential for the electricity-driven electrolyzers in 2050.	55
Figure 5.16	Network optimisation build-up of the interconnected case.	56
Figure 5.17	Network optimisation build-up of the isolated case.	56
Figure 5.18	Comparison of different LCOH values.	57
Figure 5.19	Sensitivity analysis results showing the percentual change of the LCOH by alternating the different cost values with $\pm 25\%$	62
Figure 5.20	Sensitivity analysis results showing the percentual change of the LCOH by alternating the different parameter values with $\pm 10\%$	62
Figure 7.1	Missing pipeline segment.	67

Figure 7.2	Maximum hourly supply distribution at the onshore entry points	68
Figure C.1	Estimated breakdown of the Capital Expenditures (CapEx) of a baseline offshore wind farm in 2015 (Lacal-Aránategui et al., 2018).	93

LIST OF TABLES

Table 4.1	Main techno-economic data used in this thesis.	40
Table 4.2	Renewable energy levels per country in GW (Wang et al., 2021).	42
Table 5.1	Electricity potential to produce hydrogen under the electricity-driven operational mode per country in 2030.	44
Table 5.2	Electricity potential to produce hydrogen under the electricity-driven operational mode per country in 2040.	45
Table 5.3	Electricity potential to produce hydrogen under the electricity-driven operational mode per country in 2050.	46
Table 5.4	Economic analyses regarding the LCOH for scenarios A30B1 (interconnected) and A30B2 (isolated).	49
Table 5.5	Economic analyses regarding the LCOH for scenarios A40B1 (interconnected) and A40B2 (isolated).	52
Table 5.6	Economic analyses regarding the LCOH for scenarios A50B1 (interconnected) and A50B2 (isolated).	53
Table 5.7	Economic analyses regarding the LCOH for adjusted systems over the entire phasing period. *for 2030, 2040, and 2050.	57
Table 5.8	Results of the NPV calculations for the adjusted systems of the interconnected and isolated system designs.	58
Table 5.9	Capacity factor increases of the offshore wind farm per country for the maximum hydrogen generation case and the adjusted case in 2030, 2040, 2050.	59
Table 5.10	New NPVs in MEUR resulting from changing the costs of each component with $\pm 25\%$	63
Table 5.11	New NPVs in MEUR resulting from changing parameter values with $\pm 10\%$ and removing the option to repurpose the existing natural gas transmission infrastructure.	63
Table 7.1	Maximum supply of the hydrogen system and demand of Belgium, Denmark, Germany, and the Netherlands. Demand derived from Wang et al. (2021).	67
Table A.1	Overview of all the offshore wind farms within the system, data derived from EMODnet (2021).	85
Table B.1	Overview of all the incumbent gas pipelines and their potential hydrogen capacity, data derived from EMODnet (2022).	88
Table D.1	Electrolyser hubs and their respective assigned wind farms in Belgium. '(N)' is a new wind farm.	96
Table D.2	Electrolyser hubs and their respective assigned wind farms in Denmark. '(N)' is a new wind farm. The H ₂ -in-Turbine wind farms are connected to a compressor hub, not an electrolyser hub.	96

Table D.3	Electrolyser hubs and their respective assigned wind farms in Germany. '(N)' is a new wind farm. The H ₂ -in-Turbine wind farms are connected to a compressor hub, not an electrolyser hub.	97
Table D.4	Electrolyser hubs and their respective assigned wind farms in the Netherlands. '(N)' is a new wind farm. The H ₂ -in-Turbine wind farms are connected to a compressor hub, not an electrolyser hub.	97
Table D.5	Spatial coordinates of the electrolysers. Coordinate reference system: "WGS 84 / UTM zone 31N". Authority ID: "EPSG:32631"	98

ACRONYMS

ABM Agent Based Modelling	8
ACO Ant Colony Optimisation	8
BOS Balance Of System	41
CapEx Capital Expenditures	xii
EEZ Exclusive Economic Zone	3
EMOM Electricity Merit Order Model	xi
ETM Energy Transition Model	xi
EU European Union	vi
GGT Geometric Graph Theory	7
GIS Geographical Information System	6
LHV Low Heating Value	29
LCOE Levelised Cost Of Electricity	71
LCOH Levelised Cost Of Hydrogen	vi
MI(N)LP Mixed Integer (Non-)Linear Programming	8
NOM Network Optimisation Model	x
NPV Net Present Value	vi
OpEx Operational Expenditures	32
PSO Particle Swarm Optimisation	8
P₂H₂ Power-To-Hydrogen	2
QGIS Quantum Geographical Information System	37
UNCLOS United Nations Convention on the Law of the Sea	17

NOMENCLATURE

Prefix

<i>G</i>	Giga
<i>K</i>	Kilo
<i>M</i>	Mega
<i>T</i>	Terra

Symbols

$^{\circ}\text{C}$	Degrees Celsius
<i>EUR</i>	Euro
<i>g</i>	Gram
<i>in</i>	Inch
<i>J</i>	Joule
<i>K</i>	Kelvin
<i>m</i>	Meter
<i>MEUR</i>	Million euro
<i>mol</i>	Mole
<i>s</i>	Second
<i>t</i>	Tonne
<i>W</i>	Watt
<i>Wh</i>	Watt-hour
<i>yr</i>	Year

ASSUMPTIONS

ASSUMPTION 1	<i>Electrolyser hubs can be placed on top of existing and new electricity sub stations belonging to wind farms.</i>	19
ASSUMPTION 2	<i>The hydrogen system should be able to handle the maximum possible output of hydrogen on a yearly basis.</i>	20
ASSUMPTION 3	<i>The electricity demand of each country has the same percentual increase per year.</i>	21
ASSUMPTION 4	<i>H₂-in-Turbine wind farms only exist after a certain distance threshold. Likewise, normal wind farms only exist before this distance threshold.</i>	23
ASSUMPTION 5	<i>The operational operational life of the system is proportional to the cost of the components compared to its operational life.</i>	33
ASSUMPTION 6	<i>The future wind farms will be built in disregard of the potential hydrogen system.</i>	34
ASSUMPTION 7	<i>The offshore natural gas transmission infrastructure may be repurposed for hydrogen transport.</i>	37
ASSUMPTION 8	<i>All the onshore entry points have significant future hydrogen demands.</i>	39
ASSUMPTION 9	<i>The yearly averaged minimum electricity price is the price for the use of surplus electricity.</i>	42
ASSUMPTION 10	<i>The H₂-in-Turbine turbines all have a capacity of 10 MW.</i>	92

1 | INTRODUCTION

Within the last century, human development was tied to the use of fossil fuels. Exploiting fossil fuels has certainly led to substantial technological advances within a short amount of time. However, a drawback of these types of fuels is the pollution by so-called greenhouse gasses acquainted with using them; the Earth can not tolerate more without considering the consequences. These adverse effects of fossil fuel use are visible in many forms, of which the most notable forms are connected to climate change (Kovac et al., 2021); the majority of the scientists is convinced that the global warming should be reduced. Additionally, as a reaction to Russia's aggression towards the Ukraine and the consequent volatile and soaring energy prices, European Union (EU) member states have announced to significantly scale down their fossil fuel use to shield themselves from geopolitical threats (Czyżak et al., 2022). Using alternative energy sources has now become a geopolitical priority as well as a climate priority.

1.1 OFFSHORE WIND ENERGY

In order to battle climate change, countries have started to express efforts to reduce greenhouse gas emissions within their borders. Within the EU, this led to greenhouse gas reduction targets reaching 55 % before 2030, and 100 % in 2050 (European Commission, 2021). One commonly known method to reduce greenhouse gas emissions, is adopting more renewable energy sources (Blanco & Faaij, 2018); these energy sources entail the most natural and clean types such as wind or solar energy sources (Aktas, 2021). The EU targets have led to massive electrification efforts (i.e. powering by electricity instead of by other energy sources) and have inspired North Sea countries to initiate significant offshore wind energy investments in the North Sea (Stichting New Energy Coalition, 2019). The expected EU offshore wind capacity in the North Sea increases from 41 GW in 2030, to 76 GW in 2040, and to 102 GW in 2050 (Wang et al., 2021).

However, there also exist adverse effects to these efforts as higher renewable electricity levels may endanger the reliability of our energy systems. Renewable energy sources are namely characterised by a high variability, limited predictability and controllability; this can consequently result in high fluctuations of electricity generation and thus threatening the energy security of the system (Strbac et al., 2021). To balance the electricity grid, it is necessary to store energy. Moreover, the effectiveness of renewable energy sources with respect to decreasing greenhouse gas emissions is limited. This is as electrification of system components can not be applied within all sectors, such as in the heavy industry (Oliveira et al., 2021) or in the heavy

duty transport (Maggio et al., 2019). Additionally, there exists a specific adverse effect for wind as a renewable source; large increase in offshore wind capacity also requires moving further offshore (PBL, 2018). This results in relatively high costs and high lead times to transport its power to shore, because of the energy losses within the cable (Stichting New Energy Coalition, 2019).

1.2 OFFSHORE HYDROGEN SYSTEMS

One way to alleviate the aforementioned challenges whilst also enhancing the global energy transformation momentum, is using Power-To-Hydrogen (P₂H₂) technologies (Yue et al., 2021). P₂H₂ technologies refer to the hydrogen being produced using electrolysis; this is a process powered by electricity to split water into hydrogen and oxygen. By doing so, the hydrogen becomes an energy carrier of the electricity (IRENA, 2019). Hydrogen produced by means of renewable electricity, such as wind energy, offers a vast amount of advantages which can be exploited within the needed energy transition:

- it can balance the electricity grid in times of uncertainty by producing or by using electricity, and thus act as a storage mechanism (Ehteshami & Chan, 2014);
- it can decarbonise heavy industry sectors which do not have other green alternatives (Oliveira et al., 2021);
- it can fuel the mobility sector without releasing any greenhouse gasses (Maggio et al., 2019); and,
- the costs for transmitting hydrogen are lower than for transmitting electricity over long distances (DeSantis et al., 2021).

In Europe, the before mentioned increase of offshore wind capacity seems a good opportunity to produce hydrogen. In order to benefit the most from offshore wind energy, one increasingly recognises that it is a compelling option to transform a part of the offshore wind electricity into hydrogen by using P₂H₂ technologies. There exist three prominent configurations of such a hydrogen system; the hydrogen can be produced by using (Singlitico et al., 2021):

- onshore electrolyser hubs;
- offshore electrolyser hubs; or
- within the wind turbine itself.

The latter two configurations opt for a way of transporting hydrogen to shore. For this transmission, an aspect exists which is exploitable within the North Sea: the incumbent offshore natural gas infrastructure. One could repurpose this infrastructure which could boost the energy transition (Invernizzi et al., 2020). The idea to repurpose the existing gas infrastructure is not uncommon. For example, Gasunie (2022) — a transmission system

operator of the Netherlands — recently announced that the national incumbent natural gas infrastructure will be repurposed for hydrogen transmission. The same orientation can also be applied offshore.

1.3 THESIS SCOPE

Such a hydrogen system located in the North Sea might sound favorable, considering the aforementioned EU wind energy investments. However, the feasibility of such a system on this scale is yet to be determined (as is also substantiated within the literature review in the next chapter).

Within this thesis, only the offshore variants of hydrogen production are taken into account. For one thing, the offshore hydrogen production will require less permits due to less environmental impact, and will avoid the necessity of onshore grid reinforcements (Stuurgroep Extra Opgave, 2022). On the other hand, it offers the possibility of re-utilising existing assets in the North Sea, as well as the storage of hydrogen in for example depleted gas reservoirs.

Additionally, this thesis is demarcated by the EU countries (Figure 1.1). Hence, only EU countries with wind farms within the North Sea are considered within this project: Belgium, Denmark, Germany, and the Netherlands.

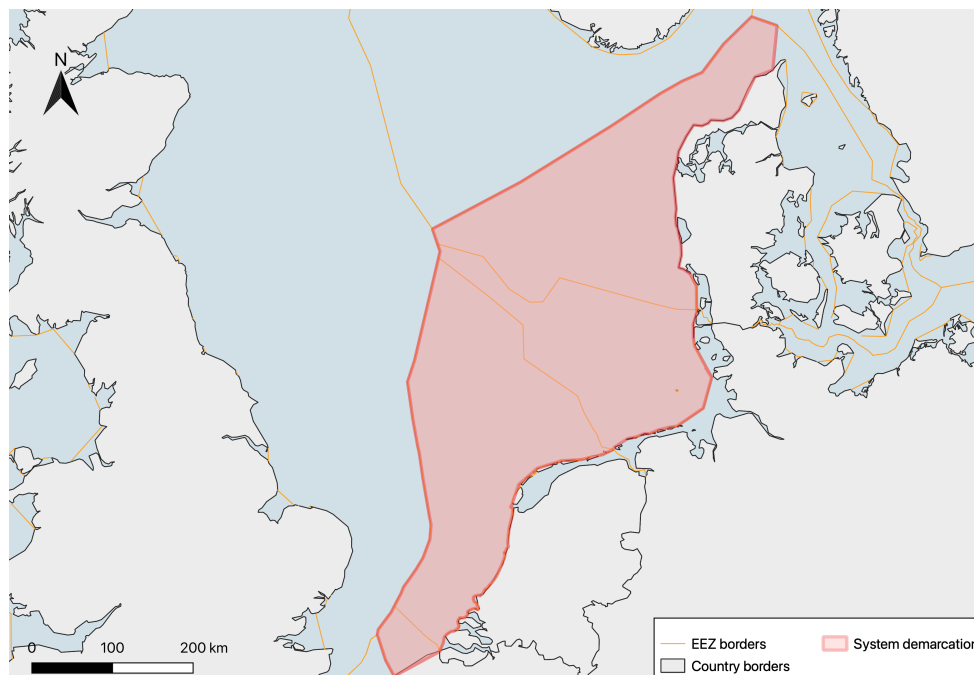


Figure 1.1: System demarcation within the North Sea

The feasibility of an EU system covering different Exclusive Economic Zones (EEZs) will, besides various techno-economic aspects, depend on international collaboration. The feasibility of the latter is not included in the scope of this thesis, since this would require a dedicated research.

To summarize: in this thesis the techno-economic feasibility of an offshore hydrogen system, powered by EU wind farms in the North Sea, is investi-

gated. In the next chapter, a literature review is conducted to develop this research objective.

2

RESEARCH FORMULATION

To define the research question of this thesis, this chapter provides first a review of the existing literature on offshore hydrogen systems and available models to evaluate transmission infrastructures. A particular focus is dedicated to the integration of a hydrogen system into the (offshore) electricity grid. This is done by finding literature on configurations of offshore (green) hydrogen production. After identifying the knowledge gaps and network optimisation models, the research main and sub-questions for this thesis are proposed.

2.1 STATE-OF-THE-ART REVIEW

2.1.1 Hydrogen Systems

Currently, around 9,75 Mt of hydrogen is annually produced in the EU; this would require 290 TWh of electricity if the hydrogen would solely been produced using (green) electrolysis (Calado & Castro, 2021). According to Kakoulaki et al. (2021), this demand can be satisfied in the EU if all the current available renewable energy sources are used to produce the green hydrogen. Moreover, the International Energy Agency (2020) states that the future hydrogen demand is expected to increase, as low-carbon hydrogen is becoming increasingly more important. This indicates the need for proper facilitation of hydrogen technologies and support tools in order to maintain a high energy security.

According to Gusain et al. (2020), hydrogen can play a grid stabilising role, and is thus able to increase the energy security of the system. Gusain et al. (2020) researched the potential use of electrolysers as a flexibility service provider. They concluded that an electrolyser is well suited to provide grid balancing services due to its fast dynamic response. Moreover, the researchers found that the technology is also suited to correct for wind forecast errors; indicating the high potential of electrolysers in future wind energy systems. The latter is especially interesting when one considers that according to the International Energy Agency (2019a), the world is entering a phase where renewable energy sources will make up an increasingly large share of our electricity supply. The International Energy Agency (2019a) mentions that as more countries move to variable renewable energy sources such as offshore wind, higher levels of curtailment (i.e. deliberate reductions of production in order to balance the electricity grid) will arise. In particular, they estimate that Europe will require more advanced technologies to ensure a higher system reliability due to the increasing shares of wind and solar energy.

Designing such a hydrogen system should be done using a long-term logic as such investment decisions are long-lived ([International Energy Agency, 2019b](#)). The decisions should focus on the dynamic geography of future renewable energy sources, as the system is expected to change over time. In that sense, decisions on what would be compatible with the current offshore energy system, are likely to differ in the future.

As a consequence of the increasing presence of renewable energy sources and rising levels of curtailment ([Calado & Castro, 2021](#)), several authors researched different hydrogen scenarios. See e.g. [Mcdonagh et al. \(2020\)](#) or [Xiao et al. \(2020\)](#). Investigated scenarios by these authors are: sell all the electricity to the grid; use all the electricity to produce hydrogen; and, a hybrid solution of the first two scenarios.

A similar study was conducted by [Hou et al. \(2017\)](#). The authors modelled two different scenarios of hydrogen production by means of offshore wind. The first scenario revolved around feeding the electricity of the wind farm directly into the electrolyser, and storing the produced hydrogen until needed. The second scenario revolved around the ability to feed the electricity into the national grid, or into the electrolyser. Projects found within (grey) literature published by non-academic entities (such as [Stichting New Energy Coalition \(2019\)](#) and [NSWPH \(2022\)](#)) mostly take a more overall view on large hydrogen systems. Their view is focused on the economic feasibility of the hydrogen side of the system. Compared to the academically published articles, they tend to incorporate more wind farms within their envisioned system. Among the researches focused on a wider spectrum of wind farms, only one study is found which incorporates the potential wind surplus on a national level ([Nadaleti et al., 2020](#)). These authors investigated hydrogen production in Brazil using hydroelectric and wind farm surplus energy. However, only based on a maximum production of three hours per day.

Other hydrogen-based studies mostly focus purely on new hydrogen transmission infrastructures on a local, regional or national level, see e.g. [Lee et al. \(2020\)](#); [André et al. \(2013\)](#); [Moreno-Benito et al. \(2017\)](#) and [Seo et al. \(2020\)](#). Such studies look from a cost-optimal perspective to the placement of pipelines on a simple spatial level. However, as also indicated by the authors, they neglect the development of the system over different years. Another gap in transmission network analyses is the lack of Geographical Information System (GIS) based studies, as explained by literature reviews conducted by [Maryam \(2017\)](#) and [Agnolucci & McDowall \(2013\)](#). Moreover, the authors explain that studies focused on larger hydrogen transmission infrastructures mainly treat the system as an isolated system. However, it is important to treat the hydrogen system as a part of an entire system. According to [L. Li et al. \(2019\)](#), this broader perspective offers more insights and solutions.

Looking at the studied researches, and given the scope of this thesis, it can be distinguished that there are some gaps in the existing literature:

- most studies do not incorporate the total available surplus of wind electricity;
- most studies do not incorporate cross border hydrogen systems;

- there is a lack of incorporating spatial details, by using for instance GIS tools (e.g. using tools which contain specified geographical data);
- most studies only focus on a cost optimisation, not incorporating other aspects of their optimal hydrogen system;
- most studies do not incorporate barriers or different spatial complexities for their hydrogen infrastructure;
- studies should evaluate how the system develops over time, and not take just one point in time; and,
- most studies do not include the reuse of offshore natural gas pipelines within their research.

Since some of these gaps specifically contemplate the transmission infrastructure, network modelling tools are evaluated in the next section.

2.1.2 Network Optimisation Models

Deploying an infrastructure for a hydrogen system which offers the aforementioned benefits, requires a vast amount of investments. In order to avoid redundant costs, a systematic approach could be beneficial. Such a systematic approach should be capable of solving multi-source multi-sink network problems. Multi-sink multi-source refers to networks with multiple 'consumers' and multiple 'producers'. Network optimisation models offer a viable option for such problems. Heijnen et al. (2019) reviewed several network optimisation approaches. The authors identified three different approaches: the use of Geometric Graph Theory, Mixex Integer (Non-)Linear Programming, and Agent Based Modelling.

Geometric Graph Theory

Geometric Graph Theory (GGT) is an approach which uses heuristics and algorithms to acquire local optimisations. The approach is based on a combination of geometric and graph theory. The graph is represented by nodes which indicate the different points within the graph; such points may represent 'producers' and 'consumers' within a network. Simultaneously, the possible connections between the nodes are represented by edges (Ackerman et al., 2014). GGT is a commonly used approach when solving cost network minimisation problems (F. Li et al., 2015). An example of using this approach is the study by Zhou et al. (2019); here, the authors used a minimum spanning tree¹ to optimise a pipeline network. Heijnen (2022) also developed an modelling approach using GGT which is focused on finding minimum cost solutions for network layouts. This model is unique in its ability to repurpose existing infrastructure into the optimisation. Additionally, the model is able to restrict certain areas from edges (Heijnen, 2022). However, a potential drawback is that it does not differentiate between different cost areas within the model.

¹ A minimum spanning tree is a subset of edges which connect all the nodes, without creating any cycles within the tree and whilst minimising the edge weight.

Mixed Integer (Non-)Linear Programming

Mixed Integer (Non-)Linear Programming (MI(N)LP) are mathematical modelling approaches. These approaches solve complicated optimisation problems and are used to identify trade-offs within the problem. MI(N)LP approaches are proven to have a wide applicability within network optimisation problems (Kantor et al., 2020). The main advantages of MI(N)LP are in its ability to concurrently and effectively balance multiple objectives (Guo & Shah, 2015). Additionally, geographical elements can be included in such approaches, making it suitable for multi-objective network problems where one optimal solution needs to be found; an example of such an MI(N)LP approach is conducted by Seo et al. (2020). A potential drawback of this approach is its requisition to perform a vast amount of preliminary work to set-up the problem. This results in a less flexible method; not being ideal for experimenting with small changes. Additionally, the researcher needs to consider all time-stamps at once, and therefore the approach is limited to static system components and thus not able to analyse dynamic systems (Urbanucci, 2018). Another possible drawback is that such an approach is not able to take into account existing network paths (Seo et al., 2020).

Agent Based Modelling

Agent Based Modelling (ABM) simulates the actions and interactions between entities. According to Heijnen et al. (2019), there exist two types of ABM approaches which are suitable for cases as represented in this thesis: Particle Swarm Optimisation (PSO) and Ant Colony Optimisation (ACO). Both are suitable for finding optimal networks. These approaches are especially useful for scenario exploration and use the manner of conduct of a living organism to find the optimal solution for optimisation problems. They can be used to minimise the cost of networked infrastructures. The ABM approaches are particularly suitable for discrete problems where potential paths are already encoded; however, they can fail to provide insights into new paths (Yang & Karamanoglu, 2020). Another potential drawback of the two ABM approaches is that they can not (yet) be applied on infrastructural problems where paths can be repurposed into the new system.

2.2 RESEARCH OBJECTIVE

As it stands, it can be concluded that there are different suitable models which are able to give insights in the viability of integrating green hydrogen system components into the (offshore) electricity grid. These models offer the ability to design a desired hydrogen infrastructure. Looking at the possibilities offered by the different network optimisation models, as well as the identified knowledge gaps in literature, the following objectives should be addressed within this thesis:

- include the wind electricity surplus as a potential for hydrogen production;
- include detailed spatial characteristics by using GIS tools;

- include barriers and other spatial complexities within the network optimisation;
- investigate the effects of the differences between isolated and interconnected hydrogen systems in the North Sea on a (trans)national scale;
- consider a phasing period over the upcoming decades; and,
- include the reuse of natural gas pipelines.

In line with these objectives, this research focuses on identifying an optimal cost-effective hydrogen system within the offshore wind energy grid of the EU in the North Sea. The main research question of this thesis is therefore defined as:

“What is the optimal EU offshore hydrogen system configuration in the North Sea”

Within this research question, the system configuration entails the locations of the different wind farms, electrolyzers, and hydrogen pipelines. The possible locations are limited by borders of the economic exclusive zones of the EU. Furthermore, given the current EU plans of the increase of offshore wind capacities, a phasing period is used from 2030, 2040, to 2050.

The main research question can be broken down into a set of sub-questions:

1. *“What are the locations of the new wind farms and of the electrolyzers?”*

To design an offshore hydrogen system, first the locations of the new wind farms are being defined. The EU plans of the increase in offshore wind capacities, are a starting point for this. Consequently, the locations of the electrolyzers can be defined.

2. *“What is the maximum amount of electricity which can be used to produce hydrogen?”*

With the defined new wind farms and electrolyzers, the maximum amount of electricity available for hydrogen production can be determined. This leads to the maximum amount of hydrogen that can be produced per electrolyser.

3. *“What is the optimal infrastructure for the transmission of hydrogen to shore?”*

After having derived the capacities and the locations of the electrolyzers, the transmission infrastructure can be defined.

4. *“How do the costs relate to the expected benefits of the different system designs?”*

The final step is performing an economic assessment to evaluate the system. Using the economic assessment, the system can also be fine-tuned.

2.3 REPORT STRUCTURE

The remainder of this thesis is structured as follows: In [Chapter 3](#) the methodologies used to answer the sub questions are described. To use the defined models, data preparation is needed, which is described in [Chapter 4](#). [Chapter 5](#) presents the results including a sensitivity analysis, after which the conclusion follows in [Chapter 6](#). Finally, in [Chapter 7](#), the results and the conclusion are discussed and recommendations are given. Additional information is found in the appendices: the offshore wind farm characteristics can be found in [Appendix A](#); the incumbent gas infrastructure characteristics in [Appendix B](#); an explanation on the techno-economic data used in this thesis in [Appendix C](#); and information on the electrolyzers in [Appendix D](#).

3 | RESEARCH METHODOLOGY

Throughout the whole research different scenarios are used, which are explained in the first section of this chapter. The other sections in this chapter explain the used methodology for the aforementioned four sub research questions:

1. The rationale on the expected wind farm placement and electrolyser placement is explained in [Section 3.2](#).
2. The methodology on how to derive electricity potential for hydrogen production is explained in [Section 3.3](#).
3. The Network Optimisation Model (used to define the transmission infrastructure) is explained and adapted for this thesis in [Section 3.4](#).
4. The methodology on the economic assessment is presented — including different hydrogen pricing scenarios — in [Section 3.5](#).

3.1 SCENARIO SET-UP

This section reflects on the different scenarios which are analysed within this thesis. The scenarios are used as further input to design the different offshore energy systems.

Top-level scenarios (A)

These scenarios reflect the phasing period within this thesis: 2030 (A₃₀) – 2040 (A₄₀) – 2050 (A₅₀), according to the [EU](#) offshore wind investment plans. The corresponding expected increase in electricity demand for each year is included within the scenarios. These scenarios are of interest as they reflect how the [EU](#)-wide energy system is expected to change over the upcoming decades, and to present indications of the feasibility of the hydrogen system phased over different years.

Lower-level scenarios (B)

This layer is divided into two different scenarios: an interconnected (B₁) and an isolated (B₂) scenario:

- B₁ reflects on the countries of interest within the system demarcation as a whole; here, the countries are interconnected and collaborating, and thus all the electrolysers and pipelines of each country may interact with each other. As an example, an electrolyser located in the

Dutch EEZ may connect via another electrolyser located in the German EEZ to shore, connecting both EEZs.

- B2 reflects on the system if all the countries within the system demarcation are isolated from each other. Hence, their electrolysers may not interact or connect with one another and pipelines may not cross EEZ borders.

These B-scenarios are of interest as they give indications on whether the countries within the system demarcation need to collaborate or if they can realise such a system on their own.

Combining the A and B scenarios, a total of six scenarios is used, as visualised in Figure 3.1. To analyse all the different scenarios, the methodology as presented in Figure 3.2 is used. The different methodologies are elaborated on in the remainder of this chapter.

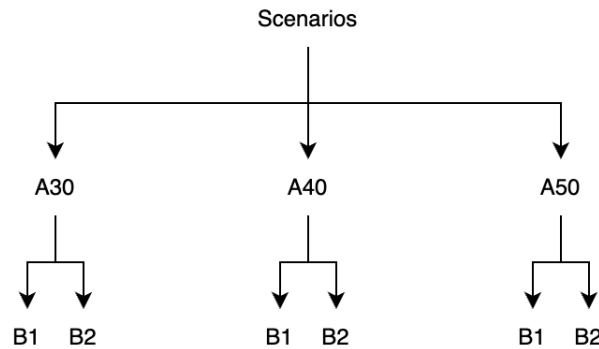


Figure 3.1: Scenarios used.

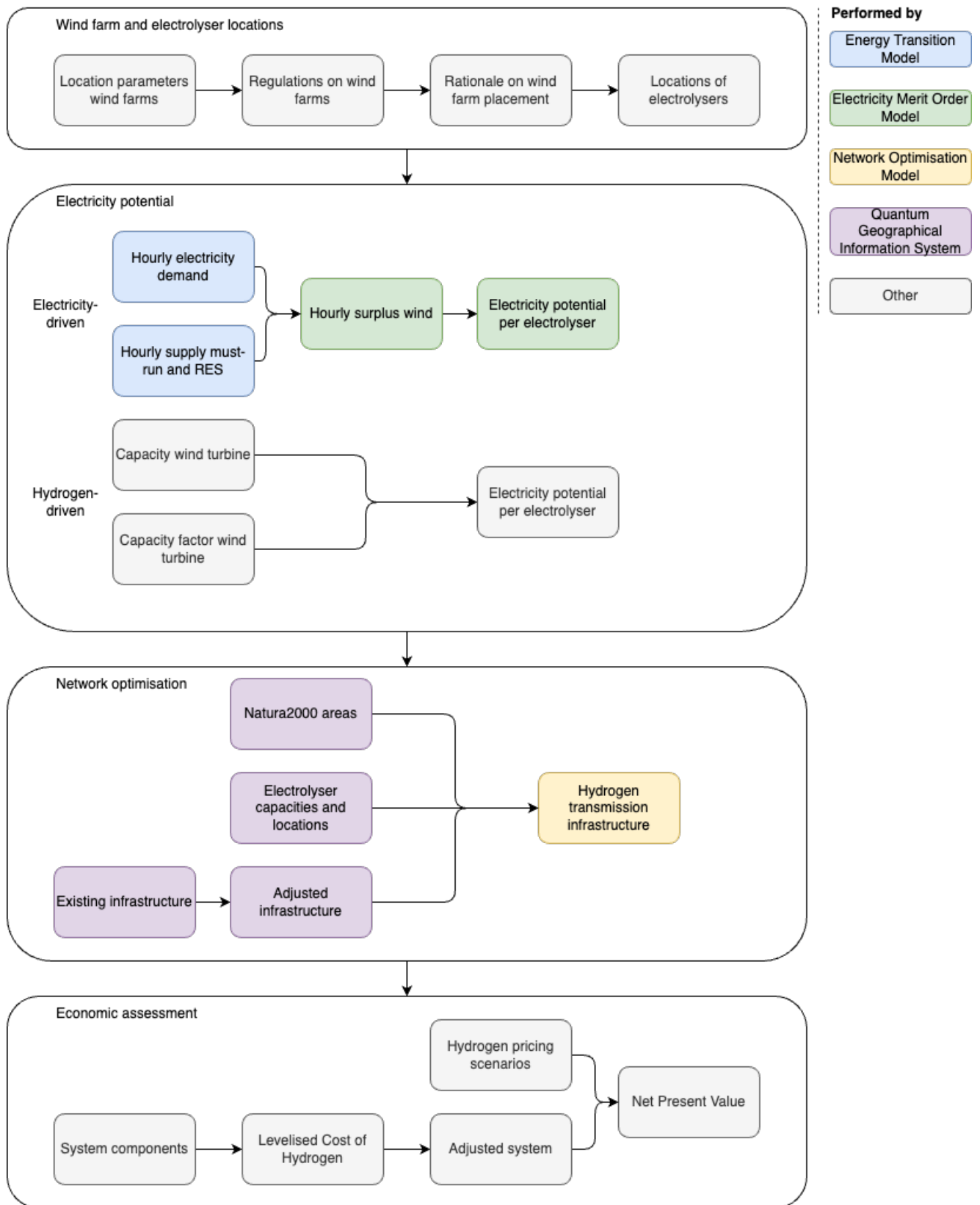


Figure 3.2: Methodology flowchart.

3.2 WIND FARM AND ELECTROLYSER LOCATIONS

This section presents the methodology on how to derive the locations of the wind farms and electrolysers. First, one should be able to accurately estimate where future wind farms will be placed. Thereafter, it is possible to (more) accurately describe the placement of the electrolysers.

3.2.1 Wind Farms

Location Parameters

To understand the rationale behind the locations of (future) wind farms, it is important to understand how location parameters influence this decision making process. Using these parameters, the North Sea (within the EEZs of Belgium, Denmark, Germany, and the Netherlands) can be analysed to find a rationale on how the wind farms will be placed. Five basic parameters can be distinguished, which are explained and evaluated below:

- **Soil conditions:** The soil conditions of the seabed, influence what kind of structure is needed to support the offshore wind farm and what kind of installation procedure is most favourable. E.g. harder soils may opt for drilling procedures, which cost more time and money when compared to e.g. impact piling¹.

The goal of analysing this parameter is to evaluate if there are soil conditions present within system demarcation that would hinder the installation of the wind farm. This appears not to be the case: According to C. Schallück (Van Oord NV, personal communication, August 2021), the soil characteristics consist primarily of sand. Hence, similar installation procedures and foundation types can be used throughout the system.

- **Water depth:** Like the soil conditions, the water depth influences the type of support structure, as well as the installation procedure. E.g. deep waters might require floating wind farms.

The water depth is analysed in order to find areas which might be too deep for the construction of wind turbines, or reaching certain depths where different support structures are needed for the wind turbines. Additionally, it is important to note how the depth increases along the coast, as deeper waters might challenge the technical feasibility of the installation (Kallehave et al., 2015). In Figure 3.3, the bathymetry of the North Sea is shown. As can be deduced from the figure, the depth of the North Sea is quite shallow within the system demarcation. The maximum depth reaches 40 m, which makes it suitable for the most commonly used support structure: monopiles (Kallehave et al., 2015).

- **Average wind speeds:** The average wind speed directly influences the potential output of the wind farm. E.g. too high or too low average

¹ I.e. using a hydraulic 'impact' hammer to drive down the monopile support structure of offshore wind farms

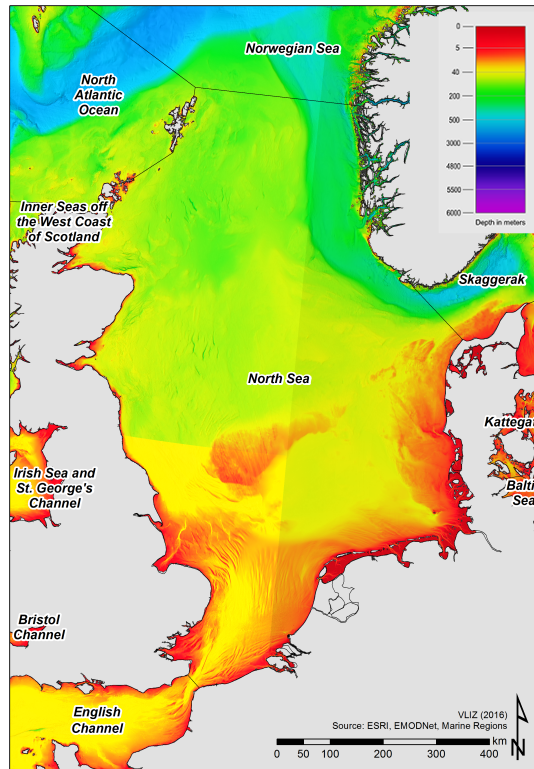


Figure 3.3: Bathymetry of the North Sea (De Hauwere, n.d.).

wind speeds, might refrain the wind turbine from generating electricity.

Figure 3.4 shows the average wind speeds. The figure shows that within the system demarcation, the average wind speeds are very similar. This does not impose any explicit challenges, nor large advantages with regard to the placement of the offshore wind farms.

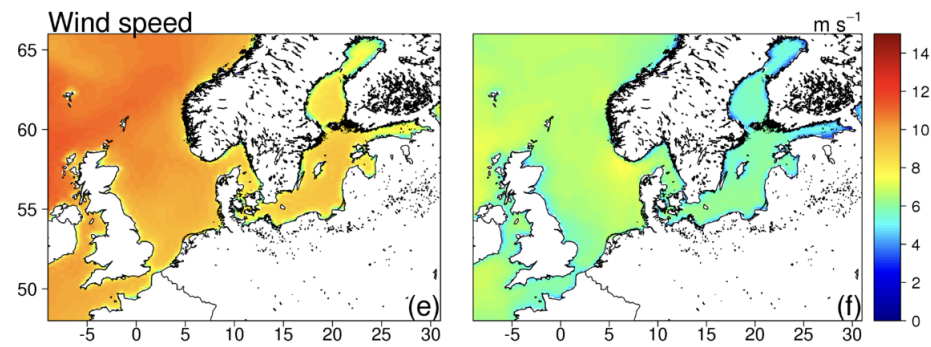


Figure 3.4: Average wind speeds in the North Sea during winter (left panel) and summer (right panel) (Bonaduce et al., 2019).

- **Sea state:** Simply put, the sea state reflects the 'roughness' of the sea. The sea state influences the design load and the design height of the structure, and consequently also the installation and maintenance costs. E.g. a very rough sea state requires the structure to endure higher loads, increasing the costs of the structure.

The sea state is analysed to derive areas where the sea state might be too rough for feasible wind farms, and to derive possible large sea state discrepancies within the system demarcation. The sea state is defined by the significant wave height, and by the mean wave period (Lavidas, 2022). The significant height of a sea state represents the average height of $\frac{1}{3}^{rd}$ of the highest waves measured within the record (Lavidas, 2022). The wave period defines the time for two successive crests to pass a specified point (hence one wavelength) (Lavidas, 2022). The more similar the significant wave height and the mean wave period, the more similar the sea state of the areas. Figure 3.5 presents the significant wave heights (H_s) and the mean wave periods (T_m) for the North Sea during winter and summer. As can be seen, very similar sea states are present due to the relative equivalent significant wave heights and wind speeds throughout the system demarcation. Although, the further from shore, the more challenging the sea state becomes. However, in general, the sea state is considered to be moderate.

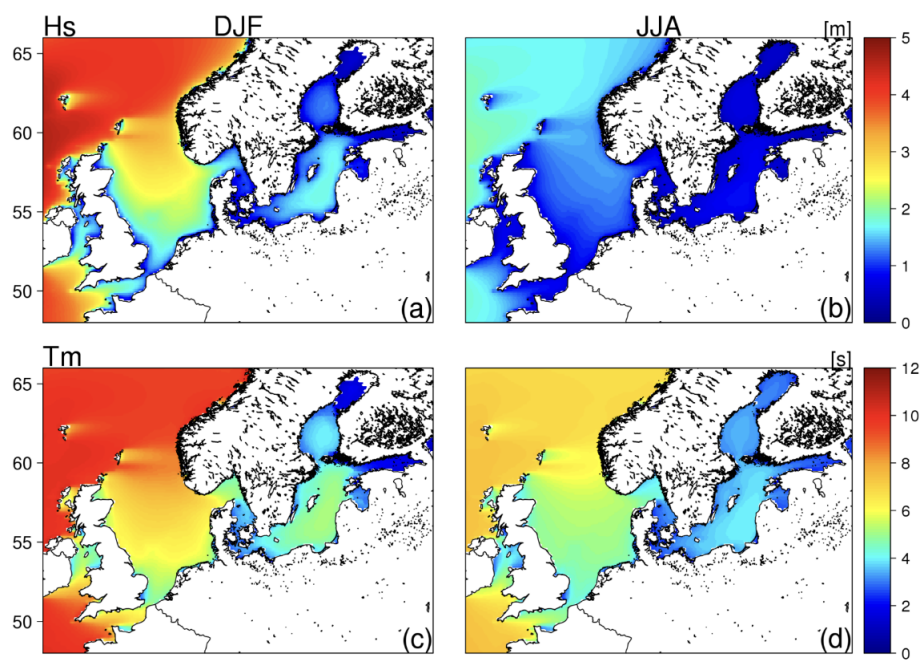


Figure 3.5: Showing the significant wave height (a + b) and the mean wave period (c + d) during winter (left panels) and summer (right panels) (Bonaduce et al., 2019).

- **Distance to shore:** The distance to the shore influences the maintenance and installation costs of the wind farm, as well as the transmission costs of the electricity. E.g. a wind farm far from shore requires a longer transmissions distance to shore, which increases the transmission infrastructure costs and electricity losses.

Hence, this parameter is the most easy to define. The further the distance, the higher the costs of installation, maintenance, and transmission.

Wind Turbine Placement

A final point of interest within the wind farm placement reflects on the placement of the turbines themselves. When designing a wind farm, it is important to consider the wake effect. The wake effect refers to the area behind the rotor of the wind turbine where the wind speed is reduced, reducing the effective power of the other turbines (Van der Male, 2021). Van der Male (2021) explains that when one designs (offshore) wind farms, the power output of the wind farm as a whole is to be optimised. The power output is directly related to the corresponding wind speed around the rotor. Hence an optimal distance between the various wind turbines is needed to minimise the wake effect. To acquire the distancing between the wind turbines, the rotor diameter of the wind turbines is used. The spacing becomes 5 times the diameter (Grady et al., 2005).

Rationale Based on Location Parameters

Considering the location parameters, a rationale can be defined on how future wind farms are likely to be placed. As stated above, nor do the soil conditions, the water depth, or the average wind speed vary along the system demarcation to such an extent that they are likely to greatly influence the decision making process on the location of the wind farms. However, the sea state varies (to some extent), and so does the distance to the shore. The sea state becomes more rough (although still moderate) further from shore. Additionally, the costs acquainted with the installation and maintenance of the wind farm increase along the distance from shore.

Using this, a simple rationale can be derived for the locations of the offshore wind farms: the wind farms are placed from the coast outwards.

Regulatory Constraints

Although it is defined that the optimal placement is closest to shore, not all wind farms may be placed near shore. A set of constraints exists with respect to placement of the wind farms.

The United Nations Convention on the Law of the Sea (UNCLOS) defines that states located alongside international waters, have the right to regulate and authorise the construction and use of systems for economic purposes within the waters of the EEZs (UN General Assembly, 1982). As the construction and use of wind farms located within the EEZs are economic activities, such developments are allowed. Within the EEZs, this right is limited by the obligation to have due regard (i.e. take proper care or concern) to the rights of other states as is described within the UNCLOS (UN General Assembly, 1982). This entails that other states have the right of navigation and the right to lay offshore pipelines and cables.

Additionally, the right of deploying economic activities within the offshore EEZs is limited by the state's duty to protect and preserve the marine environment (UN General Assembly, 1982). As a consequence, there only exists a number of potential wind farm locations.

As a result, governments have defined specified wind farm development zones within their EEZs. These development zones are chosen conform the

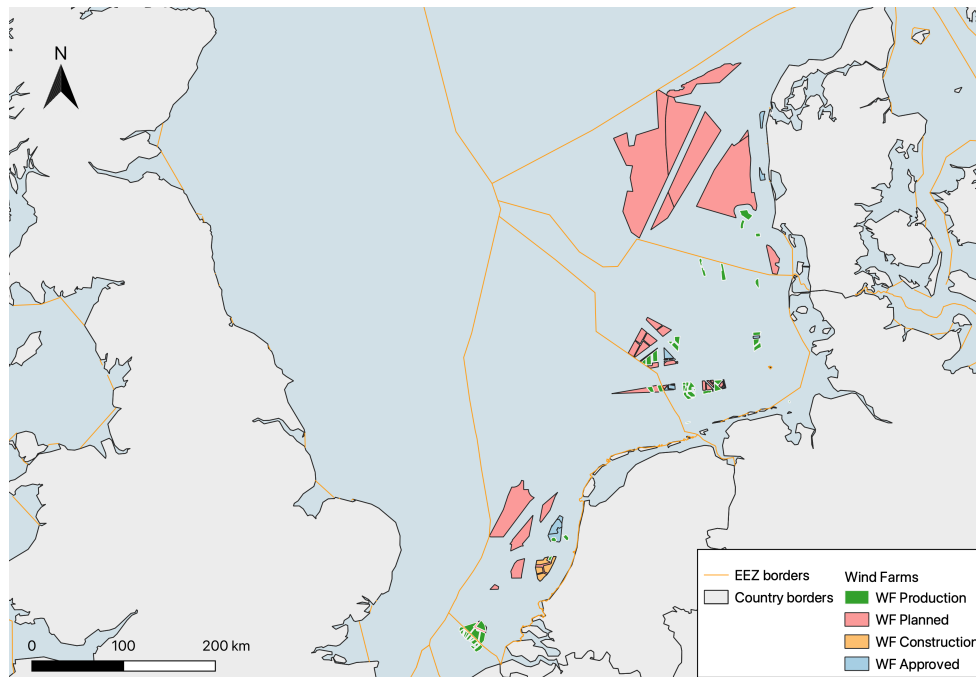


Figure 3.6: Map of the wind farms locations presented by [EMODnet \(2021\)](#).

laws stated within the [UNCLOS](#). The new wind farms within this thesis are placed conform these specified development zones.

The offshore wind farm development zones consist of a set of 96 different (potential) wind farms within the North Sea. This data-set is defined by [EMODnet \(2021\)](#). Within this set, 86 wind farms have a pre-defined capacity (see [Appendix A — Table A.1](#) for an overview). The data-set comprises of a total of four different wind farms states: *production (active)*, *construction (inert)*, *planned (inert)*, and *approved (inert)*. [Figure 3.6](#) gives a representation of the wind farms. Additional to the wind farms presented within the data-set of [EMODnet \(2021\)](#), [4C Offshore \(n.d.\)](#) also presents an overview of wind farm development zones. First, the data-set of [EMODnet \(2021\)](#) will be used as the data-set is prepared by the European Commission. If the needed locations exceed the proposed sites by [EMODnet \(2021\)](#), the additional development zones presented by [4C Offshore \(n.d.\)](#) are included.

Concluding Remark

Together with the wind farm (development) zones (presented by [EMODnet \(2021\)](#) and [4C Offshore \(n.d.\)](#)) and with the optimal wind farm location rationale (moving from the coast outwards) described before, it is possible to define how the new wind farm locations are expected to develop over time: The new wind farms will be placed within the wind farm development zones. Along 2030, 2040, and 2050, the wind farms will gradually move outwards from the coast.

3.2.2 Electrolysers

Aside from the wind farms, the offshore hydrogen system includes electrolysers in order to produce the hydrogen. The offshore electrolysers can be placed in two different ways: general offshore electrolyser hubs, or in-turbine electrolysers.

First, the electrolyser hub. It is important to note that the electrolyser hub does not solely consist of an electrolyser. The hub also consists of a desalination unit, and a compressor. The desalination unit is needed as the electrolyser uses water as an input. The unit removes salt and other impurities from the seawater to produce fresh water. Moreover, as the electrolyser output pressure is not same as the operating pressure of the pipeline, a compressor is needed. When trying to optimise the placement of the electrolyser hub, the output should be maximized whilst minimizing the costs. To achieve this, it is assumed that the electrolyser hubs may be placed on top of existing and new electricity sub stations belonging to wind farms ([Assumption 1](#)). The sub stations are used for the following reasons:

- it is possible to allocate the costs of the foundation over the sub station and the electrolyser hub, reducing the costs;
- there are less energy losses due to lower transmission distances via cables;
- per sub station and electrolyser hub, only one environmental impact assessment needs to be done, thus reducing the costs; and,
- reducing the spatial uses within the North Sea, as no additional 500 *m* between structures is need (as defined by the [UNCLOS](#)).

As an example, the location of such sub stations can be seen in [Figure 3.7](#).

For the in-turbine electrolysers, the electrolyser and the desalination unit are placed within the wind turbine of a wind farm. However, a separate compressor station is needed. This station is placed close to these wind farms. The hydrogen produced within the turbines will directly be fed into the compressor station, from where the hydrogen is fed into the hydrogen transmission infrastructure.

Both types of electrolysers (electrolyser hubs and in-turbine electrolysers) are included in this thesis. In the next section, a more detailed elaboration is given on both types, as well as the methodology on how much electricity could be used by both electrolyser types to produce hydrogen.



Figure 3.7: A depiction of the locations of the offshore sub stations of wind farms NLD10, NLD11, NLD12, NLD13, NLD22. Derived from (4C Offshore, n.d.)

■: Offshore sub station ■: Wind farm
—: Infield cable —: Export cable

3.3 ELECTRICITY POTENTIAL

The offshore hydrogen system is influenced by a concurrent demand of hydrogen and electricity, both generated using the wind turbines located in the North Sea. Efforts to generate green hydrogen by means of offshore wind should not hinder the transition towards clean electricity systems. Hence, the question is what quantity of hydrogen could be supplied by the system located in the North Sea. This is rather complex because the system is subject to a number of different factors such as the hydrogen demand, electricity demand, hydrogen supply, and electricity supply. This section proposes an approach to answer this question.

To determine the supplyable quantity of hydrogen, one important assumption is made: The system should be able to handle the maximum possible output of hydrogen on a yearly basis ([Assumption 2](#)). Hence, the system will be supply driven, not demand driven. If in the end the possible yearly hydrogen supply exceeds the hydrogen demand, the hydrogen supply can be downscaled.

Two operational modes are used to investigate the maximum electricity potential which can be used by the electrolyzers to produce hydrogen:

- Electricity-driven: The electrolyser only uses the surplus of electricity from the offshore wind farms. The surplus can be seen as excess supply of electricity ([International Energy Agency, 2019a](#)). Hence, a priority is given to the electricity demand of a country.

- **Hydrogen-driven:** The electrolyser uses the entire generated electricity of the wind turbines. Hence all the electricity generated by a turbine is transformed into hydrogen. This mode only uses so-called H₂-in-Turbine wind farms. These wind farms have (among other components) electrolysers within the wind turbines.

3.3.1 Electricity Supply Potential for Hydrogen — Electricity-driven

To define the quantity of potential electricity which can be used within the electricity-driven operational mode, several steps are taken. The steps are partially done by making use of the Energy Transition Model (ETM)², and partially done by an Electricity Merit Order Model (EMOM)³ built for this thesis. How the ETM and the EMOM are intertwined, is explained in more detail in the steps below:

1. The system has been divided with respect to the countries taken into account: Belgium, Denmark, Germany, and the Netherlands. Each country is treated as a closed system, and therefore imports and exports of electricity are not considered⁴. Hereafter, the hourly demands for 2020 of each country are derived within the ETM. Thereafter, within the EMOM, an additional yearly electricity demand increase is assumed per country (Assumption 3). This demand increase is set at 1,1 %/yr for 2020 to 2050 (McKinsey&Company, 2010).
2. As renewable electricity should be treated as "renewable first — if possible", the maximum hourly supply of the 'must-run' plants and the plants with a marginal cost of 0 EUR/MWh of the country of interest are derived using the ETM. The must-run plants are combined heat and power plants that satisfy a certain heat demand and do not primarily run to sell power, as proposed by the ETM. Additionally, nuclear power plants are also considered as must-run plants due to their long start up times which can reach up to 12 hours (Energy Administration Information, 2020). The plants with a marginal costs of 0 EUR/MWh are, but not limited to, offshore and onshore wind, and offshore and onshore photovoltaic sources.
3. Using the hourly demand derived in step one and the maximum supply derived in step two, the potential of electricity which can be used to produce hydrogen using the must-run plants and the plants with a

² The ETM is an open-source and interactive energy model developed by Quintel Intelligence (n.d.). Within this model, the user can build and explore different energy scenarios for countries by adjusting for instance the energy mix, prices, demand sources, and supply sources of a country. The model outputs fact-based results due to repetitive updating of the model and due to years of data collection. Using this, proper insights can be created when analysing large energy systems.

³ The EMOM is a model built specifically for this thesis. This Excel model is able to compare the hourly electricity demand and supply values of a country within a specific year. The demand and supply classes are very sector specific and exist of a set of 140+ different types per country. As a consequence, the model is able to accurately define the electricity surplus.

⁴ The reason for doing so, is as otherwise the ETM will balance the energy systems of each country using imports or exports. This is unfavourable when trying to derive the maximum available surplus of each country.

marginal cost of 0 *EUR/MWh* is derived using the [EMOM](#). This is done by subtracting the hourly demand of the country from the hourly maximum supply of the power plants in question. The residual supply is the overall potential which could technically be used to produce hydrogen.

4. As only the surplus offshore wind is of interest, the potential electricity of offshore wind needs to be derived within the [EMOM](#). This is done by comparing the residual hourly supply derived in step three to the maximum estimated hourly output of all the offshore wind farms of the country of interest. First, if the residual supply is less or equal to 0 *MW*, the potential electricity for hydrogen is also 0 *MW*. Second, if the residual supply is greater than 0 *MW* and the residual supply is greater or equal to the maximum hourly supply of the offshore wind farms, then the maximum hourly electricity potential for hydrogen production is equal to the hourly maximum offshore wind electricity production. And finally the third option, if the residual supply is greater than 0 *MW* and the residual supply is less than the maximum hourly supply of the offshore wind farms, then the maximum hourly electricity potential for hydrogen production is equal to the hourly residual supply.
5. As not all countries have all wind farms located within the system demarcation, it is important to define the proportion of available wind electricity which can be used to produce hydrogen within the system. For simplicity, this is done by comparing the overall wind capacity of a country to the wind capacity of that specific country within the system. By doing so, the fraction of the wind capacity within the system demarcation compared to the overall wind capacity can be multiplied with the electricity potential originating from offshore wind of that respective country which is derived during step four.
6. As the [EEZs](#) within the system belong to various countries, the total electricity potential for hydrogen production for the entire hydrogen system also needs to be established. This is done by summing all the separate hourly electricity potentials of each country as derived in step five.

To illustrate the method, [Figure 3.8](#) shows an energy chart of an arbitrary given case derived using the [ETM](#) and the [EMOM](#). As explained, the must-run plants and renewable energy sources are compared to the hourly demand to derive the potential wind surplus. Within this figure, the maximum generated wind electricity is stacked on top the must-run plants and the remainder of the renewable energy sources. Hence, the area of wind electricity above the demand curve represents the surplus of wind electricity which could be used to produce hydrogen.

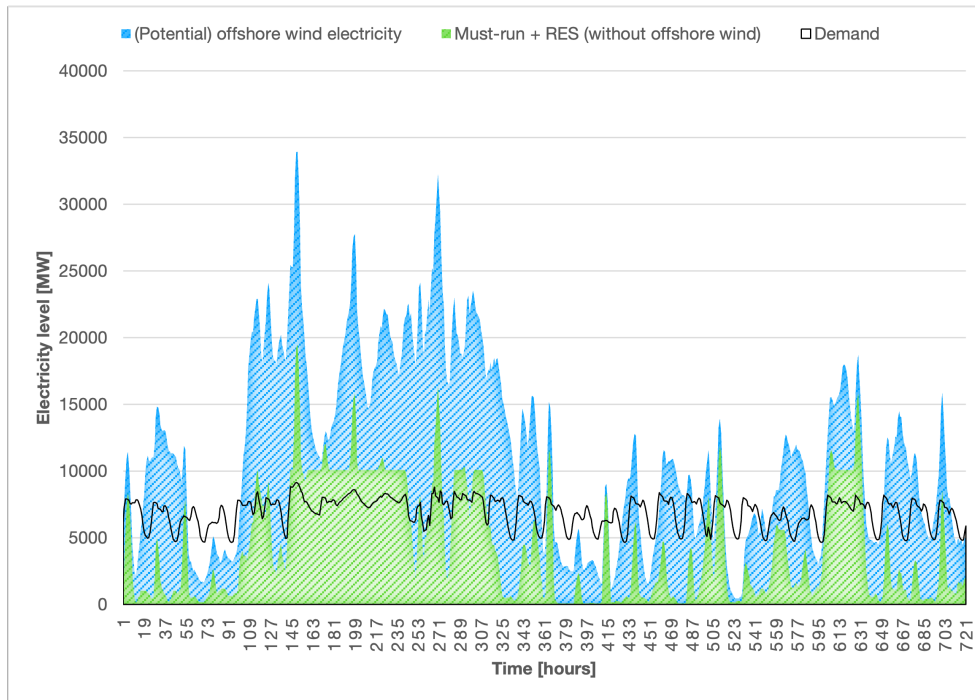


Figure 3.8: Stacked energy chart of an arbitrary case indicating the available wind surplus within a month.

3.3.2 Electricity Supply Potential for Hydrogen — Hydrogen-driven

Additional to using the surplus of electricity generated of the offshore wind farms to produce hydrogen, dedicated wind farms which only produce hydrogen within the wind turbines can also be used. To determine which wind farms will be dedicated to hydrogen production, a cost-parity point is used. This point is based on economic feasibility to transport energy via pipelines or cables over certain distances. By comparing the two transmission options, it is possible to determine the distance threshold after which energy transmission by pipeline would be more economically feasible. Wind farms which fall under the hydrogen-driven operation mode, are assumed to only exist after this threshold (*Assumption 4*). The threshold is calculated by extrapolating and intersecting a data-set on the *CapEx* with respect to transmission costs via cable and pipelines for a transmission capacity.

To visualise the distance threshold, *Figure 3.9* shows a depiction. As can be seen, before the threshold there is electricity generation present. The electricity may be transported via the sub station to shore, or the electricity may be converted into hydrogen at the electrolyser hub. After the threshold the hydrogen-driven (H_2 -in-Turbine) operational mode is used. Hence, only hydrogen is produced and thus no array cables transport electricity to a sub station.

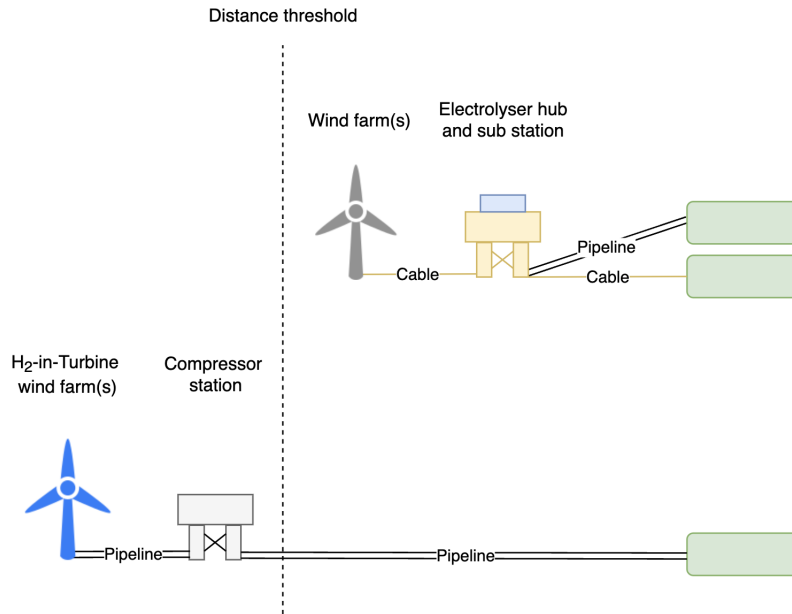


Figure 3.9: Distance threshold between the two operational modes.

The hydrogen supply potential for the hydrogen-driven wind farms is only hampered by the efficiency losses of the electrolyzers and the capacity factor of the wind farms. All the electricity generated by the offshore wind turbines is directly fed into the electrolyzers within each turbine. This means that the capacity of the hydrogen-driven wind farms acts as a firm indication regarding their hydrogen supply potential. A great indication for how much energy an offshore wind farm produces is the capacity factor. This factor is determined by dividing the actual annual output of a wind farm by the annual output if the wind farm would always run on its maximum capacity. Estimations on the capacity factor can be used to derive the annual output of the wind farms. The total yearly electricity potential can be calculated by using [Equation 3.1](#):

$$AEY = C_f \cdot P_{rated} \cdot 8760 \quad (3.1)$$

where AEY is the annual energy yield, thus the electricity generated within a year in MWh ; C_f is the capacity factor in %; and P_{rated} is the rated power of the wind turbine/wind farm in MW , hence the total capacity.

3.4 NETWORK OPTIMISATION MODEL

The purpose of the Network Optimisation Model ([NOM](#)) is to derive the optimal infrastructure for the transmission of hydrogen to shore (the third sub question of this thesis). As has been established in the research formulation ([Chapter 2](#)), the model should preferably be able to:

- repurpose existing natural gas pipelines for hydrogen transport;
- be able to route around defined obstacles; and,

- be able to add different spatial complexities (i.e. cost surfaces) for new pipelines.

The Geometric Graph Theory (GGT) modelling approach (Section 2.1.2) built by Heijnen (2022) seems to be the best approach given the network modelling requirements within this thesis. Namely, the model is able to repurpose existing infrastructures and able to route around obstacles for new infrastructures. This capability is not offered by the Agent Based Modelling (ABM) or the Mixed Integer (Non-)Linear Programming (MI(N)LP) approaches. Unfortunately, the model is not able to add different cost surfaces for new pipelines, nor is this ability offered by the ABM or the MI(N)LP approaches. Hence, this aspect shall not be incorporated within this thesis.

This section further describes the GGT NOM which is used to design the hydrogen pipeline infrastructure within the system. First, a general explanation on GGT is given on order to get acquainted with the terminology and mathematical structure of the theory. Thereafter, an explanation is given on the GGT NOM built by Heijnen (2022) after which this model is adapted such that it can be applied to this research.

3.4.1 Geometric Graph Theory

The term GGT often refers to a large body of research focused on graphs defined by their geometric characteristics (Erdős et al., 2013). To take a more simplified view, within the theory a graph G may exist which is located in a plane with possibly intersecting lines (*edges*) which potentially connect a set of points (*nodes*) (Voloshin, 2009). Such a graph is then described by $G = (N, E)$. The most standard type of graph is an *undirected graph*; as the name implies, here the edges of the graph are a 'two-way road' (Rahman, 2017). Figure 3.10a presents a simple undirected graph, and Figure 3.10b presents how an undirected graph can be seen as a two-way directed graph.

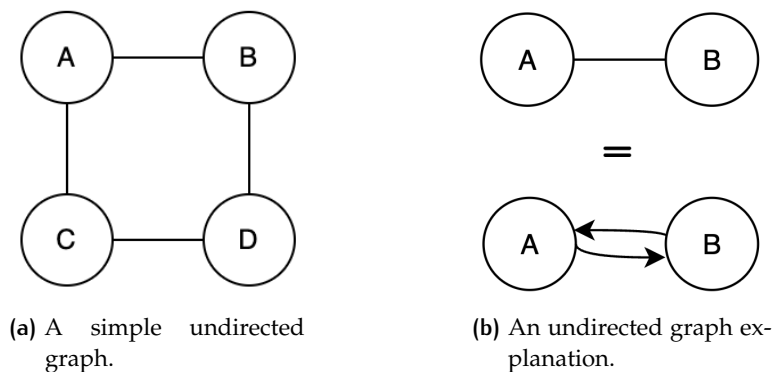


Figure 3.10: Two simple graphs.

The second type of graph is a *directed graph*. A graph is called a directed graph if each edge of the graph has a specified flow direction (Rahman, 2017). Hence, in a sense the edges are a 'one-way street', such as gas pipelines. Figure 3.11 presents a simple directed graph. Within this specific graph, a clockwise flow is only possible.

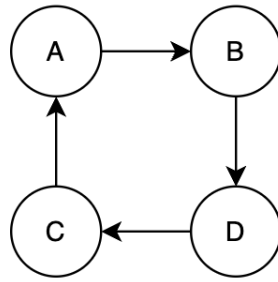
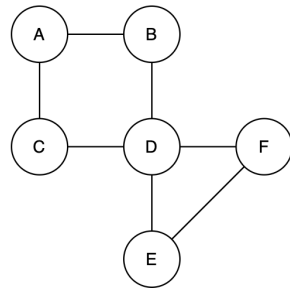
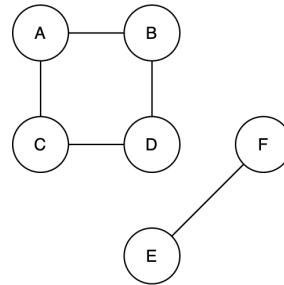


Figure 3.11: A simple directed graph.

The graph presented in [Figure 3.12a](#) is a *connected graph*, on the contrary [Figure 3.12b](#) presents a *disconnected graph*. A graph G is considered to be connected if there is a possible path between each pair of nodes located within the graph, otherwise the graph is considered to be a *disconnected graph* ([Rahman, 2017](#)).



(a) A simple connected graph.



(b) A simple disconnected graph.

Figure 3.12: A connected and a disconnected graph

There are different ways to connect a graph. One of them is a *complete graph*, where all nodes are connected to all edges. Another is by means of a *tree topology*. A tree is a connected graph which contains no cycles ([Rahman, 2017](#)). A cycle can be described as a closed path. Hence, in a cycle you can 'walk in circles'.

The final theorem of interest is the *weighted graph*. A graph is weighted if there is a weight assigned to each edge ([Rahman, 2017](#)). The weight of an edge can represent anything. Commonly, they represent the costs, the capacity, or the length of the edge.

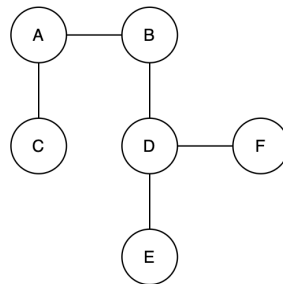


Figure 3.13: A simple graph with a tree topology.

3.4.2 Network Optimisation Model

The **NOM** developed by Heijnen (2022) is a model constructed in Python. The model makes use of a set of algorithms which provide the user with an optimal minimum-cost network-layout. Before applying the algorithms, the **NOM** sets up the case which is to be analysed by (1) reading the input data; (2) analysing the demand-supply patterns; and, (3) determining a representative set of demand-supply profiles. After having set up the input data of the **NOM**, the network optimisation algorithms are performed. Firstly, (4) the minimum spanning tree is determined; thereafter, (5) the minimum-cost spanning tree is determined; and finally, (6) the minimum-cost Steiner tree is determined. The last step of the model is step (7); here, a last improvement round is done by repeating step (5) and step (6).

Step 1 — Reading the input data

In order to read the input data, a number of different files are used with different input variables. Firstly, there exists the coordinates-file. Within this file, the set of coordinates of the nodes is presented; the coordinates represent the supply or demand nodes (*sources* or *sinks* respectively) within the system. In the second file, the supply and demand profiles of the sources and sinks for a given time step are given. Sources are given a positive demand, indicating that they supply to the network. On the contrary, sinks have a negative demand. The third file lists all the existing edges within the network, and represent the existing connections of the system. The connections are presented by two coordinates, defining the endpoints of an connection, and their specific capacity. The next input file is dedicated to defining the obstacles within the model. The obstacles are defined as polygons through which new connections can not run; existing connections can however. The final input file is dedicated to describing the routing restrictions. When using routing restrictions, the possible connections are restricted to a set of pre-defined network connections

In order to assess the quality of the different network topologies, the model uses a cost-function which is defined as follows:

$$C(G) = \sum_{e \in E_n(G)} l_e q_e^\beta + spc \cdot s(G) + cpc \sum_{e \in E_o(G)} l_e (q_e - rq_e)^\beta \quad (3.2)$$

where $E_n(G)$ represents the set of all the new edges within network G ; l_e is the length of edge e ; q_e represent the capacity of edge e ; β is the capacity-cost exponent, which indicates the scaling cost of increasing a capacity of an edge; spc represents the extra costs of the splitting points $s(G)$. Additionally, the existing connections $E_o(G)$ can have an extension of their capacity rq_e by assigning a value to cpc .

Step 2 — Analysing the demand-supply patterns

This step analyses the supply-demand profiles per time step given as input in the model. Here, a visual representation is given within the model regard-

ing the time steps and the supply-demand values of the sinks and sources analysed within the model.

Step 3 — Determining the representative set of demand-supply profiles

Within this step, one can define the number of representative supply-demand profiles. Within this thesis, this is not used as only one relevant time step is used to calculate the optimal network. This is because the supply values of the system increase and decrease uniformly. And since overcapacity generally results in less regret than undercapacity, the maximum supply-demand values are used to determine the optimal network.

Step 4 — Determining the minimum spanning tree

The next step within the model is the generation of the minimum spanning tree of the network. A minimum spanning tree is a tree topology where the sum of the weight or length of the edges used within the tree topology is minimised. [Figure 3.14](#) (left) shows an example of an output of a minimum spanning tree by the model.

Step 5 — Determining the minimum-cost spanning tree

After having determined the minimum spanning tree, the model defines the minimum-cost spanning tree. Within this optimisation, the costs of the edges are also included. The connections of the minimum spanning tree are here iteratively swapped in order to find a solution with a lower cost. In [Figure 3.14](#) (middle) a representation is shown of such a new tree.

Step 6 — Determining the minimum-cost Steiner tree

The possibility exists that a shorter network is present when new splitting points are added to the network. These splitting points are referred to as Steiner nodes; including such Steiner nodes within the tree results in the minimum-cost Steiner tree, as is presented in [Figure 3.14](#) (right).

Step 7 — Last improvement round

The final step repeats Step 5 and 6 in order to find better results.

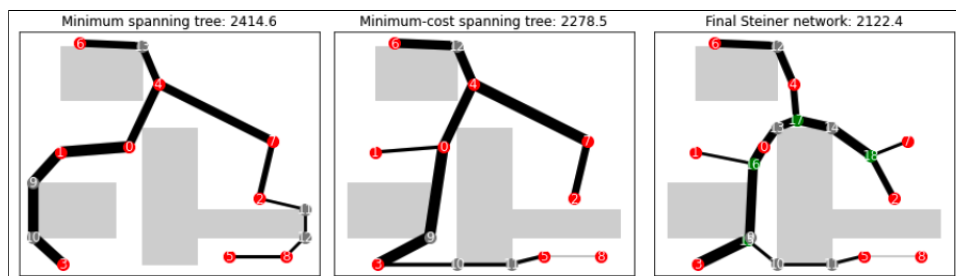


Figure 3.14: Example of a minimum spanning tree, minimum-cost spanning tree, and Steiner tree output with obstacles (grey polygons) by the NOM (Heijnen, 2022).

Existing connections

Existing connections can allow for a cheaper final network. Using existing connections within the network, the same steps are executed to find the best topology. [Figure 3.15](#) shows two network topologies where the right network has existing connections (blue lines) included within the network.

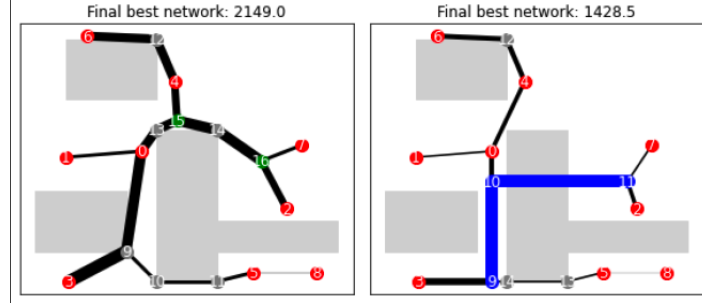


Figure 3.15: Comparison of a final network topology without (left) and with (right) existing connections by the NOM ([Heijnen, 2022](#)).

3.4.3 Model Adaption

Cost Function

The transmission capacity of the hydrogen pipelines depends of a number of parameters. Hence, the original cost function of the NOM needs to be rewritten. The capacity is based on the pipeline size, operating pressure, temperature, flow speed, and the Low Heating Value (LHV) of hydrogen ([González Díez et al., 2020](#)). This can more formally be expressed as:

$$C_p = \dot{n} \cdot M_{H_2} \cdot LHV_{H_2} \quad (3.3)$$

in which

$$\dot{n} = \frac{P\dot{V}}{RT} = \frac{Pv_p A_p}{RT} \quad (3.4)$$

where M_{H_2} is the molar mass of H_2 ; LHV_{H_2} is the low heating value of H_2 ; P is the pressure inside the pipe; v_p is the flow speed; A_p is the area of the pipe; R is the gas constant; and, T is the temperature of the reference point.

The original cost function of the NOM is defined by [Equation 3.2](#). This cost function is to some extent used as a basis for the new cost function. Using [Equation 3.2](#), [C.1](#), and [3.4](#), a new cost function can be acquired. The new cost function of the pipelines is defined by [Equation 3.5](#):

$$C(G) = \sum_{e \in E_n(G)} C_n \cdot \left[\frac{\sqrt{10^9 \cdot C_{new} \cdot R \cdot T_e}}{s \sqrt{0,25 \cdot 3600 \cdot \pi \cdot LHV_{H_2} \cdot M_{H_2} \cdot P_e \cdot v_e}} \cdot l_e \right] + \sum_{e \in E_o(G)} C_o \cdot \left[\frac{\sqrt{10^9 \cdot C_{existing} \cdot R \cdot T_e}}{s \sqrt{0,25 \cdot 3600 \cdot \pi \cdot LHV_{H_2} \cdot M_{H_2} \cdot P_e \cdot v_e}} \cdot l_e \right] \quad (3.5)$$

where C_n and C_o represent the installation costs of the new and original pipelines respectively; s represents the conversion factor to cope with different units of measurement; C_{new} and $C_{existing}$ are the capacity of the new and existing edge respectively⁵; R is the gas constant; T is the temperature of the reference point; LHV_{H_2} is the low heating value of H_2 ; M_{H_2} is the molar mass of H_2 ; P is the pressure inside the pipe; v_p is the flow speed; and, l_e is the length of the pipeline.

Super-Sink

Aside from the adjusted cost function so far, there exists another adoption acquainted with the cost function: this part is affiliated with a so-called 'super-sink' which is added to the [NOM](#). The super-sink represents the total demand of the analysed system. This additional sink is used to optimally distribute the hydrogen along the coast of the [EU](#). To accomplish this, there are existing connections running from the sinks along the coast, to the super-sink. Those existing connections have an extremely large capacity and have no cost affiliated when being used. In this manner, the model is 'tricked' to optimally distribute the hydrogen along the coast: The model treats the super-sink as the only sink present within the system; and at the same time, the super-sink is positioned far from the existing normal sinks. By doing so, the [NOM](#) will always prefer using the available existing connections routing from the normal sinks to the super-sink, instead of building new connections. In this manner, the model automatically distributes the hydrogen supply along the sinks on the coast. In [Figure 3.16](#), a the location of hypothetical sink is presented.

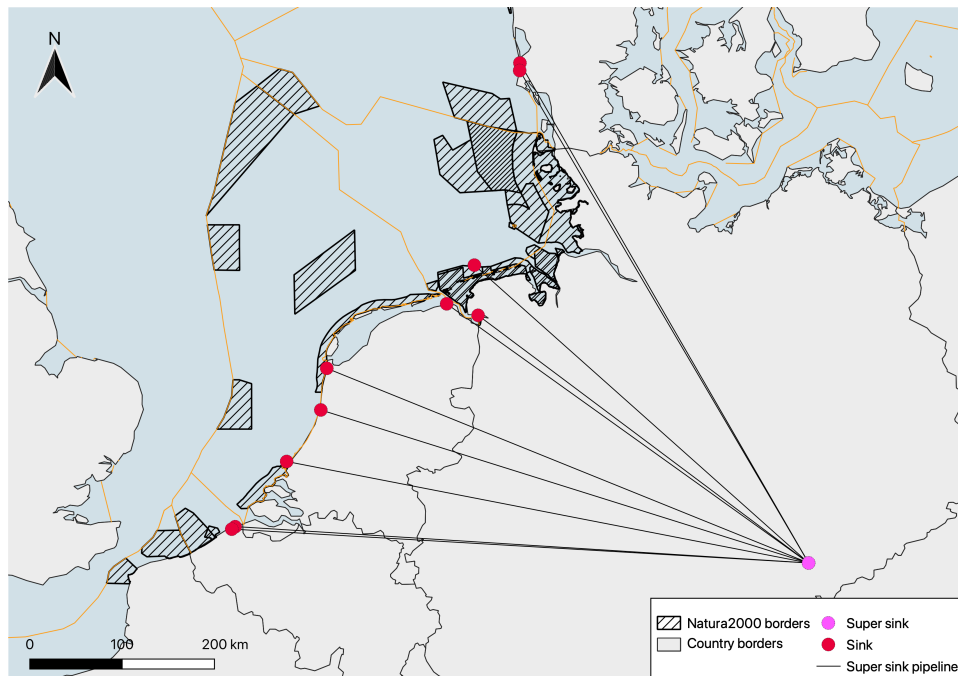


Figure 3.16: Visualisation of the super sink.

⁵ It should be noted that when implementing it in such a way, the entire existing edge will be refurbished, regardless of the capacity needed of the existing edge.

Pseudo-code of the Cost-function

In [Algorithm 3.1](#), the new cost function is shown. Within the pseudo-code, the additional undefined variable X is the capacity of the existing connection to the super-sink. Within this thesis, this capacity is based on a diameter of 1000 in, which is practically speaking infinite.

Algorithm 3.1: Cost function

Input: edge

Output: edge costs

```

1 for new edge do
2    $cost = C_n \cdot \left[ \frac{\sqrt{10^9 \cdot C_{new} \cdot R \cdot T_e}}{s \sqrt{0,25 \cdot 3600 \cdot \pi \cdot LHV_{H_2} \cdot M_{H_2} \cdot P_e \cdot v_e}} \cdot l_e \right]$ 
3   save cost as identity to specific edge
4   add cost to total costs
5 for existing edge do
6   if capacity < X then
7      $cost = C_o \cdot \left[ \frac{\sqrt{10^9 \cdot C_{existing} \cdot R \cdot T_e}}{s \sqrt{0,25 \cdot 3600 \cdot \pi \cdot LHV_{H_2} \cdot M_{H_2} \cdot P_e \cdot v_e}} \cdot l_e \right]$ 
8     save cost as identity to specific edge
9     add cost to total costs
10  if capacity ≥ X then
11  | cost = 0

```

Step 1 — 6

These steps are not adjusted within the [NOM](#), except for the new cost function as described above.

Step 7

As this step often does not improve the results of the [NOM](#) in many cases ([Heijnen, 2022](#)), this step is removed from the [NOM](#) to increase the calculation speed.

Export

A final step is added to the [NOM](#) to export the results of the [NOM](#). Here, the results are exported to a set of different files which for instance can be imported into the [GIS](#) tool or into Excel for data analysis.

3.5 ECONOMIC ASSESSMENT

In order to determine the economic effectiveness of the hydrogen systems (the fourth sub question of this thesis), there is a need to analyse the costs and the benefits of the different systems. This is done by calculating the Levelised Cost Of Hydrogen and the Net Present Value.

3.5.1 Levelised Cost of Hydrogen

The Levelised Cost Of Hydrogen (LCOH) represents the break-even point of an energy generation system. It is a good indicator in the cost-effectiveness of an energy generation system as it does not presume any assumptions on the energy price at which it would be sold. Additionally, the LCOH can be used to compare multiple and different energy systems without framework conditions affecting the assessment (Papapetrou & Kosmadakis, 2022). Simply put, the LCOH is calculated by dividing the total costs of the system by the total produced energy of the system. The LCOH is determined using the general Equation 3.6:

$$LCOH = \frac{\sum_{t=1}^n \frac{I_t + M_t + F_t}{(1+r)^t}}{\sum_{t=1}^n \frac{E_t}{(1+r)^t}} \quad (3.6)$$

where I_t are the CapEx in EUR in year t ; M_t are the Operational Expenditures (OpEx) in EUR in year t ; F_t represent the fuel expenditures in EUR in year t ; E_t is the produced energy in MWh in year t ; r is the discount rate %; and finally, n is the expected operational life of the system.

3.5.2 Net Present Value

The Net Present Value (NPV) is used to analyse the expected profitability of the investments. The NPV is calculated using Equation 3.7.

$$NPV = \sum_{t=1}^n \frac{R_t}{(1+i)^t} \quad (3.7)$$

where R_t represents the net cash flow in MEUR in year t ; and, i represents the discount rate in %.

The NPVs of the systems depend greatly on the future estimated prices of hydrogen. To calculate the NPV, different hydrogen prices are taken into account. The hydrogen prices are derived from a set of five different scenarios. These scenarios are based on the potential market sizes and estimates on the threshold prices to replace the incumbent technologies (Ruth et al., 2020). The five scenarios are:

1. A reference scenario: within this scenario, a strong market competition (low natural gas prices) is assumed as well as the current hydrogen technology status.
2. The research and development advances + infrastructure scenario: within this scenario, the expected development of hydrogen technologies and the expected demand growth are incorporated.
3. The low natural gas resource/high natural gas price scenario: here the natural gas market is adjusted by decreasing the natural gas availability but increasing the natural gas demand.

4. The aggressive electrolysis research and development scenario: in this scenario, the electrolyzers have access to the electricity grid whilst wind and solar energy are more competitive with natural gas generation.
5. The lowest-cost electrolysis scenario: this scenario considers an optimistic development of hydrogen technologies.

The results of the work by [Ruth et al. \(2020\)](#) can be found in [Figure 3.17](#) and translate to 1,63 EUR/kg, 2,11 EUR/kg, 2,21 EUR/kg, 2,21 EUR/kg, and 1,92 EUR/kg respectively.

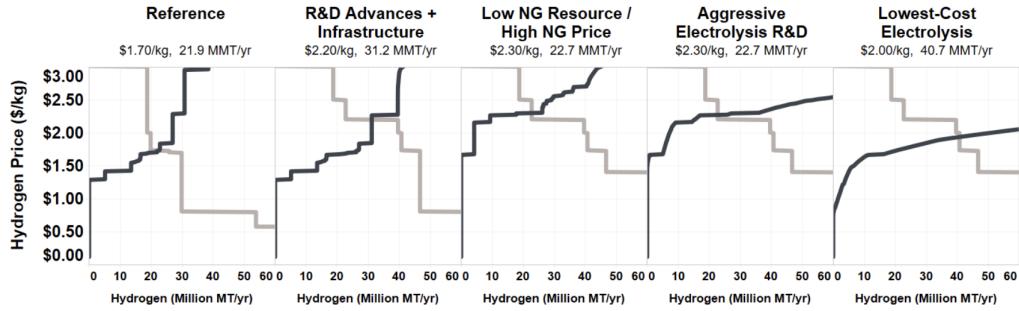


Figure 3.17: Estimation of future demand-supply curves for hydrogen.
— : Supply — : Demand

3.5.3 Additional Remarks

An important remark regarding the calculations for the economic assessment, reflects on the expected operational life of the system: as not all components of the system have the same estimated operational life, an assumption is made: The total operational life is assumed proportional to the cost of the components compared to its operational life ([Assumption 5](#)). Hence, e.g. a component with a low total added cost to the system as a whole, will have a low impact on the total assumed operational life. A mathematical expression of the total operational life is as follows:

$$n_{tot} = \sum \frac{n_i \cdot C_i}{C_{tot}} \quad (3.8)$$

where n_{tot} is the total operational life of the system in years; n_i is the operational life of the system component i in years; C_i is the [CapEx](#) of the system component i in *MEUR*; and, C_{tot} is the [CapEx](#) of the system as a whole in *MEUR*.

Additionally, it should be noted that within the economic assessment, the costs of the wind farms and of the transmission infrastructure of the electricity, are not taken into account. These costs are treated as sunk costs. Sunk costs reflect on costs that already have been made, and which cannot be recovered ([Mankiw, 2018](#)). The hydrogen system is considered to be a potential 'add-on' of the electricity system. With this rationale, it is assumed that the future electricity systems will be built, in disregard of the potential

hydrogen system ([Assumption 6](#)). Hence all the components of the electricity system are considered to be sunk costs.

Finally, it should be noted that not only the construction or repurposing of the offshore components are taken into account within the economic assessments. Components are also to be deconstructed. The [UNCLOS](#) defines that a removal of abandoned or obsolete structures or installations is obligated ([UN General Assembly, 1982](#)). Hence, after their expected operational life, the system components will be decommissioned, which induces additional costs.

4 | DATA PREPARATION

Data preparation is needed before the different models discussed in the previous chapter can be used. In the first section of this chapter, it is explained how the individual electrolyzers get their capacity assigned to. In [Section 4.2](#), the locations of the obstacles used within this research are defined. In [Section 4.3](#), data concerning the existing gas transmission infrastructure are adjusted, and the locations of the onshore entry points are presented. And finally, in [Section 4.4](#), an overview of the main techno-economic data is presented, as well as estimations on the future renewable energy source levels of each country.

4.1 ELECTROLYSERS

By following the methodology described in [Section 3.2](#), it is possible to define specific electrolyser locations within the North Sea. However, using the methodology described in [Section 3.3](#), only the total of country specific electricity potential for hydrogen production will be determined. Hence, the specific capacities still need to be assigned to the individual electrolyzers before the data can be used in the Network Optimisation Model (NOM).

4.1.1 Electrolyser Hub

The assigned electrolyser hub capacity is in proportion to the capacity of the wind farms onto which the electrolyser hub is connected. A mathematical expression of the rationale is presented in [Equation 4.1](#):

$$E_{hub,max} = E_{pot,max} \cdot \frac{\sum P_{i,connected}}{\sum P_{all}} \quad (4.1)$$

where $E_{hub,max}$ is the maximum energy output of the hub *MWh*; $E_{pot,max}$ is the maximum electricity available for hydrogen production *MWh*; $P_{i,connected}$ is the capacity of wind farm *i* which is connected to the electrolyser hub; and P_{all} reflects all the wind farms within the system. Moreover, as the electricity which is available for hydrogen production is determined on an hourly basis, $E_{hub,max}$ is equal to the capacity of the electrolyser hub in *MW*.

4.1.2 In-Turbine Electrolysers

For the H₂-in-Turbine wind farms, the electrolyser capacity of each turbine is the same as the capacity of the wind turbine itself. Additionally, as a separate compressor station is needed to which the H₂-in-Turbine wind farms

are connected. The capacity of the compressor station is the same as the sum of the capacities of the electrolysers connected to the compressor.

4.2 NATURA2000 AREAS

As explained in [Section 3.2](#), the [UNCLOS](#) states that countries should preserve their marine environment. Defining the effects of a project is normally done on a case-by-case basis, by means of e.g. an environment impact assessment. However, due to the sheer size of the project in question, such assessments would require an extensive amount of time. Instead of this, Natura2000 sites are used in this thesis. In order to preserve the marine environment, to reduce the negative environmental impact of the hydrogen system design, and for simplification purposes, this research treats Natura2000 sites as areas where the construction of new system components is prohibited. A data-set presented by the [European Environment Agency \(2022\)](#) is used for the Natura2000 areas. This data-set is adjusted to include only the Natura2000 areas which fall within the system demarcation (see [Figure 4.1](#)). In order for the [NOM](#) to be able to treat the Natura2000 areas as obstacles, the coordinates of the corners of the Natura2000 areas has been derived and exported to the [NOM](#). This is done in a simplified manner in order to reduce the amount of coordinates.

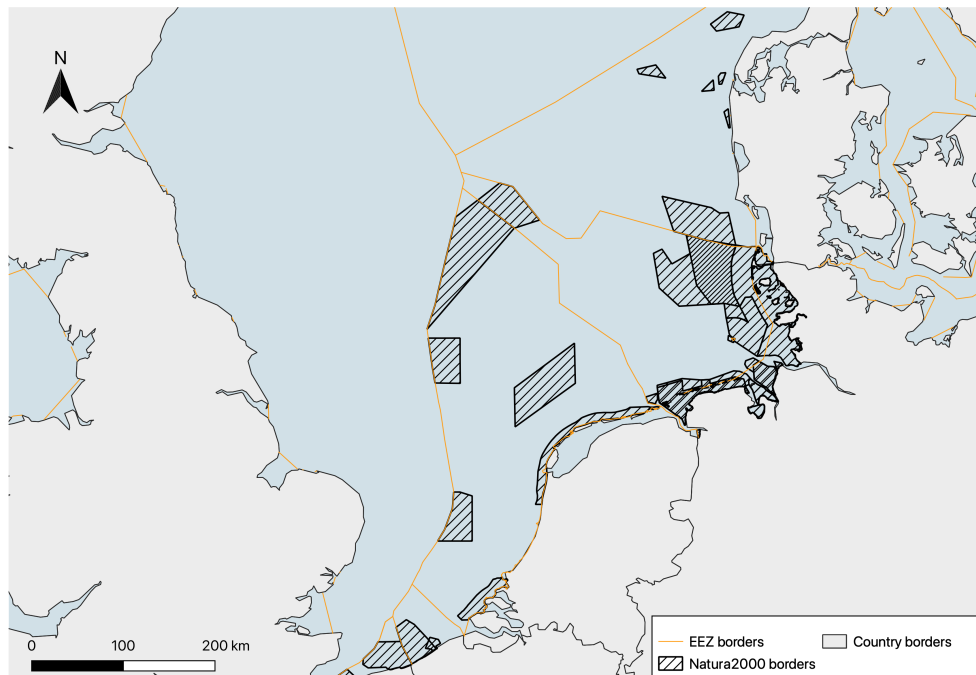


Figure 4.1: Map of the Natura2000 sites within the system of interest, derived from [European Environment Agency \(2022\)](#).

4.3 EXISTING TRANSMISSION INFRASTRUCTURE AND ONSHORE ENTRY POINTS

4.3.1 Existing Connections

In this thesis, it is assumed that all the offshore natural gas pipelines may be reused for hydrogen transport ([Assumption 7](#)). The existing natural gas infrastructure in the North Sea is derived from [EMODnet \(2022\)](#). Before using the data-set within the [NOM](#), the data-set is edited within Quantum Geographical Information System ([QGIS](#)) and by using the programming tool Python.

After importing the data-set into [QGIS](#), the pipelines outside this system demarcation are removed using the *intersect* tool of [QGIS](#). The intersect tool extracts overlapping portions of different layers, e.g. the pipelines within the presented system demarcation. Thereafter, the data-set is *filtered* on gas pipelines. Next, the data-set is *simplified*. As, for example, a bend in a pipeline is actually represented by a very large amount of edges. By simplifying, [QGIS](#) recreates the same layer and input features; however, the layer contains a lower number of edges. Simplification results in straighter pipelines and a lower number of total edges, which reduces the calculation time of the [NOM](#). Hereafter, the pipelines are *exploded*. By exploding the pipelines, each pipeline is treated as a line with only a start and an end point, and no intermediary points in between. Thereafter, all the pipelines which have a start or an end point within a Natura2000 area are removed. This must be done as the [NOM](#) treats Natura2000 areas as obstacles¹. And finally, the pipeline data-set is exported to a CSV-file in order for Python to be able to read it.

The new pipeline data-set is presented in [Figure 4.2](#).

¹ As a reminder: Within the [NOM](#), the existing connections may only cross obstacles, and may not start or end within the defined obstacles.

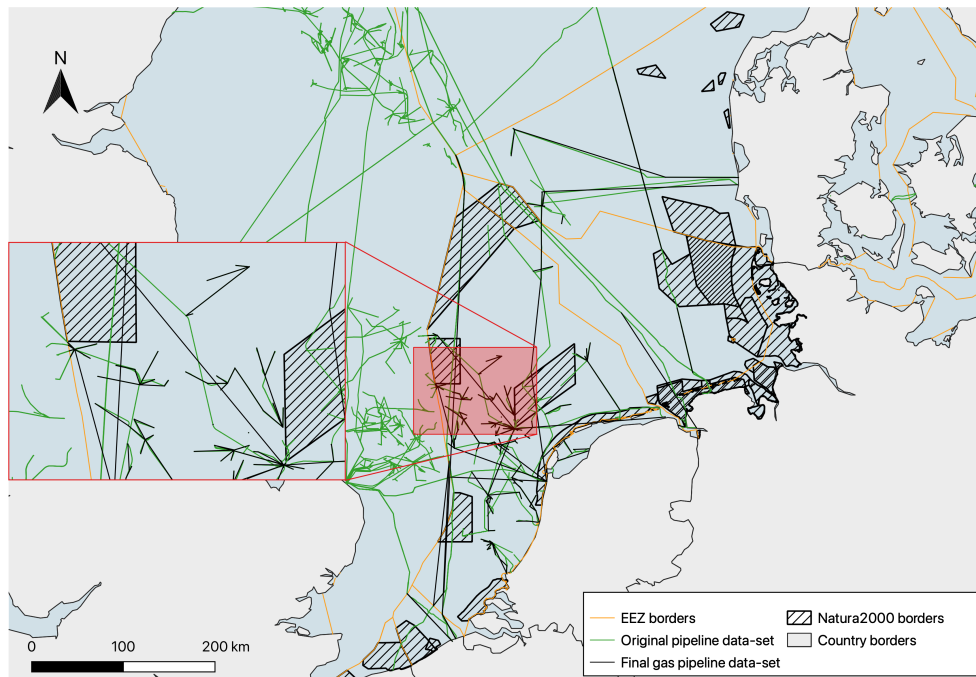


Figure 4.2: Changes between the starting and final data-set of the pipelines.

As the file might contain errors and can not directly be used within the [NOM](#), the file needs to be cleaned and adjusted by using the pseudo-code presented in [Algorithm 4.1](#). First, the data-set is filtered and cleaned such that only the desired gas pipelines are taken into account. Thereafter, the pipelines are grouped according to their own characteristics, and adjusted such that they can be saved within the needed text-file of the [NOM](#). Here, the undefined variable X represents a pipeline diameter. Pipelines with a smaller diameter than X are not incorporated within the [NOM](#). The main reason for this is to reduce the calculation time of the [NOM](#). Within this thesis, the value is set at 6 *in*. The total costs of the system only increases marginally when only using pipelines with this value, but the calculation time decreases exponentially.

Algorithm 4.1: Existing connections input derivation

Input: pipelines.csv**Output:** existing_connections.txt

```

1 for pipelines.csv do
2   remove pipelines with "ID" = "NULL"
3   remove pipelines with "diameter" = "NULL"
4   remove pipelines with "diameter" < X
5   remove duplicate pipelines
6 let xxs be a X-coordinate (x, x1) dataframe of a pipeline grouped by
   "Length", "ID", "Angle", "Diameter"
7 let xyys be a Y-coordinate (y, y1) dataframe of a pipeline grouped by
   "Length", "ID", "Angle", "Diameter"
8 let ec be a dataframe with the "X" and "Y" coordinates and the
   "Diameter" of the pipeline
9 for ec do
10  remove NAN data
11  assign corresponding capacity pipeline based on "diameter"
12  rearrange as "x,y,x1,y1,capacity"
13  rearrange as "(x,y) \tab (x1,y1) \tab capacity"
14  save as existing_connections.txt

```

4.3.2 Onshore Entry Points

The onshore entry points (sinks) are based on the existing gas infrastructure. These points are chosen as they most-likely already have gas treatment facilities, and are located near industrial clusters which are assumed to have significant hydrogen demand in the future ([Assumption 8](#)). In [Figure 4.3](#), an overview is given of the different onshore entry points. One entry point has not been incorporated; this entry point is marked with a "*". The reason for doing so is as the pipelines corresponding to that entry point, only transport gas between two of the Wadden Islands and the shore.

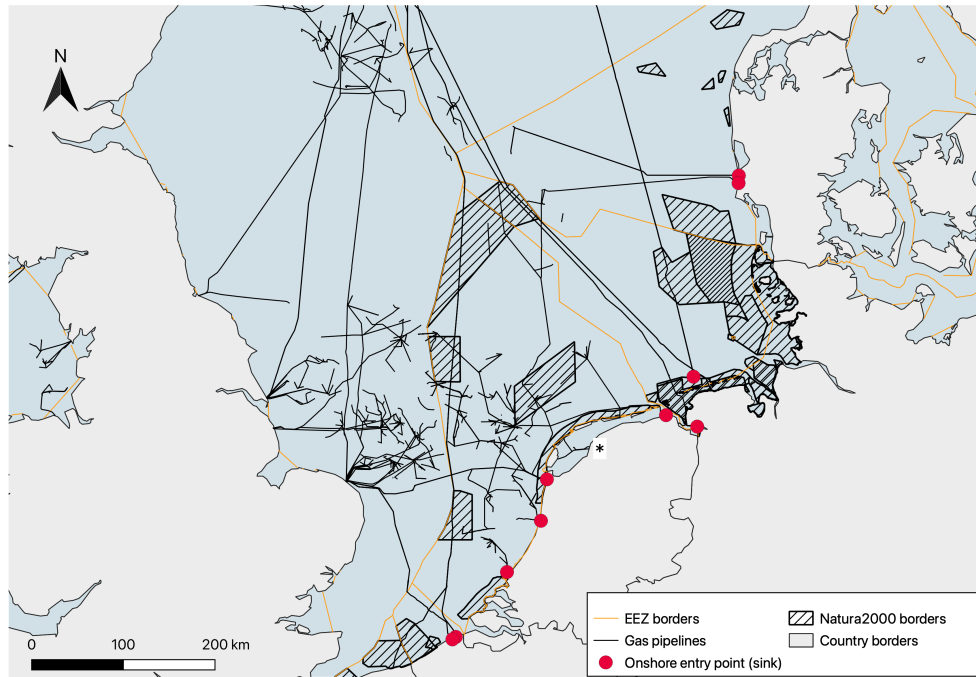


Figure 4.3: Sinks with the associated gas pipelines. The entry point with a "*" is not taken into account as it only transports gas over the Wadden Sea.

4.4 TECHNO-ECONOMIC DATA

In [Table 4.1](#), an overview is presented of the main techno-economic data used within this study. Techno-economic parameters that are left out of the scope, are re-compression stations and additional converters. This is done as the [NOM](#) does not consider these possibilities. Additionally, there exists the possibility to split a pipeline into two (or more) new pipelines; however, after consultation with industry experts by [Brosschot \(2022\)](#), the decision is made that no additional costs are acquainted with splitting a pipeline. For a more elaborate and inclusive explanation of the parameters, see [Appendix C](#).

In [Table 4.2](#) the renewable energy potential of each country is presented, as defined by [Wang et al. \(2021\)](#).

Table 4.1: Main techno-economic data used in this thesis.

Component	Parameter	Value	Unit	Source(s)
Electrolyser	Operational life	20	years	(IRENA, 2020)
	CapEx	600	EUR/kW	(Danish Energy Agency, 2021) (NSE et al., 2020)
	OpEx	4	% of the CapEx	(IRENA, 2020)
	Output pressure	30	bar	(Danish Energy Agency, 2021) (NSE et al., 2020)
	Efficiency	71;76;80 ²	%	(Wang et al., 2020)

² For 2030, 2040, and 2050 respectively.

Desalination plant				
Operational life	30	years		(WRADC, 2011)
CapEx	1883,7		EUR/MW _e	(Nayar et al., 2016)
OpEx	0	-		(NSE et al., 2020)
Compressor				
Operational life	20	years		(EPA, 2006)
CapEx	2665,04		EUR·W ³	(González Díez et al., 2020)
OpEx	8		%	(NSE et al., 2020)
Pipelines				
Operational life	40	years		(Chis, 2015)
CapEx (new)	121.000		EUR/in – km	(Procainsa SA, 2016)
CapEx (refurbished)	10		% of the CapEx of new	(ICF International, 2014)
OpEx	7		% of the CapEx	(Miao et al., 2021)
Operating pressure	80	bar		(Wang et al., 2020)
Flow speed	20	m/s		(CEER, 2019)
(self-study)				(Staurland & Aamodt, 2004)
Wind farm				
Operational life	25	years		(González Díez et al., 2020)
CapEx	2000		EUR/kW	(Topham et al., 2019)
CapEx H ₂ -in-Turbine wind farms	89 ⁴		% of the CapEx	(Sens et al., 2022)
OpEx	118		EUR/kW/yr	(Lacal-Aránegui et al., 2018)
Capacity factor	48,7 ⁵		%	(Stehly et al., 2020)
Distance between turbines	965	m		(Stehly et al., 2020)
				(Grady et al., 2005)
				(self-study)
Other				
Discount rate	8	%		(International Energy Agency, 2021)
Decommissioning costs offshore structures	4 ⁶		% of the CapEx	(Topham & McMillan, 2017; Kaiser & Snyder, 2012)
Temperature North Sea (water)	10	°C		(MacKenzie & Schiedek, 2007)

³ For the calculations of \dot{W} , see [Appendix C](#).

⁴ There is a lower price for the H₂-in-Turbine wind farms due to lower Balance Of System (BOS) costs (i.e. no array cables). The stated CapEx does not include the costs of the electrolyser, desalination unit, or compressor.

⁵ This is only used for the H₂-in-Turbine wind farms.

⁶ This number only reflects offshore wind farms. However, due to a lack of literature describing all decommissioning costs of offshore energy systems, this value is used for all system components.

Table 4.2: Renewable energy levels per country in GW (Wang et al., 2021).

Country	2030				2040				2050			
	PV ground	PV offshore	Wind onshore	Wind offshore	PV ground	PV offshore	Wind onshore	Wind offshore	PV ground	PV offshore	Wind onshore	Wind offshore
Belgium	10	7	4	3	10	14	4	4	10	22	4	5
Denmark	11	6	10	8	18	8	10	21	25	11	11	28
Germany	98	69	20	15	98	110	20	21	98	153	20	28
Netherlands	27	10	12	10	27	20	12	36	27	31	12	48

Finally, for the economic assessment, an electricity price is needed for the calculation of the **LCOH** and **NPV**. A price of 8,33 *EUR/MWh* is assumed for 2030, 2040, 2050 (**Assumption 9**). This is roughly the consistent minimum value of the estimated electricity price for 2030 to 2050, as can be seen in **Figure 4.4**. The reasoning for not taking an electricity price of 0 *EUR/MWh* — which would theoretically be the case when using surplus wind energy — is because within this thesis, must-run plants are also considered to calculate the electricity potential for the electricity-driven operational mode. I.e. the marginal costs of the must-run plants fluctuate between 2 and 20 *EUR/MWh*, and are thus considered to be the 5th percentile mark in **Figure 4.4**. For the hydrogen-driven operational mode, the H₂-in-Turbines do not have any electricity prices, as the H₂-in-Turbines are considered to be a part of the hydrogen generation system. However, there do exist electricity prices for compressor stations. These prices are the medians for 2030, 2040, and 2050, as presented in **Figure 4.4**.

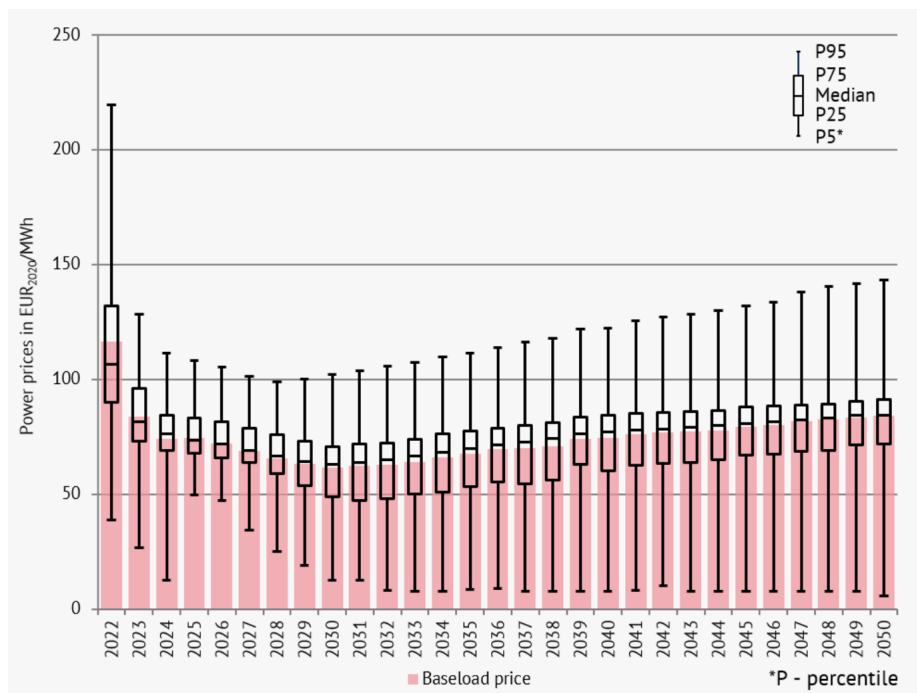


Figure 4.4: Estimation of the electricity prices in the EU over the upcoming years (Schmitt, 2022).

5 | RESULTS

In this chapter, the results of the conducted research are presented. In [Section 5.1](#), research question “*What are the locations of the new wind farms and of the electrolyzers?*” is answered. Thereafter, in [Section 5.2](#), research question “*What is the maximum amount of electricity which can be used to produce hydrogen?*” is answered. Based on the results of the electrolyser locations and the electricity potential, the last two research questions “*What is the optimal infrastructure for the transmission of hydrogen to shore?*” and “*How do the costs relate to the expected benefits of the different system designs?*” are answered in [Section 5.3](#). And finally, in [Section 5.4](#), a sensitivity analysis is performed.

5.1 ELECTROLYSER LOCATIONS

The build-up of the electrolyser locations phasing over 2030, 2040, and 2050, is shown in [Figure 5.1](#). Within the figure, the electrolyser hubs as well as the compressor stations (of the H₂-in-Turbine wind farms) are indicated as nodes (points). The nodes which are marked by a green circle are the compressor stations. As previously stated in the methodology ([Chapter 3](#)), a cost-parity point is used to determine a distance-threshold after which dedicated H₂-in-Turbine wind farms are placed. The resulting threshold is 122,2 km, signifying that after 122,2 km, transmission of energy by pipeline is economically more feasible than by cable (for a transmission capacity of 1 GW).

It can clearly be seen that the network builds itself outwards from shore during the time periods. Although, there are a few exceptions. The exceptions are due to two different reasons:

1. existing wind farms are already positioned further offshore; and,
2. the data-set of [EMODnet \(2021\)](#) did not include enough locations. This resulted in a later use of extra wind farm locations out of the data-set of [4C Offshore \(n.d.\)](#).

A detailed overview of all the wind farms connected to the different electrolyser hubs can be found in [Appendix D](#).

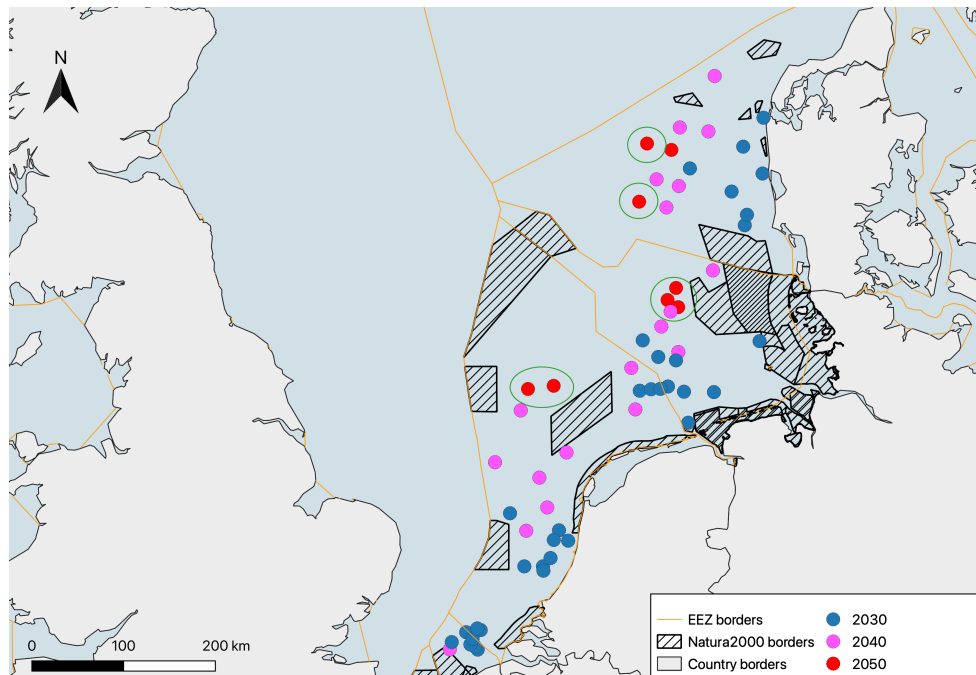


Figure 5.1: Build-up electrolyser hubs and compressor stations for 2030, 2040, to 2050. The nodes which are marked by a green circle are the compressor stations of the H₂-in-Turbine wind farms.

5.2 MAXIMUM ELECTRICITY POTENTIAL FOR HYDROGEN PRODUCTION

5.2.1 Electricity Supply Potential for Hydrogen 2030

The electricity supply potential to produce hydrogen in 2030 within the EEZ of Belgium in the North Sea is depicted in [Figure 5.2a](#); for Germany, in [Figure 5.2b](#); for Denmark, in [Figure 5.2c](#); and for the Netherlands, in [Figure 5.2d](#). Additionally, in [Table 5.1](#), the electricity potential *GWh/yr* is numerically shown.

In 2030, no wind farms are hydrogen-driven, all the wind farms are electricity-driven.

Table 5.1: Electricity potential to produce hydrogen under the electricity-driven operational mode per country in 2030.

	Belgium	Denmark	Germany	Netherlands
Electricity potential in <i>GWh</i>	408	5.552	4.397	10.803

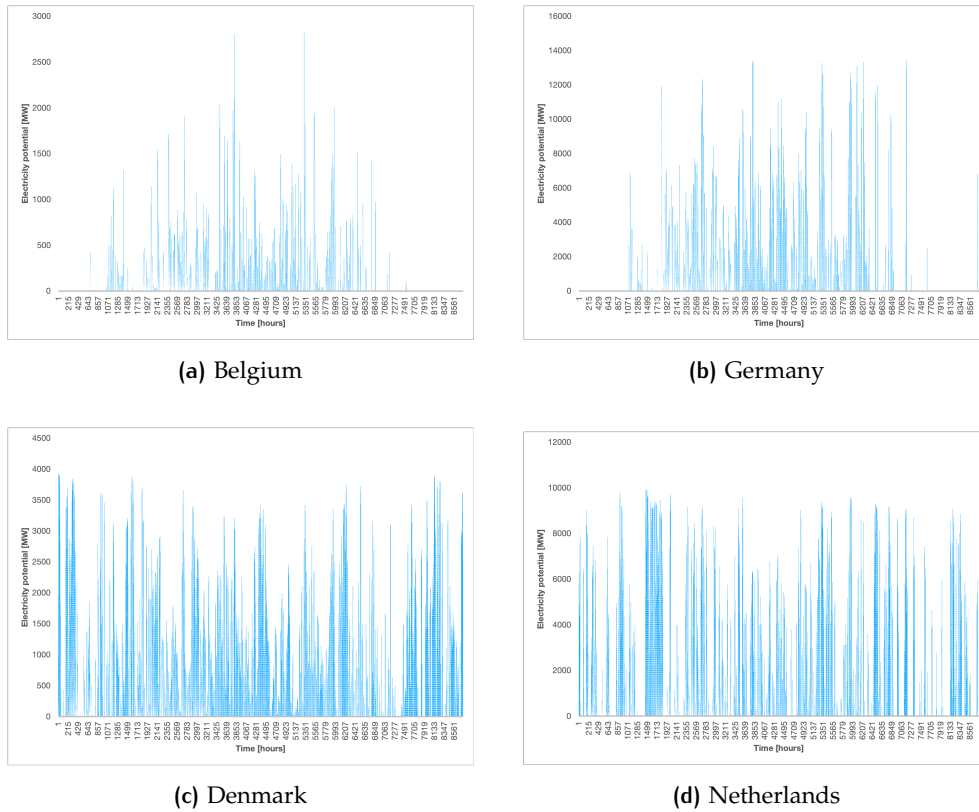


Figure 5.2: Electricity potential for the electricity-driven operational mode derived by the [ETM](#) and the [EMOM](#) for 2030.

5.2.2 Electricity Supply Potential for Hydrogen 2040

The electricity supply potential to produce hydrogen in 2040 with the electricity-driven wind farms within the [EEZ](#) of Belgium in the North Sea is depicted in [Figure 5.3a](#); for Germany, in [Figure 5.3b](#); for Denmark, in [Figure 5.3c](#); and for the Netherlands, in [Figure 5.3d](#). Additionally, in [Table 5.2](#), the electricity potential which can be used for hydrogen production under the electricity-driven operational mode is shown.

In 2040, only Germany has also hydrogen-driven wind farms. These wind farms offer 11.273 *GWh/yr* of electricity for hydrogen production.

Table 5.2: Electricity potential to produce hydrogen under the electricity-driven operational mode per country in 2040.

	Belgium	Denmark	Germany	Netherlands
Electricity potential in <i>GWh</i>	808	32.474	7.071	80.604

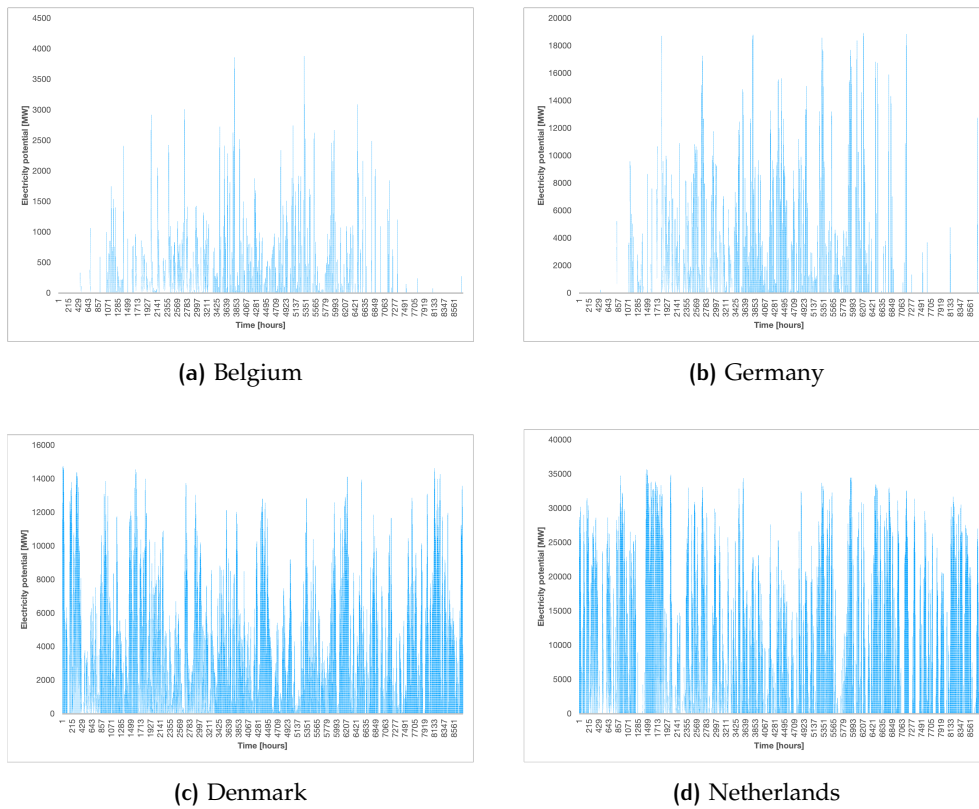


Figure 5.3: Results of the electricity potential for the electricity-driven operational mode derived by the *ETM* and the *EMOM* for 2040.

5.2.3 Electricity Supply Potential for Hydrogen 2050

The electricity supply potential to produce hydrogen in 2050 with the electricity-driven wind farms within the *EEZ* of Belgium in the North Sea is depicted in [Figure 5.4a](#); for Germany, in [Figure 5.4b](#); for Denmark, in [Figure 5.4c](#); and for the Netherlands, in [Figure 5.4d](#). Additionally, in [Table 5.3](#), the electricity potential which can be used for hydrogen production under the electricity-driven operational mode is shown.

In 2050, Denmark, Germany, and the Netherlands all have also H_2 -in-Turbine wind farms. These wind farms offer 96,6 *TWh/yr* of electricity for hydrogen production.

Table 5.3: Electricity potential to produce hydrogen under the electricity-driven operational mode per country in 2050.

	Belgium	Denmark	Germany	Netherlands
Electricity potential in <i>GWh</i>	1.228	36.880	10.266	84.333

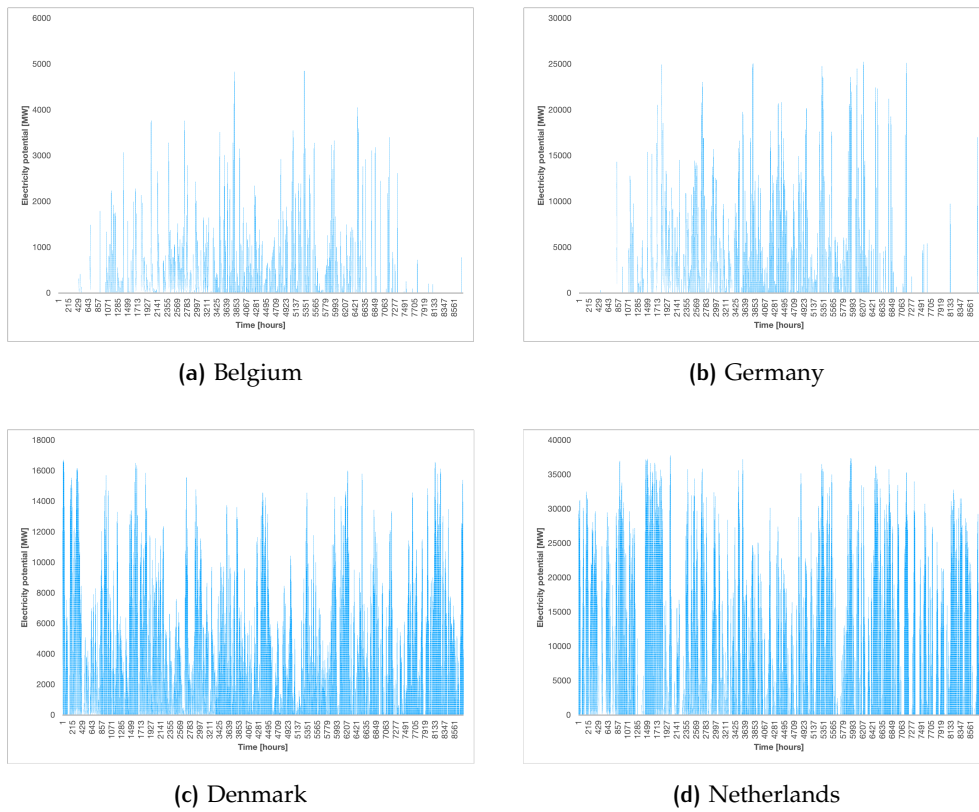


Figure 5.4: Electricity potential for the electricity-driven operational mode derived by the [ETM](#) and the [EMOM](#) for 2050.

5.3 NETWORK AND ECONOMIC ASSESSMENT

5.3.1 Scenario 2030 (A30B1 and A30B2)

The optimal network lay-outs derived using the [NOM](#) for the 2030 scenarios are shown in [Figure 5.5](#) and [Figure 5.6](#) for the interconnected and isolated designs respectively. The difference between the two system designs reflects on the possibility of cross-border interconnections between the [EU](#) countries. This can be seen in the south-west of the system; a pipeline crosses the [EEZ](#) border between Belgium and the Netherlands within the interconnected design ([Figure 5.5](#)). This is not the case within the isolated design ([Figure 5.6](#)). As a consequence, the hydrogen transport to the the most southern sink of the Netherlands decreases, and increases to Belgium in the interconnected design. The same applies to the north of the Netherlands and Germany. However here, the most northern sink of the Netherlands is not used within the interconnected system design.

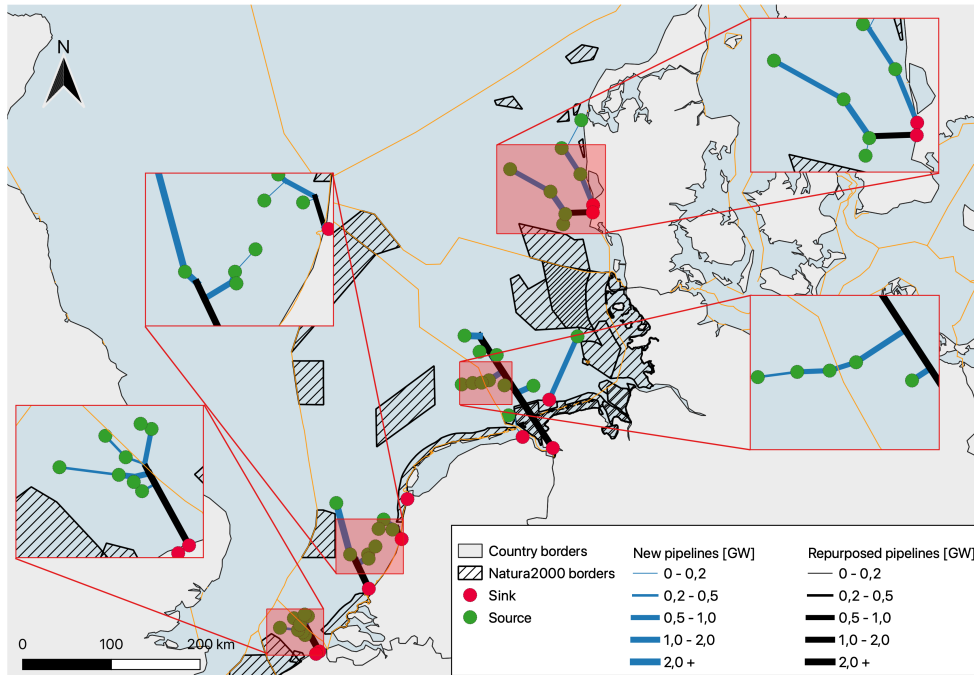


Figure 5.5: Network optimisation in 2030 for scenario A30B1 (interconnected).

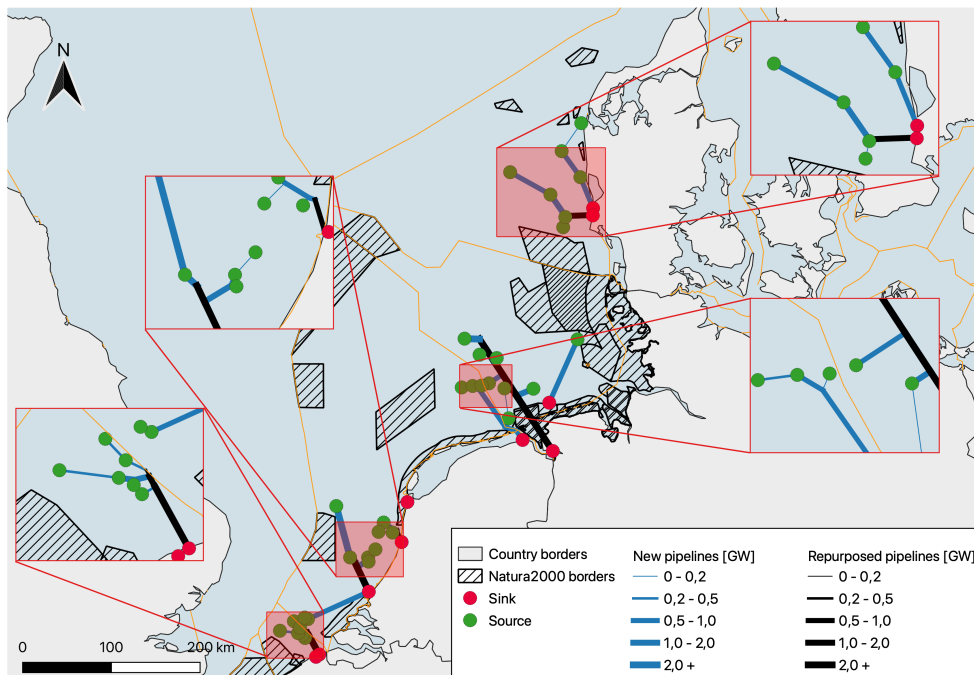


Figure 5.6: Network optimisation in 2030 for scenario A30B2 (isolated).

As expected, the case where the EU countries may cross borders has a lower infrastructure CapEx compared to the case where the EU countries act separately: the transmission infrastructure costs are 703 MEUR and 926 MEUR respectively. Although this might sound significant, when comparing the CapEx of the hydrogen systems as a whole (which includes the

pipelines, electrolysers, desalination plants, and compressors¹), this is relatively insignificant. The total CapEx of the interconnected case is 18.976 MEUR, and of the isolated case 19.199 MEUR. This small difference can also be seen when one calculates the LCOH of the system, as shown in Table 5.4.

Table 5.4: Economic analyses regarding the LCOH for scenarios A30B1 (interconnected) and A30B2 (isolated).

Scenario/Variable	CapEx MEUR	OpEx MEUR/yr	Fuel costs MEUR/yr	Lifetime years
A30B1	18.976	789	176	21
A30B2	19.199	804	176	21
	Produced H ₂ TWh/yr	Produced H ₂ kt/yr	LCOH EUR/MWh	LCOH EUR/kg
A30B1	15	451	208,66	6,95
A30B2	15	451	214,08	7,13

The analyses present two quite similar LCOH values 6,95 EUR/kg and 7,13 EUR/kg for scenario A30B1 (interconnected) and A30B2 (isolated) respectively. However, these values are not cost competitive when compared to grey² hydrogen, nor when compared to green hydrogen as produced in 2020, as can be seen in Figure 5.7. The relatively high LCOH values can be explained by analysing and comparing the electrolyser capacities and the electricity potential for the electricity-driven wind farms.

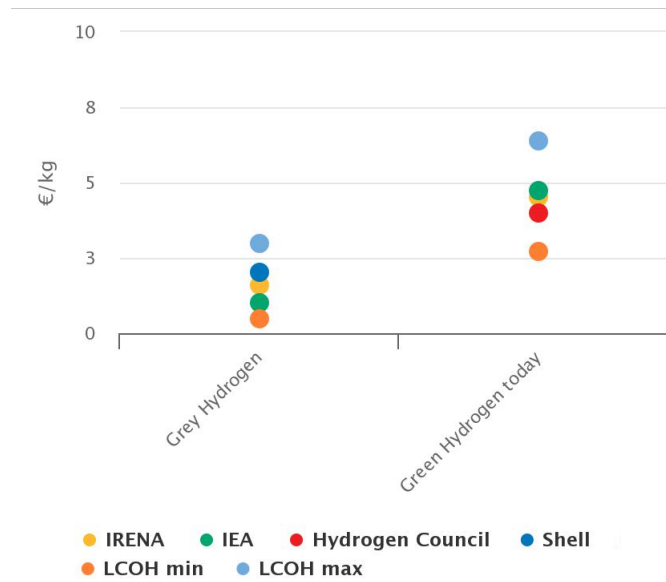


Figure 5.7: LCOH values evaluated of different organisations for 2020 (Braun & Hesel, 2020).

- 1 The costs of the offshore wind farms are not considered as they are treated as sunk costs for the production of hydrogen.
- 2 Hydrogen produced using fossil fuels (Hermesmann & Müller, 2022).

Figure 5.8 shows the box plot and the probability density function of the overall electricity potential for the electricity-driven electrolyzers in 2030. The electrolyser capacity of a hub is valued at the maximum surplus of wind farm(s) to which the electrolyser is connected to maximize the hydrogen output. However, as the results indicate, from an economic point of view this results in an over-investment. As can be deduced from Figure 5.8, the electricity potential in the North Sea rarely reaches the peak values and is mostly faced towards the lower end of the distribution of the electricity potential. This lowers the capacity factor of the electrolyser and consequently increasing the LCOH (Breeze, 2021).

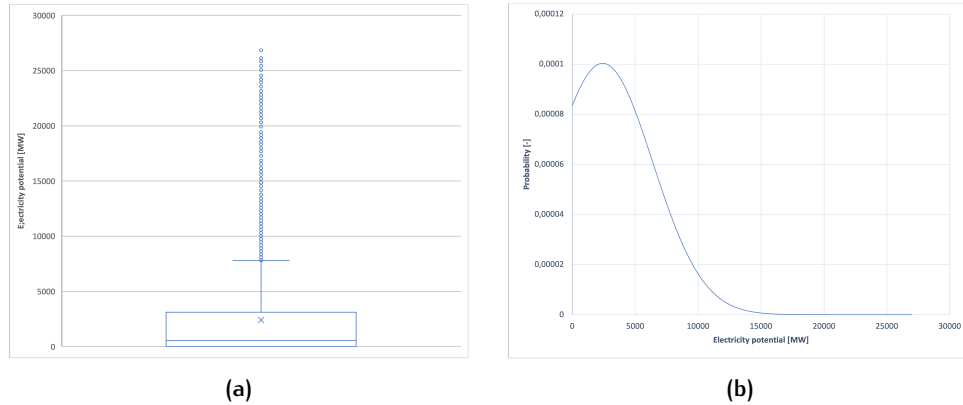


Figure 5.8: box plot (a) and the probability density function (b) of the electricity potential for the electricity-driven electrolyzers in 2030.

5.3.2 Scenario 2040 (A40B1 and A40B2)

The designs constructed by the NOM for 2040 are shown in Figure 5.9 and Figure 5.10 for the interconnected and isolated cases respectively. Once again the CapEx of the hydrogen infrastructure is lower for the interconnected case when compared to the isolated case with a transmission infrastructure CapEx of 1.195 MEUR and 1.359 MEUR respectively. A new system component which emerges in 2040 is the H₂-in-Turbine wind farm (thus the hydrogen-driven operational mode). Figure 5.11 shows a depiction of the two H₂-in-Turbine wind farms in Germany. The connections between the turbines and the H₂-in-Turbine source (i.e. the compressor station) are generated by the NOM. From the compressor station, the generated hydrogen will enter the rest of the system.

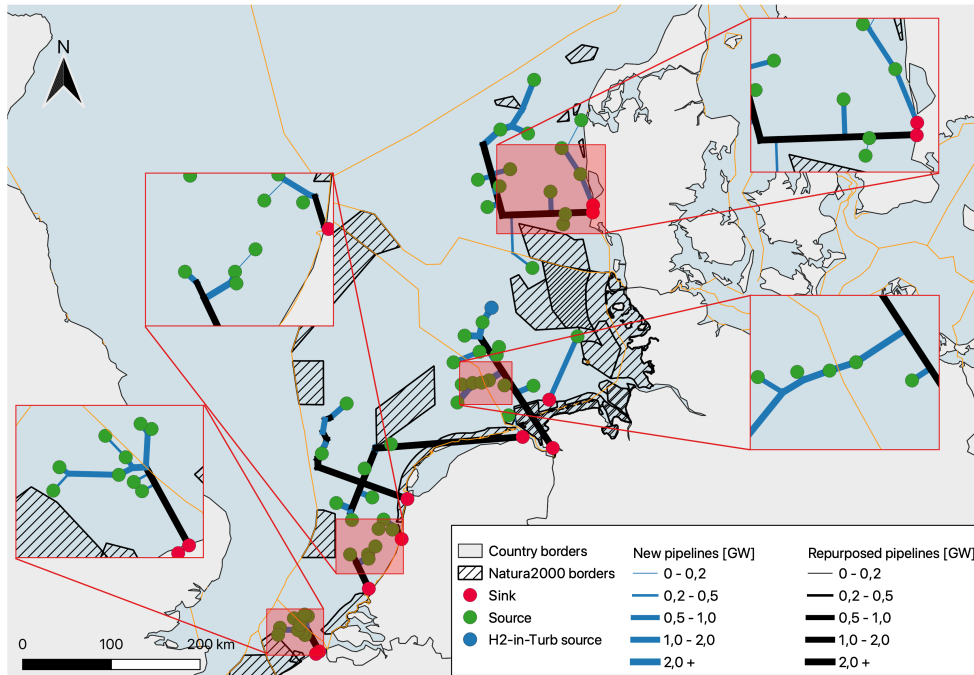


Figure 5.9: Network optimisation in 2040 for scenario A40B1 (interconnected).

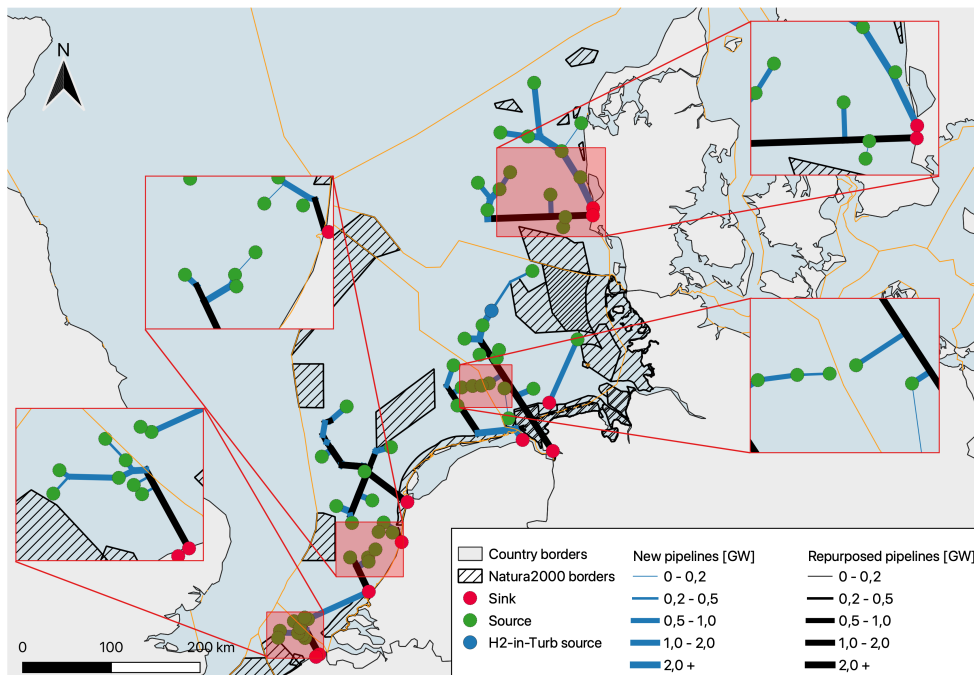


Figure 5.10: Network optimisation in 2040 for scenario A40B2 (isolated).

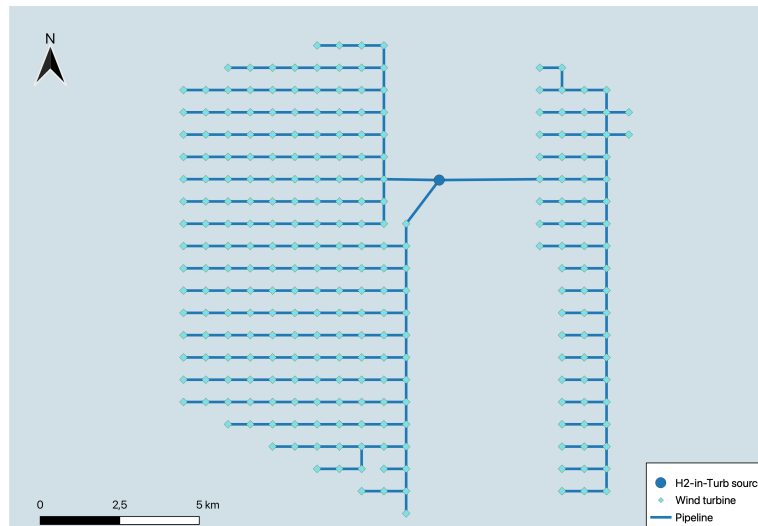


Figure 5.11: The H₂-in-Turbine wind farm lay-out in Germany 2040.

Table 5.5 present the results of the economic analyses regarding the LCOH of scenario A₄₀B₁ and A₄₀B₂ (i.e. the interconnected and isolated scenarios for 2040). As can be noted when comparing scenarios A₃₀ and A₄₀ with one another, the LCOH is reduced during the transition towards 2040. The new values of the LCOH almost reach cost competitive levels. Once again, this can be reflected back on the distribution of the surplus levels which are the input of the electricity generation for the electricity-driven electrolyzers. Figure 5.12 presents the box plot and the probability density function of the A₄₀ scenarios. When comparing this to A₃₀, it can be seen that the box plot shifts upwards, and the probability density function shifts to the right, insinuating a higher capacity factor of the electrolyzers. This is because a higher level of hydrogen generation is more often reached using the installed electrolyzers. Consequently, this results in a lower value for the LCOH. The shift in the increase of the overall electricity potential is caused by the steep increase in renewable energy source penetration and by the relative low increase in the overall electricity demand compared to 2030. This results in higher and more constant levels of electricity potential for the electricity-driven electrolyzers.

Table 5.5: Economic analyses regarding the LCOH for scenarios A₄₀B₁ (interconnected) and A₄₀B₂ (isolated).

Scenario/Variable	CapEx <i>MEUR</i>	OpEx <i>MEUR/yr</i>	Fuel costs <i>MEUR/yr</i>	Lifetime years
A ₄₀ B ₁	50.741	2.210	1.008	21
A ₄₀ B ₂	50.905	2.222	1.008	21
	Produced H ₂ <i>TWh/yr</i>	Produced H ₂ <i>kt/yr</i>	LCOH <i>EUR/MWh</i>	LCOH <i>EUR/kg</i>
A ₄₀ B ₁	100	3.011	89,88	2,99
A ₄₀ B ₂	100	3.011	90,18	3,00

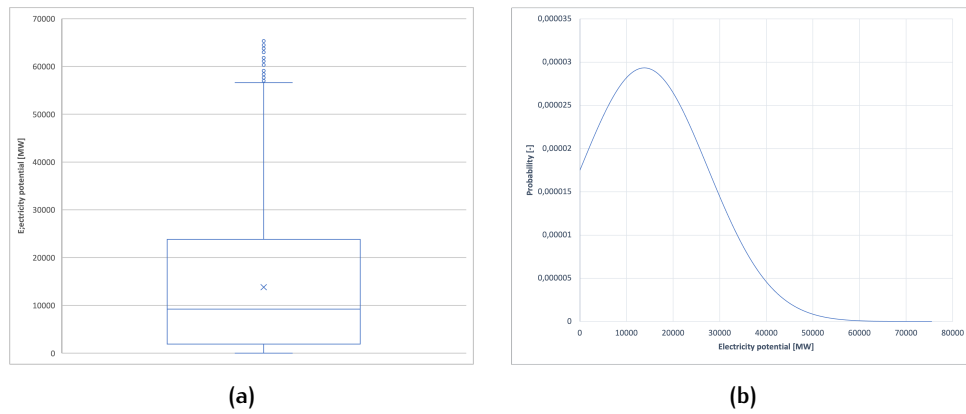


Figure 5.12: box plot (a) and the probability density function (b) of the electricity potential for the electricity-driven electrolyzers in 2040.

5.3.3 Scenario 2050 (A50B1 and A50B2)

The final scenarios reflect on 2050. The visual results of the **NOM** can be found in Figure 5.13 and Figure 5.14 for the interconnected and isolated cases respectively. Again, the interconnected case offers cheaper transmission infrastructure **CapEx** when compared to the isolated case in 2050 with a **CapEx** of 1.780 *MEUR* and 1.855 *MEUR* respectively. In 2050, these costs are remarkably insignificant when compared to the overall **CapEx** of both systems, which are 112.462 *MEUR* and 117.180 *MEUR* respectively. These high **CapEx** are mainly due to the installation of the new offshore H₂-in-Turbine wind farms, which account for more than one-third of the total **CapEx** with a **CapEx** of 40.303 *MEUR* in both cases.

Table 5.6: Economic analyses regarding the **LCOH** for scenarios A50B1 (interconnected) and A50B2 (isolated).

Scenario/Variable	CapEx <i>MEUR</i>	OpEx <i>MEUR/yr</i>	Fuel costs <i>MEUR/yr</i>	Lifetime years
A50B1	112.462	5.650	1.105	23
A50B2	112.538	5.655	1.105	23
	Produced H ₂ <i>TWh/yr</i>	Produced H ₂ <i>kt/yr</i>	LCOH <i>EUR/MWh</i>	LCOH <i>EUR/kg</i>
A50B1	183	5.504	105,78	3,52
A50B2	183	5.504	107,00	3,56

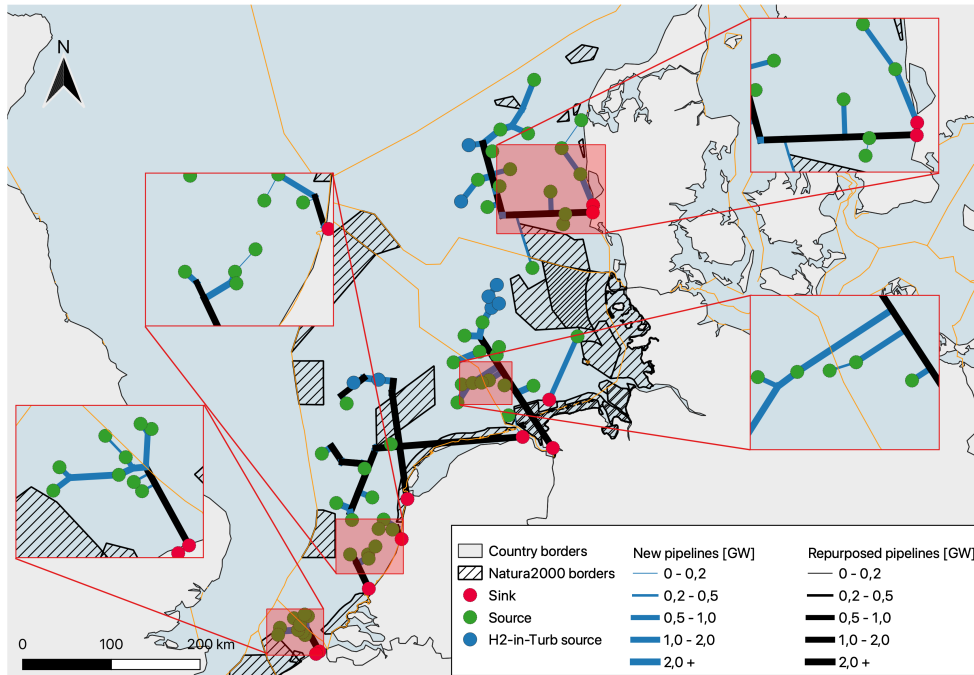


Figure 5.13: Network optimisation results visualisation in 2050 for scenario A50B1 (interconnected).

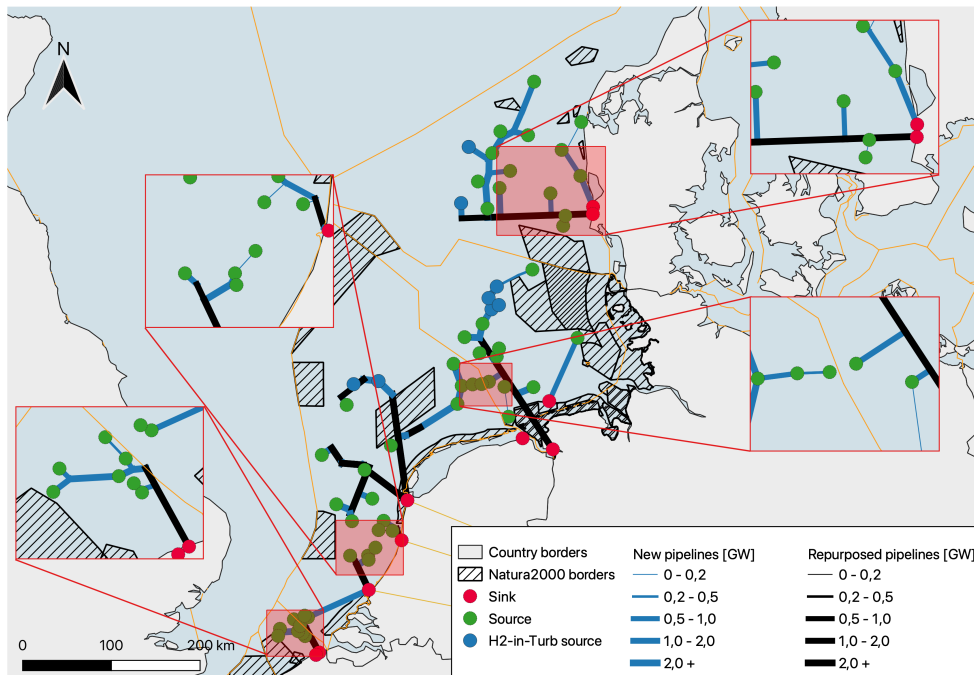


Figure 5.14: Network optimisation results visualisation in 2050 for scenario A50B2 (isolated).

The results for the **LCOH** are shown in [Table 5.6](#). A remarkable and counter intuitive result for 2050 is that the **LCOH** in 2050 for both cases increases when compared to 2040. This is most-likely due to the following reason: Once again, there is a shift within the electricity potential which can be used

by the electricity-driven electrolyzers. When comparing the box plots and probability density functions of 2050 (Figure 5.15) with 2040 (Figure 5.12), it can be deduced that a smaller proportion of the electricity potential in 2050 reaches above the median. This consequently results in a lower capacity factor of the electrolyzers and thus a higher LCOH.

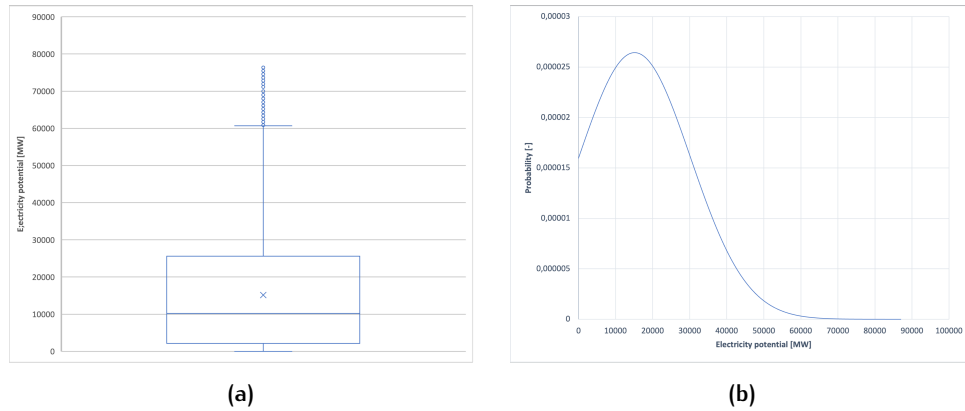


Figure 5.15: box plot (a) and the probability density function (b) of the electricity potential for the electricity-driven electrolyzers in 2050.

5.3.4 Analysis of the system as a whole (2030–2040–2050)

Another way is to analyse the system over the whole phasing period. Here, the system is build-up with the system infrastructure of 2050 as a 'starting point' (Figure 5.16 and 5.17). Therefore in the year 2030, a subset of the 2050 pipelines are built; namely the pipelines which are (also) used in 2030. Hence, for the year 2030, the pipelines used in 2050 to connect the sinks and sources used in 2030 are build, as is also the case for 2040 and 2050. As implied, the total pipeline infrastructure CapEx increases over time; and thus during the whole period, a distribution of operational and capital expenditures acquainted with the infrastructure are present. The same applies to the electrolyzers, desalination units, compressors, and H₂-in-turbine plants. Consequently, the electricity costs of the hydrogen system also increase during the analysed period.

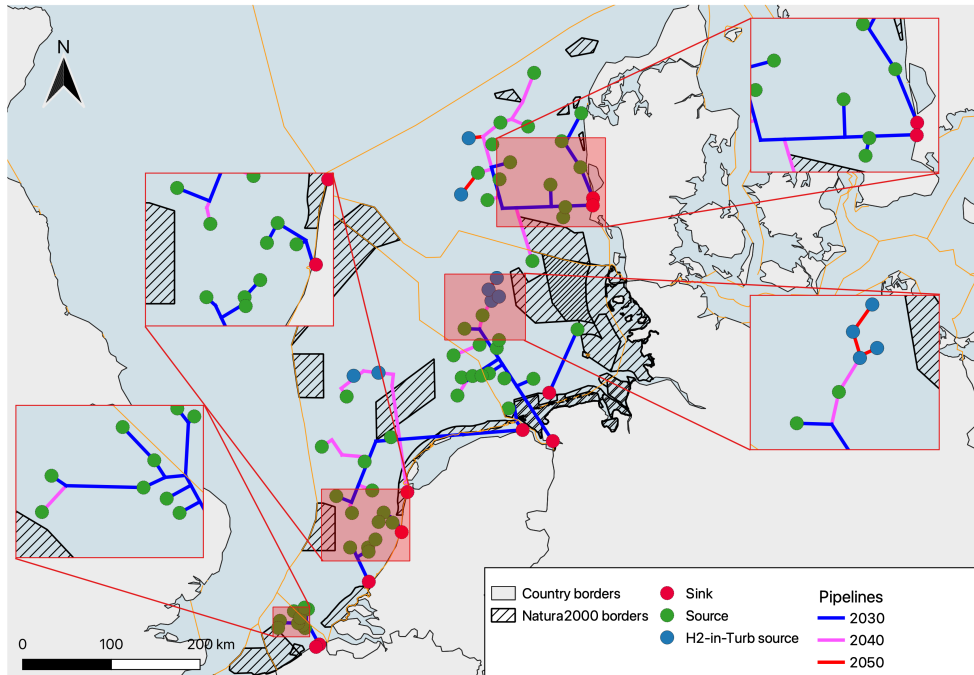


Figure 5.16: Network optimisation build-up of the interconnected case.

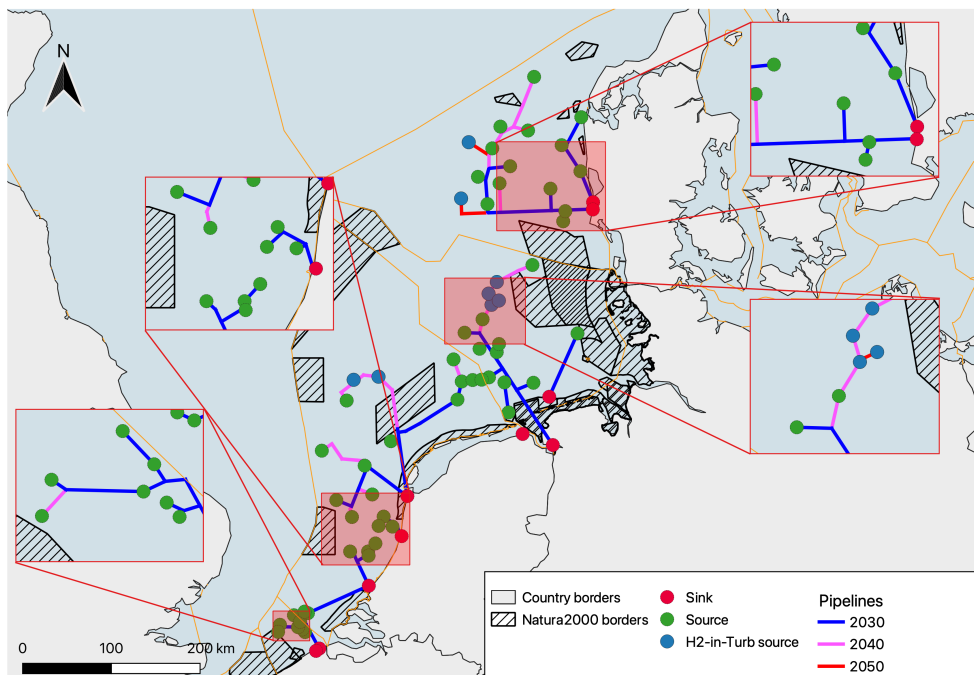


Figure 5.17: Network optimisation build-up of the isolated case.

Adjusting the System

The economic analyses of the hydrogen systems over the whole period result in a overall **LCOH** of 3,81 EUR/kg and 3,87 EUR/kg for the interconnected and isolated cases respectively. However, the results in [Section 5.3.1](#), [5.3.2](#), and [5.3.3](#) all indicate that the electrolyser capacity is an important factor

when designing an hydrogen system. A capacity based on the maximum surplus is most likely leading to higher **LCOH**. This is due to a lower capacity factor as a consequence of the high amount of electricity supply potential outliers present within the system. Optimising the **LCOH** whilst keeping the hydrogen infrastructure and H₂-in-Turbine wind farms constant, results in a lower total capacity of the electricity-driven electrolyzers. The new electrolyser capacities for 2030, 2040, and 2050 all lie within the median and the third quartile of the electricity potential for the electricity-driven electrolyzers. The new **LCOH** values for the hydrogen system decrease to 2,08 *EUR/kg* and 2,10 *EUR/kg* for the interconnected and isolated systems respectively whilst still reaching a total yearly production of 4,27 *TWh*, 67,70 *TWh*, and 141,67 *TWh* in the years 2030, 2040, and 2050 accordingly (Table 5.7). The newly presented **LCOH** values are cost-competitive compared to other researches focused on offshore hydrogen production. More specifically, they are relatively low (Figure 5.18).

Table 5.7: Economic analyses regarding the **LCOH** for adjusted systems over the entire phasing period.

*for 2030, 2040, and 2050.

Scenario/Variable	CapEx <i>MEUR</i>	OpEx* <i>MEUR/yr</i>	Fuel costs* <i>MEUR/yr</i>	Lifetime years
Interconnected (Adjusted)	66.253	95	50	43
		801	650	
		3194	670	
Isolated (Adjusted)	66.349	98	50	43
		809	650	
		3202	670	
	Produced H ₂ * <i>TWh/yr</i>	Produced H ₂ * <i>kt/yr</i>	LCOH <i>EUR/MWh</i>	LCOH <i>EUR/kg</i>
Interconnected (Adjusted)	4	128	62,61	2,08
	68	2.031		
	142	4.251		
Isolated (Adjusted)	4	128	62,92	2,10
	68	2.031		
	142	4.251		

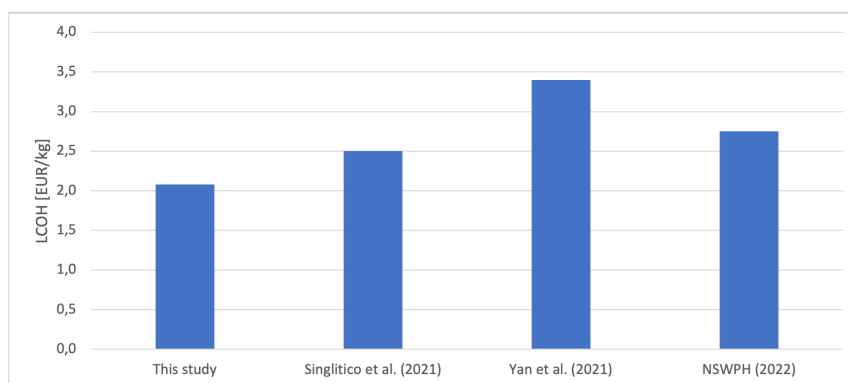


Figure 5.18: Comparison of different **LCOH** values.

Economic Assessment of the Adjusted System

With the new adjusted systems for the electricity potential, the NPV can be calculated to capture the value of the potential investments. The NPVs of both (interconnected and isolated) systems greatly depend on the future estimated prices of hydrogen. To calculate the NPV, different hydrogen prices are taken into account. As explained during the methodology (Section 3.5.2), the hydrogen prices are based on a set of five different scenarios. The different pricing scenarios are 1,66 EUR/kg (reference scenario), 2,15 EUR/kg (R&D advances + infrastructure), 2,24 EUR/kg (low NG resource/high NG price), 2,24 EUR/kg (aggressive electrolysis R&D), and 1,95 EUR/kg (lowest-cost electrolysis). The corresponding results of the NPV calculations for the two adjusted systems can be found in Table 5.8.

Table 5.8: Results of the NPV calculations for the adjusted systems of the interconnected and isolated system designs.

Scenario	NPV MEUR	NPV MEUR
	interconnected system	isolated system
Reference	-5.591	-5.824
R&D advances + infrastructure	1.266	1.034
Low NG resource/ high NG price	2.526	2.293
Aggressive electrolysis R&D	2.526	2.293
Lowest-cost electrolysis	-1.533	-1.765

As can be seen in Table 5.8, both system designs have the same negative and positive NPV scenarios. The negative scenarios are the reference (low natural gas price) and the lowest-cost electrolysis scenario; both being the least realistic scenarios. Developing the system under these scenarios indicate poor investment choices. The three more realistic scenarios all have positive NPVs. It can be noted that due to the recent geopolitical events between Russia and Ukraine, the third³ scenario seems to become the most realistic and thus also the most representative for the business case of the two system designs.

Effect on the Offshore Wind System

The hydrogen system also offers a positive secondary effect to the North Sea energy system. A steep increase in renewable energy source penetration, indirectly leads to a lower capacity factor of the offshore wind farms. This is because the electricity demand is met faster by the must-run and renewable plants. If no additional actions are taken, this results in more idle offshore wind farms, which consequently indicate over-investment in wind power capacity (Xuemei, 2013). The system designs proposed within this thesis offer

³ Here the natural gas market is adjusted by decreasing the natural gas availability but increasing the natural gas demand.

an option to mitigate this problem as the potential surplus is not unused but redirected to electrolyser hubs to generate hydrogen. The results show the percentual capacity factor increases (Table 5.9); especially for Denmark and the Netherlands, where the increase in renewable energy source penetration is relatively high compared to their yearly increasing electricity demand.

Table 5.9: Capacity factor increases of the offshore wind farm per country for the maximum hydrogen generation case and the adjusted case in 2030, 2040, 2050.

	Capacity factor increase (max.) %			Capacity factor increase (adj.) %		
	2030	2040	2050	2030	2040	2050
BEL	5,3	8,0	10,0	0,3	1,4	8,3
DEU	11,0	12,9	14,2	0,8	11,0	8,8
DNK	79,9	220,2	221,6	20,4	141,0	175,6
NLD	40,7	149,8	137,6	6,9	84,7	72,2

Concluding Remark

When comparing the two (adjusted) system designs, a (small) preference to the interconnected design can be expressed: This preference is based on the slightly higher NPVs. Although, both system designs offer good investment opportunities.

5.4 SENSITIVITY ANALYSIS

In this section, the sensitivity analysis is presented. A sensitivity analysis is performed to explore the robustness of the research done with the different models. The analysis is focused on parameters which are to such an extent uncertain, that they might influence the outcomes of the research fundamentally (Balaman, 2019). These parameters are changed by a certain percentage whilst the other parameters are kept constant. The changes are made in the cost-optimal system design (the adjusted interconnected design).

5.4.1 Parameter Overview

The changed parameters are divided into two categories: the costs and the technical parameters. Both categories are explained below.

Cost Parameters

The cost parameters are perturbed by assigning a multiplier of $\pm 25\%$, as is proposed by Singlitico et al. (2021). The following cost parameters are changed:

- Pipeline:

The costs of installing and maintaining offshore hydrogen transmission infrastructures are not well known. There are currently no large scale offshore hydrogen transmission projects planned, nor completed.

- **Electricity:**
Electricity price forecasting is a complex process subject to a large number of variables. Most rigorous approaches and data-sets are not made publicly available (Lago et al., 2021). This results in high uncertainties with respect to the used prices.
- **Compressor:**
Compressors are not uncommon within offshore transmission infrastructures. However, the costs of deploying compressors also depend on the costs of the support structure. Under [Assumption 1](#), it is stated that the electrolyser hubs (i.e. also the compressors) can be built on sub stations of the wind farms. However, if this is not the case, additional the cost of each compressor increases if additional support structures are needed.
- **Desalination:**
Using the same rationale as for the compressor, the costs of the desalination unit might also differ.
- **Electrolyser:**
The only offshore electrolyser project is currently PosHYdon (PosHYdon, 2021). However, the electrolyser capacity of this project is only 1 MW. Hence, the costs of deploying electrolysers on the proposed scale of this thesis is uncertain. Additionally, under [Assumption 1](#), the costs of the electrolyser might increase if the electrolyser can not be placed on the sub station.

Technical Parameters

The technical parameters are changed by assigning a multiplier of $\pm 10\%$. 10% is used instead of 25% as otherwise the changes would become unrealistically high or low. The following technical parameters are changed:

- **Electrolyser efficiency:**
There are discrepancies between estimated electrolyser efficiencies. This may be a result of not yet having deployed such large scale electrolysers. Additionally, it is uncertain what type of electrolysers may be used, which influences the efficiency.
- **Electrolyser lifetime:**
Not only does the lifetime of an electrolyser depend on the type of electrolyser (d'Amore Domenech et al., 2020). It is also relatively unknown as large scale electrolysers have not yet been deployed offshore. Therefore, the lifetime of the electrolyser is also taken into account within the analysis.

- Temperature:

The subsea temperature of the North Sea is not consistent throughout the entire sea. Additionally, the temperature of the North Sea is expected to increase over the coming years (Reidmiller et al., 2018; Schrum et al., 2016). Hence the subsea temperature is also incorporated within the sensitivity analysis.

- Pipeline pressure:

There are no regulations regarding the standards on transmission infrastructures of hydrogen (Cauchois et al., 2021; Andreasson & Roggenkamp, 2020). Hence, the used pipeline pressure is to some extent uncertain.

- Pipeline flow speed:

Similar to the pipeline pressure, there are no regulations or standards regarding the flow speed (Cauchois et al., 2021; Andreasson & Roggenkamp, 2020).

Additionally, the option to reuse the incumbent natural gas transmission infrastructure is also removed. This is because it is currently unknown if the transmission infrastructure may be repurposed in the near future.

5.4.2 Sensitivity Analysis Results

In Figure 5.19 and 5.20, the effects of changing parameters on the LCOH are shown. Moreover, in Table 5.10 and 5.11 the new NPVs are given.

Remarkably, the changing of five parameters influences negligently the LCOH of the system. These parameters are the costs of the compressor station, costs of the desalination unit, the temperature, and the pipeline pressure and flow speeds. The low effects of these changes indicate robust results.

However, the pipeline and electricity costs do have a (small) impact on the results. Additionally, if it is not possible to repurpose the existing gas infrastructure, the total CapEx of the offshore gas pipeline infrastructure increases with 36%. This results in an LCOH increase of 2,54%. In Figure 5.19 and 5.20, it is shown that changing the three elements does not result in additional negative NPVs. Although, the second NPV scenario is almost reaching zero for the analysed parameters. As a consequence, the robustness of the modelling results could be questioned.

Finally, different aspects of the electrolyser influences heavily the robustness of the results: The costs, lifetime, and efficiency of the electrolyser all have notable effects on the NPVs of the system. The increase of the costs as well as the decrease of the lifetime and efficiency all result in more negative NPVs for the presented hydrogen price scenarios. Especially the efficiency: The decrease in electrolyser efficiency results in negative NPVs for all pricing scenarios (Table 5.11). The new electrolyser efficiencies would be 64, 68 and 72% for 2030, 2040, and 2050 respectively. The new efficiencies are no unusual values. All these efficiencies are within the range of estimations of electrolyser efficiencies up to 2050 (IRENA, 2020).

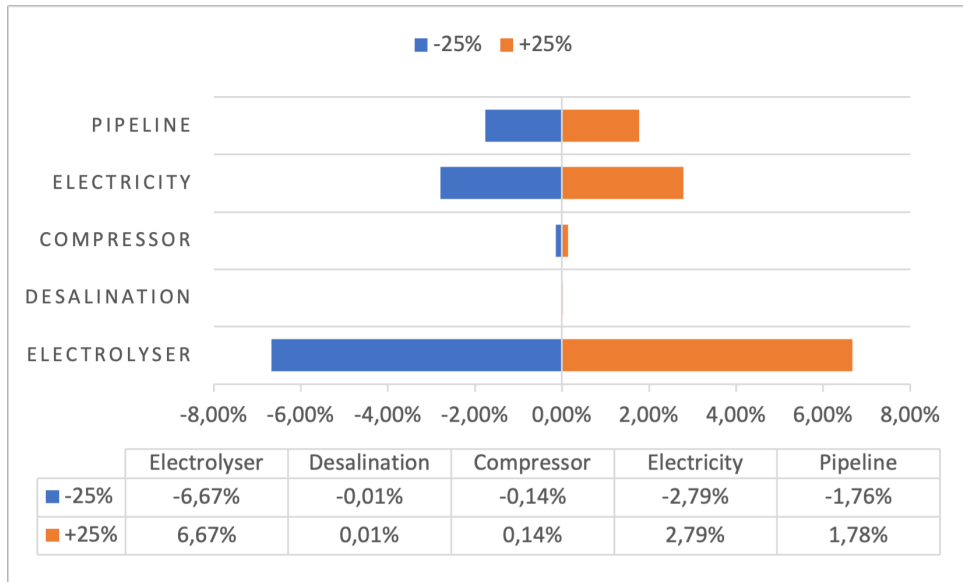


Figure 5.19: Sensitivity analysis results showing the percentual change of the LCOH by alternating the different cost values with ± 25%.

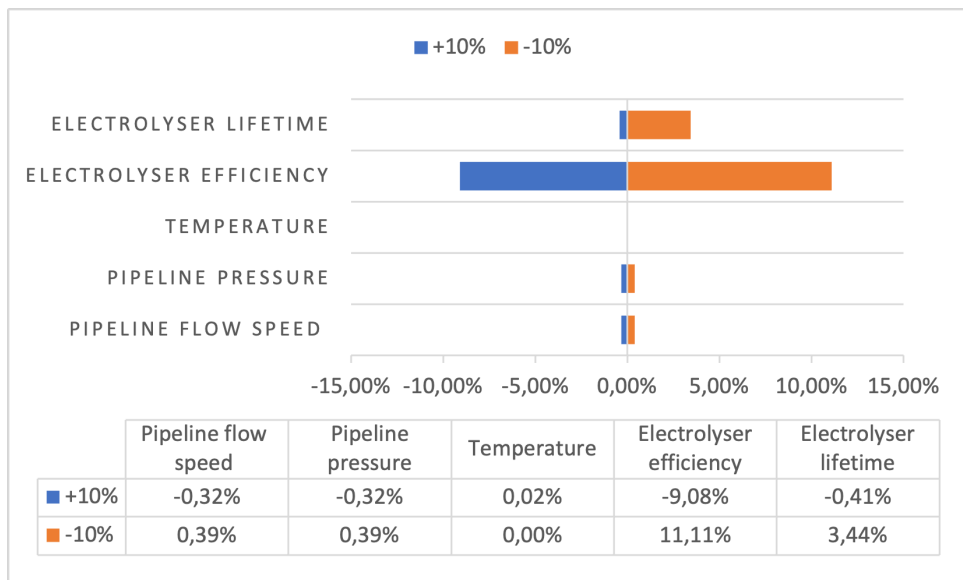


Figure 5.20: Sensitivity analysis results showing the percentual change of the LCOH by alternating the different parameter values with ± 10%.

Table 5.10: New NPVs in MEUR resulting from changing the costs of each component with $\pm 25\%$.

Scenario	Pipeline		Electricity		Compressor		Desalination		Electrolyser	
	+25%	-25%	+25%	-25%	+25%	-25%	+25%	-25%	+25%	-25%
Reference	-6.465	-5.434	-6.760	-5.133	-5.986	-5.907	-5.951	-5.942	-7.892	-4.001
R&D advances + infrastructure	393	1.423	97	1.724	871	950	907	915	-1.035	2.856
Low NG resource/ high NG price	1.652	2.682	1.356	2.984	2.131	2.210	2.166	2.174	225	4.116
Aggressive electrolysis R&D	1.652	2.682	1.356	2.984	2.131	2.210	2.166	2.174	225	4.116
Lowest-cost electrolysis	-2.406	-1376	-2.702	-1.074	-1.928	-1.849	-1.892	-1.884	-3.834	57

Table 5.11: New NPVs in MEUR resulting from changing parameter values with $\pm 10\%$ and removing the option to repurpose the existing natural gas transmission infrastructure.

Scenario	Electrolyser lifetime		Electrolyser efficiency		Temperature		Pipeline pressure		Pipeline flow speed		No reuse of pipeline
	+10%	-10%	+10%	-10%	+10%	-10%	+10%	-10%	+10%	-10%	
Reference	-5.828	-6.950	-3.627	-8.269	-5.953	-5.946	-5.854	-6.061	-5.854	-6.061	-6.687
R&D advances + infrastructure	1.029	-93	3.916	-2.097	904	911	1.004	796	1.004	796	170
Low NG resource/ high NG price	2.289	1.167	5.301	-963	2.164	2.171	2.263	2.056	2.263	2.056	1.429
Aggressive electrolysis R&D	2.289	1.167	5.301	-963	2.164	2.171	2.263	2.056	2.263	2.056	1.429
Lowest-cost electrolysis	-1.769	-2.892	837	-4.616	-1.895	-1.887	-1.795	-2.002	-1.795	-2.002	-2.629

6 | CONCLUSION

The objective of this thesis is to establish the feasibility of an offshore hydrogen system, powered by European Union (EU) wind farms in the North Sea. The analysis is done by a multi-sink multi-source approach. A phasing period from 2030, 2040, to 2050 is used to align with the EU investment plans in offshore wind energy.

6.1 FEASIBILITY

The results of the research indicate that a hydrogen system in the North Sea can offer vast investment opportunities with a cost-competitive Levelised Cost Of Hydrogen (LCOH). The proposed (interconnected) system design has a LCOH of 2,08 EUR/kg and a positive Net Present Value (NPV) for the most relevant pricing scenario's. This LCOH is relatively low compared to other researches, which mostly are between 2 and 3,5 EUR/kg. To reach a positive business case, it is important to correctly scale the electrolyzers. The economic assessment revealed that when using the maximum available electricity to scale the electrolyzers, the LCOH of the system increases. This is due to the highly fluctuating supply of electricity. When a lower capacity of the electrolyzers is used, a higher capacity factor of the electrolyzers is reached, decreasing the LCOH.

Both the isolated system design (with country specific electrolyzers and pipelines) and the interconnected system design (where electrolyzers and pipelines of each country may interact with each other) are feasible options. The calculated total costs of the interconnected system are (slightly) lower than those of the isolated design (respectively Capital Expenditures (CapEx)) of 66.253 MEUR and 66.349 MEUR.

The main uncertainty in the performed research concerns the costs and efficiencies of the electrolyzers. If lower efficiencies or higher costs are taken, the hydrogen system becomes unfeasible.

6.2 OPTIMAL DESIGN

The optimal system design uses the hydrogen infrastructure design of 2050 as a 'starting point', since the hydrogen transmission infrastructure changes greatly over the phasing period. So, in 2030, a subset of the pipelines of the 2050 design should be built to connect the 2030 sinks and sources. The same applies to 2040. Using technical and regulatory constraints, the results show that by the phased build-up, the wind farms will move further from shore (following the dedicated wind farm development zones), as will the

electrolysers. After 122,2 km from shore, the in-turbine electrolysers (i.e. H₂-in-Turbine wind farms which connect to a centralised compressor station) are present. Hence, below this threshold, electrolyser hubs (i.e. an electrolyser station which is connected to multiple wind farms) are present.

Additionally, the future transmission infrastructure should take advantage of the incumbent natural gas infrastructure, refurbishing this infrastructure next to using new pipelines. The results indicate that when only using new pipelines, the transmission infrastructure costs increase with 36%.

Both the electricity-driven (electrolyser hubs) mode and the hydrogen-driven (H₂-in-turbine electrolysis) mode offer a large amount of electricity potential to produce hydrogen. However, this potential fluctuates greatly during the year, which needs to be coped with in order for a reliable hydrogen system. The electricity-driven supply potential concerns the electricity surplus of the connected wind farms, and the hydrogen-driven supply potential concerns the total produced electricity of the corresponding H₂-in-Turbine wind farms: in 2030 the total maximum electricity potential (15,02 TWh) is entirely produced under the electricity-driven mode, in 2040 (total of 100,36 TWh) only Germany has also hydrogen driven wind farms, and in 2050 (total of 183,44 TWh) also Denmark and the Netherlands have both kinds of wind farms, while Belgium only uses the electricity surplus of electricity-driven mode.

Using the surplus of electricity for hydrogen production, has an additional benefit: The capacity factor of the wind farms (i.e. the productivity of the wind farms) can increase up to even 220% if the different surplus are being used. This should be taken into account in future investment and policy choices.

7

DISCUSSION AND RECOMMENDATIONS

In this chapter, the discussion and recommendations are presented. In [Section 7.1](#), the conclusion of this thesis is addressed by interpreting and discussing the results. Thereafter, in [Section 7.2](#), recommendations are stated corresponding to the implications and limitations of this thesis.

7.1 DISCUSSION

7.1.1 Transmission Infrastructure

This thesis proposes a (new) set pipelines which should be used to transport hydrogen from the North Sea to shore. Within this thesis — aside from the transmission distance and Natura2000 areas — there are no additional spatial complexities incorporated which affect the costs of a pipeline. In reality the costs of offshore hydrogen pipelines vary along with the location, topographic features, and the year of construction ([Miao et al., 2021](#)). As a consequence, inaccurate results may occur. Additionally, the [European Commission \(2020\)](#) states that 30% of the sea must be protected. And within 10% of the sea, multi-use is not allowed, hence no infrastructure may be placed here. None of these additional complexities are incorporated within this thesis.

Aside from the new hydrogen infrastructure, this thesis also incorporates existing infrastructure. The existing natural gas pipelines may be reused when economically feasibly. The results indicate that if the network is built solely with new pipelines, the costs increase with 36% when compared to also reusing old pipelines. The benefit of reusing pipelines is apparent. However, the assumption to be able to reuse the existing natural pipelines is optimistic. It might not be the case that the natural gas pipelines can be used as of 2030. Only in Denmark, the decision has been made that the oil and gas extraction will cease ([Klima-, Energi- og Forsyningsministeriet, 2020](#)). And, this pledge reflects 2050; not 2030.

Moreover, as also indicated in [Section 4.3](#), the existing pipelines are edited: They are filtered, simplified, and exploded, after which pipelines are removed which end or start within Natura2000 areas. Not only does the editing result in less accurate results, but the last step also sometimes results in missing segments of pipelines. This can be seen in [Figure 7.1](#). The highlighted section of the map shows a pipeline from the original data-set, which crosses a Natura2000 area. However, the same pipeline segment is removed within the final data-set. This is a result of a bend in the original pipeline within the Natura2000 area. Because the pipelines are edited, bends are represented by a set of straight segments. These straight segments are

substituted for the bend, however, these straight segments are not necessarily connected by the Quantum Geographical Information System (QGIS). As a consequence, in the last step that segment of the pipeline is removed as the individual segments have ending or starting points within the Natura2000 Area.

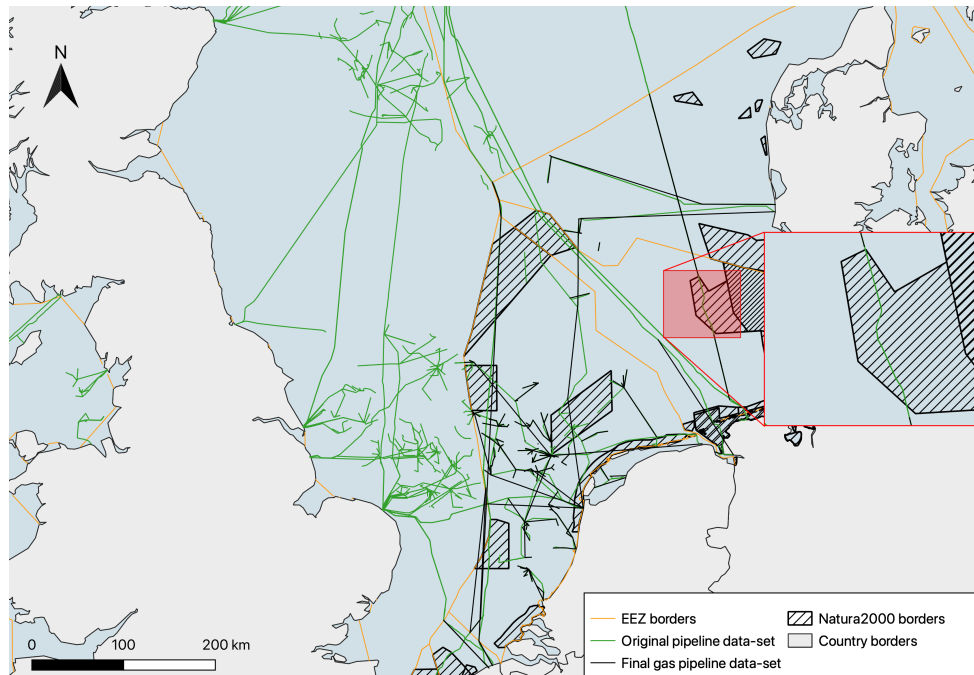


Figure 7.1: Missing pipeline segment.

The inaccuracies and uncertainties of the new and reused infrastructure lead to question the optimality of the infrastructure. It is unknown how the infrastructure might change if the before-mentioned aspects are incorporated. But, it is expected that this does not significantly influence the estimated feasibility of the system. This is because the costs of the hydrogen transmission infrastructure are quite small compared to the other components of the hydrogen system in question.

7.1.2 Onshore Entry Points

The proposed hydrogen system has a supply driven design. This means that the system is only concerned with the production and distribution of hydrogen. In Table 7.1, the maximum possible supply of the system and the demand of EU countries are shown. On itself this does not seem to be a problem as the demand exceeds the potential supply of the system.

Table 7.1: Maximum supply of the hydrogen system and demand of Belgium, Denmark, Germany, and the Netherlands. Demand derived from Wang et al. (2021).

	2030	2040	2050
Maximum supply <i>TWh</i>	15,02	100,36	183,44
Demand <i>TWh</i>	115,45	445,82	719,21

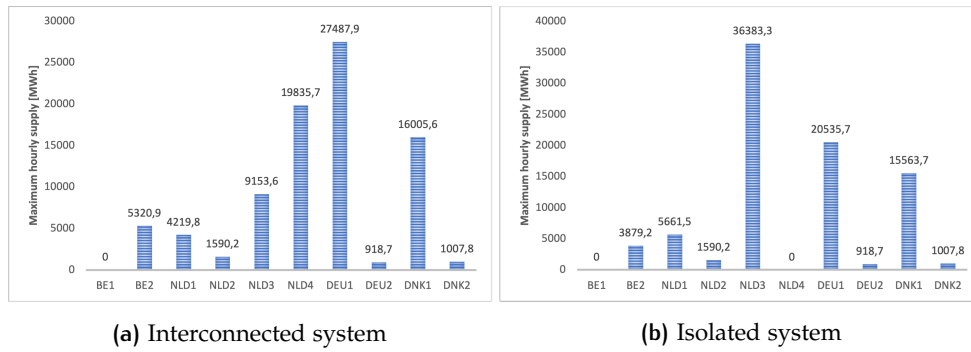


Figure 7.2: Maximum hourly supply distribution at the onshore entry points

In the (supply driven) design however, use is made of a super-sink to optimally allocate the hydrogen between the different onshore entry points. This method disregards the specific (and fluctuating) demand of the entry points from where the hydrogen would be transported to e.g. the respective industrial clusters. Not taking the specific demand value of these clusters into account, might lead to a non-optimal distribution. Figure 7.2 shows the maximum supply at the onshore entry points. As an example, onshore entry point 'NLD2' represents the harbor of Rotterdam, a large industrial district. However, the supply in 'NLD3' (in Den Helder), is much higher. In reality, this will not be the case. As a consequence, if a hydrogen system in the North Sea will be realised, specific demands per entry point should be included in the design.

7.1.3 Electrolysers

To define the location of the electrolysers, the locations of the current and future wind farms are used (i.e. electrolyser hubs and compressor stations). The electrolyser hubs are connected to a subset of the 'normal' offshore wind farms, and the compressor stations are connected to a subset of the H₂-in-Turbine wind farms.

The quantity and locations of both types of electrolysers depend on the estimations on the total capacity of the wind farms in the North Sea in 2030, 2040, and 2050. In this thesis, a proposition of the new offshore wind capacities by Wang et al. (2021) is used. However, during the course of this research, new plans were made public. The current geopolitical events between Russia and the Ukraine have resulted in more efforts of the EU to deploy renewable energy (Rijksoverheid, 2022). More specific, the recent Esbjerg Declaration defines that the North Sea will become the green power plant of Europe (Rijksoverheid, 2022). As a result, additional wind farms and electrolyser locations are expected. This would change the design and output of the hydrogen system.

Moreover, each electrolyser hub is placed on top of an electricity sub station connected to multiple wind farms (Assumption 1). In reality, this might not be the case. Consequently, the optimal placement might differ. Although, this method is not very uncommon, as it is also hypothesised by NSWPH (2021).

The in-turbine electrolyser wind farms are placed after a certain threshold (122 km). This threshold is based on the CapEx of a transmission capacity of 1 GW for both pipelines and cables. However, this comparison is basic and questionable; the system design indicates that the transmission capacity is usually more than 1 GW. Besides, the transmission capacities are very nonuniform, hence using 1 GW as an overall measurement is to some extent unsuitable. And finally, the optimal threshold depends on a greater number of parameters and aspects, not only the CapEx, as is assumed in this thesis. Hence, in hindsight, a better method would have been to use a threshold of 100 km, such as suggested by Peters et al. (2020).

Additionally, the sensitivity analysis identified new insights regarding the electrolysers. The results indicate that the outcome of the research is highly influenced by the costs and the efficiencies of the electrolysers: If lower efficiencies or higher costs are taken, the hydrogen system becomes unfeasible. Not only are the costs of the electrolysers relatively uncertain. But the used efficiencies in this thesis (as proposed by Wang et al. (2020)) might also be lower in reality. If that is the case, the proposed system might only be feasible with for example high hydrogen prices.

7.1.4 Economic Assessment

To be able to value the hydrogen system, an economic assessment is performed. The designed hydrogen system is considered as a potential 'add-on' for the offshore wind system. Within the economic assessment, 'normal' offshore wind farms and their respective infrastructure are treated as sunk costs. This methodology is used because it is assumed that the offshore wind system will be built regardless. This marginalised approach consequently results in lower costs of the proposed hydrogen system, as the costs of the wind farms are excluded. In order to be able to treat the wind system as sunk costs, it must be certain that the offshore wind system will be realised.

The estimated offshore wind farm capacity for 2030, 2040, and 2050 is derived from Wang et al. (2021). As also indicated earlier, the plans for offshore wind farm capacity are recently increased due to the geopolitical events between Russia and the Ukraine (Rijksoverheid, 2022). This creates an uncertainty regarding the maximum amount of electrolysers which could be placed offshore, as explained in Section 7.1.3. However, this also results in a higher probability that the proposed system design actually can be realised as there is now a higher probability that the used wind farms will be built. The newly proposed efforts defined in the Esbjerg Declaration will cause the estimations of Wang et al. (2021) to be more robust.

It can be argued that the outcome of this thesis might not be representative as the offshore wind system is treated as a sunk cost. However, the costs of the wind farms do not influence the costs of the hydrogen transmission infrastructure, nor do they change the lay-out of the transmission infrastructure. Moreover, it can be expected that the outcome of the economic assessment will still be the same. As there is a high probability that the wind farms will be built within the North Sea, it is reasonable to assume that these new wind farms also have a positive business case. In fact,

integrating the hydrogen system within wind farm system increases their profitability, as a consequence of using their potential surplus.

7.1.5 Interconnection between Countries

In this thesis, a (slight) preference is expressed towards the interconnected system design over the isolated design based on a techno-economic approach. However, such a decision should be evaluated on an EU level, using a dedicated research on the advantages and disadvantages of both options from a political point of view. To answer the question on which type of integration is most suitable for the presented hydrogen system, the implications of collaboration between the parties need to be assessed.

Overall, collaboration between private and/or public organisations is seen as the go-to strategy. This, as governments, businesses, and communities seek to cross boundaries, opt for a collective impact, or build partnerships. Looking back at the results of the economic assessment described in [Section 5.3](#), it could also be concluded that collaboration is once again to best strategy. Especially when one assumes that the advantages of collaboration are self-evident due to the created synergies ([Keast et al., 2017](#)). For example, there may exist an advantage by using interconnections to mitigate the intermittent characteristics of offshore wind, which affect the system output. This advantage within the North Sea is currently also hypothesised by the Dutch ministry of economic affairs and climate policy (W. Sieval, Van Oord NV., personal communication, July 2022).

However, the costs of (international) collaboration are often considerable as they may require new developments or changes within the institutional framework in which the system is located. If multiple jurisdictions are present within the system, an extensive planning, permitting, and consultation process starts, which complicates the development of the system and can take years ([International Energy Agency, 2019b](#); [Gorenstein Dedecca et al., 2018](#); [Keast et al., 2017](#)). As an example, it took almost 13 years to plan the Nord Stream pipeline, because it went through a series of different [EEZs](#) ([Nord Stream, 2009](#)). The Nord Stream 2 project also took around 7 years, while it was constructed next to the original Nord Stream pipeline.

Additionally, conflicts between the gas contracts can also be expected (W. Sieval, Van Oord NV., personal communication, July 2022). This may be since different countries may opt for different electrolyser systems and hydrogen compositions transported through the pipelines.

7.1.6 Effect of Storage

The results of this thesis indicate that the supply of hydrogen fluctuates greatly. As a consequence of this fluctuation, downscaling of the electrolyser capacities is advised. However, the fluctuating characteristics of the hydrogen production still impede the reliability of the system. Hence, there is a need for hydrogen storage ([Tesfahunegn et al., 2011](#)). The produced hydrogen could be stored inside the pipelines by increasing the operating pressure, also called linepacking ([Kazda et al., 2020](#)). Furthermore, other options of

hydrogen storage should also be considered, such as depleted offshore gas reservoirs or other geological formations (Hassanpouryouzband et al., 2021).

7.1.7 Utilising the Surplus

The capacity factor of a wind farm is mostly based on the geographical location, and the design and the characteristics of the wind turbines (Carreno-Madinabeitia et al., 2021; Sedaghat et al., 2020), not taking into account the hourly demand and supply patterns of the energy system. As a consequence, capacity factor estimations tend to be lower than expected (Boccard, 2009). These estimations might be lower due to the high potential wind surpluses present: integrating an hydrogen system within the electricity system, can have a significant effect on the capacity factor. It can also be seen that over the years, the percentual change of capacity factor tends to increase. In some cases this even reaches an increase of 220%. In other words, without integrating the hydrogen system, there is a chance that the realised capacity factor strands further from the envisioned capacity factor over the coming years. This can result in investments which appear not to be as lucrative as hoped, possibly due to a higher Levelised Cost Of Electricity (LCOE) (Breeze, 2021). Additionally, there exists the possibility that poor policy decisions are made if based on these lacking estimations of the capacity factor. In both cases, a less optimal allocation of resources would be present. Hence, by integrating the hydrogen system, this problem can be mitigated as the estimated capacity factors would be closer to the realised capacity factor, and more accurate estimations can be made on the feasibility of the system.

7.1.8 Regulatory Framework

The design of an offshore hydrogen system should abide regulations dealing with hydrogen facilities in the North Sea. However, such regimes are currently non-existent, nor exist recommendations (Cauchois et al., 2021; Andreasson & Roggenkamp, 2020). There do exist regimes which govern offshore hydrocarbon (e.g. natural gas) installations and offshore wind farms. However, it is difficult to ascertain which regulations apply to offshore hydrogen facilities. As a consequence, the results of this thesis might not be as accurate as aspired. As an example, new regulations might define rules and standards on the hydrogen transmission infrastructure, potentially changing the acquainted costs and lay-out of the system.

Additionally, there is another adverse effect of the lack of regulatory regimes. Regulatory uncertainty reduces investments in new renewable energy projects and undermines policy goals (Fabrizio, 2013).

Hence, to be able to successfully implement the offshore hydrogen system, there is a need for regulatory regimes which facilitates the deployment. In particular, Andreasson & Roggenkamp (2020) determined several regulatory aspects which need to be addressed:

- It is unclear if hydrogen is a storage or production technology; and consequently whether hydrogen falls under the electricity directive or under the gas directive.

- Under the renewable energy directive, it is important to define how guarantees of origin interact if electricity is converted into hydrogen.
- There should be specific references regarding offshore hydrogen production by means of electrolysis in environmental and safety laws. As a consequence, it is more clear whether impact assessments are mandatory for hydrogen facilities, and whether permits are needed.

7.2 RECOMMENDATIONS

Based on the results, conclusion, and discussion, a set of recommendations can be given.

National Level:

- The reuse of natural gas pipelines is deemed beneficial. However, it is unclear how the natural gas system in the North Sea will develop policy wise over the upcoming decades. Following Denmark, governments should start to formulate policy decisions on whether or when gas extraction in the North Sea should stop. And consequently whether the existing natural gas transmission infrastructure can be reused for hydrogen transport.
- Thereupon, the transmission system operators (i.e. the entities committed to the transmission of energy on a national or regional level) should scope their plans towards transporting offshore hydrogen to onshore. Such plans should be assessed with a long-term logic.

The transmission system operators should also start planning the onshore hydrogen backbone, as is already the case in the Netherlands.

- Additionally, public and private organisations should base their resource allocation plans on more realistic capacity factors of offshore wind. Such capacity factors should include a realistic supply potential of the offshore wind farm by incorporating the electricity demand of the system.

A different approach could be that governments include mandatory electrolyser facilities along the offshore wind farm in tenders. By doing so, the capacity factor of the wind farms would increase as (a part of) the electricity surplus is also used.

European Union Level:

- Currently, there lack regulatory regimes to support hydrogen production by offshore wind at sea. These regimes should be determined.
- The EU should start deciding upon whether to build an interconnected system or multiple isolated hydrogen systems in the North Sea. It is important to make such decisions far in advance.
- Based on this decision, it is important to start shaping rules, standards, and governance for hydrogen trade.

Modelling and Further Research:

- The intermittent characteristics of the hydrogen production reduce the reliability of the system. Hence, future research should also investigate the possibilities of storage and some sort of back-up energy source (such as chemical or heat energy) which could be used for the production of hydrogen.
- It is also important to analyse how the proposed system might change if more spatial complexities are incorporated within the analysis. E.g. how will the optimal pipeline allocation differ if pipelines are also subject to depth or other cost-increasing factors or constraints. Additionally, a complete and unedited data-set of natural gas pipelines should be used, and an updated offshore wind capacity plans should be incorporated.
- Different electrolyser locations should be evaluated, e.g. old support structures of natural gas extraction platforms. Additionally, the break-even point of electrolyser efficiencies and costs should be analysed.
- Additional research should define the demand of the onshore entry points by analysing the demand clusters to which each entry point is connected. This will result in a more practical transmission infrastructure design.

Using these recommendations, it is possible to develop accurate plans regarding a future proof offshore hydrogen system for the [EU](#) in the North Sea.

BIBLIOGRAPHY

- 4C Offshore. (n.d.). *Global offshore renewable map*. 4C Offshore. Retrieved from <https://map.4coffshore.com/offshorewind/1>
- Ackerman, E., Fox, J., Pach, J., & Suk, A. (2014). On grids in topological graphs. *Computational Geometry*, 47(7), 710–723. doi: 10.1016/j.comgeo.2014.02.003
- Agnolucci, P., & McDowall, W. (2013). Designing future hydrogen infrastructure: Insights from analysis at different spatial scales. *International Journal of Hydrogen Energy*, 38(13), 5181-5191. doi: 10.1016/j.ijhydene.2013.02.042
- Aktas, A. (2021). Chapter 10 - the importance of energy storage in solar and wind energy, hybrid renewable energy systems. In A. K. Azad (Ed.), *Advances in clean energy technologies* (p. 377-403). Academic Press. doi: 10.1016/B978-0-12-821221-9.00010-4
- André, J., Auray, S., Brac, J., De Wolf, D., Maisonnier, G., Ould-Sidi, M.-M., & Simonnet, A. (2013). Design and dimensioning of hydrogen transmission pipeline networks. *European Journal of Operational Research*, 229(1), 239-251. doi: 10.1016/j.ejor.2013.02.036
- Andreasson, L. M., & Roggenkamp, M. (2020). *Regulatory framework: Legal challenges and incentives for developing hydrogen offshore*. Retrieved from https://north-sea-energy.eu/static/1f13bd895cfa3e630af1bb277f2630f2/11.-FINAL-NSE3_D2.2-D2.3-Analysis-of-legal-basis-for-offshore-hydrogen-planning-and-Legal-assessment.pdf
- Balaman, S. Y. (2019). Chapter 5 - uncertainty issues in biomass-based production chains. In *Decision-making for biomass-based production chains* (p. 113-142). Academic Press. doi: 10.1016/B978-0-12-814278-3.00005-4
- Blanco, H., & Faaij, A. (2018). A review at the role of storage in energy systems with a focus on power to gas and long-term storage. *Renewable and Sustainable Energy Reviews*, 81, 1049-1086. doi: doi.org/10.1016/j.rser.2017.07.062
- Boccard, N. (2009). Capacity factor of wind power: Realized values vs. estimates. *SSRN Electronic Journal*. doi: 10.2139/ssrn.1285435
- Bonaduce, A., Staneva, J., Behrens, A., Bidlot, J.-R., & Wilcke, R. A. I. (2019). Wave climate change in the north sea and baltic sea. *Journal of Marine Science and Engineering*, 7(6). doi: 10.3390/jmse7060166
- Braun, S., & Hesel, P. (2020). *Green hydrogen – the big unknown in the eu power system*. Retrieved from <https://www.icis.com/explore/resources/news/2020/04/29/10501835/green-hydrogen-the-big-unknown-in-the-eu-power-system/>

- Breeze, P. (2021). Chapter 9 - the cost of electricity. In P. Breeze (Ed.), *The cost of electricity* (p. 117-136). Elsevier. Retrieved from <https://www.sciencedirect.com/science/article/pii/B9780128238554000097> doi: 10.1016/B978-0-12-823855-4.00009-7
- Breunis, W. F. (2021). *Hydrogen gas production from offshore wind energy — a cost-benefit analysis of optionality through grid connection*. Retrieved from <https://repository.tudelft.nl/islandora/object/uuid%3A592c4ab2-7ab1-428b-b54c-1c44afc5ba5a>
- Brosschot, S. (2022). *Comparing hydrogen networks and electricity grids for transporting offshore wind energy to shore in the north sea region. a spatial network optimisation approach*.
- Calado, G., & Castro, R. (2021). Hydrogen production from offshore wind parks: Current situation and future perspectives. *Applied Sciences*, 11(12), 5561. doi: 10.3390/app11125561
- Carreno-Madinabeitia, S., Ibarra-Berastegi, G., Sáenz, J., & Ulazia, A. (2021). Long-term changes in offshore wind power density and wind turbine capacity factor in the iberian peninsula (1900–2010). *Energy*, 226, 120364. doi: 10.1016/j.energy.2021.120364
- Cauchois, G., Renaud-Bezot, C., Simon, M., Gentile, V., Carpenter, M., & Even Torbergsen, L. (2021). *Re-stream – study on the reuse of oil and gas infrastructure for hydrogen and ccs in europe*. DNV.
- CEER. (2019). *Pan-european cost-efficiency benchmark for gas transmission system operators*. Council of European Energy Regulators. Retrieved from <https://www.ceer.eu/documents/104400/-/-/90707d6c-6da8-0da2-bce9-0fbbc55bea8c>
- Chis, T. (2015). The life cycle as an offshore pipeline. *International Conference of Scientific Paper AFASES 2015*.
- Czyżak, P., Uusivuori, E., Ilas, A., & Candlin, A. (2022). *Shocked into action: Answering multiple threats to their security, european countries are accelerating the shift from fossil fuels towards renewables*. Ember. Retrieved from <https://ember-climate.org/app/uploads/2022/06/Ember-EU-national-plans-slash-fossil-fuels.pdf>
- Danish Energy Agency. (2021). *Technology data for renewable fuels*. Retrieved from <https://ens.dk/en/our-services/projections-and-models/technology-data/technology-data-renewable-fuels>
- De Hauwere, N. (n.d.). *Bathymetry of the north sea*. Marineregions.org. Retrieved from <https://www.marineregions.org/maps.php?album=3747&pic=115811>
- DeSantis, D., James, B. D., Houchins, C., Saur, G., & Lyubovsky, M. (2021). Cost of long-distance energy transmission by different carriers. *iScience*, 24(12), 103495. doi: 10.1016/j.isci.2021.103495

- Doherty, N. (2018). *Rampion offshore wind farm, united kingdom*. Retrieved from <https://unsplash.com/photos/pONBhDyOFoM>
- d'Amore Domenech, R., Óscar Santiago, & Leo, T. J. (2020). Multicriteria analysis of seawater electrolysis technologies for green hydrogen production at sea. *Renewable and Sustainable Energy Reviews*, 133, 110166. doi: 10.1016/j.rser.2020.110166
- Ehteshami, S. M. M., & Chan, S. (2014). The role of hydrogen and fuel cells to store renewable energy in the future energy network – potentials and challenges. *Energy Policy*, 73, 103–109. doi: 10.1016/j.enpol.2014.04.046
- Elberry, A. M., Thakur, J., Santasalo-Aarnio, A., & Larmi, M. (2021). Large-scale compressed hydrogen storage as part of renewable electricity storage systems. *International Journal of Hydrogen Energy*, 46(29), 15671–15690. doi: 10.1016/j.ijhydene.2021.02.080
- EMODnet. (2021). *Emodnet_ha_windfarms_20211210*. Retrieved from <https://www.emodnet-humanactivities.eu/search-results.php?dataname=Wind+Farms+%28Polygons%29>
- EMODnet. (2022). *Emodnet human activities, pipelines*. Retrieved from <https://www.emodnet-humanactivities.eu/search-results.php?dataname=Pipelines>
- Energy Administration Information. (2020). *About 25% of u.s. power plants can start up within an hour*. Retrieved from <https://www.eia.gov/todayinenergy/detail.php?id=45956>
- EPA. (2006). *Using pipeline pump-down techniques to lower gas line pressure before maintenance*. United States Environmental Protection Agency. Retrieved from https://www.epa.gov/sites/default/files/2016-06/documents/ll_pipeline.pdf
- Erdős, P., Lovász, L., Ruzsa, I. Z., & Sós, V. T. (2013). *Erdos centennial*. Springer.
- European Commission. (2020). *Communication from the commission to the european parliament, the council, the european economic and social committee and the committee of the regions — eu biodiversity strategy for 2030*. European Commission. Retrieved from <https://eur-lex.europa.eu/legal-content/EN/TXT/?uri=CELEX%3A52020DC0380>
- European Commission. (2021). *The eu blue economy report 2021*. Publications Office of the European Union. Retrieved from https://maritime-spatial-planning.ec.europa.eu/sites/default/files/the-eu-blue-economy-report-2021_en.pdf
- European Environment Agency. (2022). *Natura 2000 data - the european network of protected sites*. Retrieved from <https://www.eea.europa.eu/data-and-maps/data/natura-13>

- Fabrizio, K. R. (2013). The effect of regulatory uncertainty on investment: Evidence from renewable energy generation. *Journal of Law, Economics, and Organization*, 29(4), 765–798. doi: 10.1093/jleo/ewso07
- Gasunie. (2022). *Gasunie starts construction of national hydrogen network in the netherlands*. Retrieved from <https://www.gasunie.nl/en/news/gasunie-starts-construction-of-national-hydrogen-network-in-the-netherlands>
- González Díez, N., Van Der Meer, S., Bonetto, J., & Herwijn, A. (2020). *Technical assessment of hydrogen transport, compression, processing offshore*. North Sea Energy.
- Gorenstein Dedecca, J., Lumberras, S., Ramos, A., Hakvoort, R. A., & Herder, P. M. (2018). Expansion planning of the north sea offshore grid: Simulation of integrated governance constraints. *Energy Economics*, 72, 376–392. doi: <https://doi.org/10.1016/j.eneco.2018.04.037>
- Grady, S., Hussaini, M., & Abdullah, M. (2005). Placement of wind turbines using genetic algorithms. *Renewable Energy*, 30(2), 259–270. doi: 10.1016/j.renene.2004.05.007
- Guo, M., & Shah, N. (2015). Bringing non-energy systems into a bioenergy value chain optimization framework. *12th International Symposium on Process Systems Engineering and 25th European Symposium on Computer Aided Process Engineering*, 2351–2356. doi: 10.1016/b978-0-444-63576-1.50086-8
- Gusain, D., Cvetkovic, M., Bentvelsen, R., & Palensky, P. (2020). Technical assessment of large scale pem electrolyzers as flexibility service providers. *2020 IEEE 29th International Symposium on Industrial Electronics (ISIE)*. doi: 10.1109/isie45063.2020.9152462
- Hassanpouryouzband, A., Joonaki, E., Edlmann, K., & Haszeldine, R. S. (2021). Offshore geological storage of hydrogen: Is this our best option to achieve net-zero? *ACS Energy Letters*, 6(6), 2181–2186. doi: 10.1021/acsenergylett.1c00845
- Heijnen, P. W. (2022). Minimum-cost network-layout with multi-sinks and multi-sources. Retrieved from <https://gitlab.tudelft.nl/pheijnen/optimal-networklayout>
- Heijnen, P. W., Chappin, E. J., & Herder, P. M. (2019). A method for designing minimum-cost multisource multisink network layouts. *Systems Engineering*, 23(1), 14–35. doi: 10.1002/sys.21492
- Hermesmann, M., & Müller, T. (2022). Green, turquoise, blue, or grey? environmentally friendly hydrogen production in transforming energy systems. *Progress in Energy and Combustion Science*, 90, 100996. doi: 10.1016/j.pecs.2022.100996
- Hou, P., Enevoldsen, P., Eichman, J., Hu, W., Jacobson, M. Z., & Chen, Z. (2017). Optimizing investments in coupled offshore wind -electrolytic hydrogen storage systems in denmark. *Journal of Power Sources*, 359, 186–197. doi: 10.1016/j.jpowsour.2017.05.048

- ICF International. (2014). *North american midstream infrastructure through 2035: Capitalizing on our energy abundance*. INGAA Foundation. Retrieved from <https://www.ingaa.org/File.aspx?id=21498>
- International Energy Agency. (2019a). *More of a good thing – is surplus renewable electricity an opportunity for early decarbonisation?* Retrieved from <https://www.iea.org/commentaries/more-of-a-good-thing-is-surplus-renewable-electricity-an-opportunity-for-early-decarbonisation>
- International Energy Agency. (2019b). *Power systems across borders*. Retrieved from <https://www.iea.org/reports/integrating-power-systems-across-borders>
- International Energy Agency. (2020). *Hydrogen*. Retrieved from <https://www.iea.org/reports/hydrogen>
- International Energy Agency. (2021). *Iea g20 hydrogen report: Assumptions*. Retrieved from <https://iea.blob.core.windows.net/assets/29b027e5-fefc-47df-aed0-456b1bb38844/IEA-The-Future-of-Hydrogen-Assumptions-Annex-CORR.pdf>
- Invernizzi, D. C., Locatelli, G., Velenturf, A., Love, P. E., Purnell, P., & Brookes, N. J. (2020). Developing policies for the end-of-life of energy infrastructure: Coming to terms with the challenges of decommissioning. *Energy Policy*, 144, 111677. doi: 10.1016/j.enpol.2020.111677
- IRENA. (2019). *Innovation landscape brief: Renewable power-to-hydrogen*. International Renewable Energy Agency. Retrieved from https://www.irena.org/-/media/Files/IRENA/Agency/Publication/2019/Sep/IRENA_Power-to-Hydrogen_Innovation_2019.pdf
- IRENA. (2020). *Green hydrogen cost reduction: Scaling up electrolyzers to meet the 1.5°C climate goal*. International Renewable Energy Agency. Retrieved from https://irena.org/-/media/Files/IRENA/Agency/Publication/2020/Dec/IRENA_Green_hydrogen_cost_2020.pdf
- Kaiser, M. J., & Snyder, B. (2012). Modeling the decommissioning cost of offshore wind development on the u.s. outer continental shelf. *Marine Policy*, 36(1), 153–164. doi: 10.1016/j.marpol.2011.04.008
- Kakoulaki, G., Kougias, I., Taylor, N., Dolci, F., Moya, J., & Jäger-Waldau, A. (2021). Green hydrogen in europe – a regional assessment: Substituting existing production with electrolysis powered by renewables. *Energy Conversion and Management*, 228, 113649. doi: 10.1016/j.enconman.2020.113649
- Kallehave, D., Byrne, B. W., LeBlanc Thilsted, C., & Mikkelsen, K. K. (2015). Optimization of monopiles for offshore wind turbines. *Philosophical Transactions of the Royal Society A: Mathematical, Physical and Engineering Sciences*, 373(2035), 20140100. doi: 10.1098/rsta.2014.0100
- Kantor, I., Robineau, J.-L., Bütün, H., & Maréchal, F. (2020). A mixed-integer linear programming formulation for optimizing multi-scale material and energy integration. *Frontiers in Energy Research*, 8. doi: 10.3389/fenrg.2020.00049

- Kazda, K., Tomasgard, A., Nørstebø, V., & Li, X. (2020). Optimal utilization of natural gas pipeline storage capacity under future supply uncertainty. *Computers Chemical Engineering*, 139, 106882. doi: <https://doi.org/10.1016/j.compchemeng.2020.106882>
- Keast, R., Charles, M., & Modzelewski, P. (2017). *The cost of collaboration: More than budgeted for?* Power to Persuade. Retrieved from <http://www.powertopersuade.org.au/blog/the-cost-of-collaboration-more-than-budgeted-for/13/4/2017>
- Klima-, Energi- og Forsyningsministeriet. (2020). *Bred aftale om nordsøens fremtid*. Retrieved from <https://via.ritzau.dk/pressemeddelelse/bred-aftale-om-nordsoens-fremtid?publisherId=9426318&releaseId=13605632>
- Kovac, A., Paranos, M., & Marcus, D. (2021). Hydrogen in energy transition: A review. *International Journal of Hydrogen Energy*, 46(16), 10016-10035. (Hydrogen and Fuel Cells) doi: 10.1016/j.ijhydene.2020.11.256
- Lacal-Aránegui, R., Yusta, J. M., & Domínguez-Navarro, J. A. (2018). Off-shore wind installation: Analysing the evidence behind improvements in installation time. *Renewable and Sustainable Energy Reviews*, 92, 133-145. doi: 10.1016/j.rser.2018.04.044
- Lago, J., Marcjasz, G., De Schutter, B., & Weron, R. (2021). Forecasting day-ahead electricity prices: A review of state-of-the-art algorithms, best practices and an open-access benchmark. *Applied Energy*, 293, 116983. doi: 10.1016/j.apenergy.2021.116983
- Lavidas, G. (2022). *Waves, current & soil*. TU Delft. Retrieved from <https://brightspace.tudelft.nl/d2l/le/content/401379/viewContent/2646954/View>
- Lee, C. H., Chong, D. Y. L., Hemmati, S., Elnegihi, M. M., Foo, D. C., How, B. S., & Yoo, C. (2020). A p-graph approach for the synthesis of national-wide bio-hydrogen network from palm oil mill effluent. *International Journal of Hydrogen Energy*, 45(35), 17200-17219. doi: 10.1016/j.ijhydene.2020.04.179
- Li, F., Liu, Q., Guo, X., & Xiao, J. (2015). A survey of optimization method for oil-gas pipeline network layout. *Proceedings of the 2015 International Conference on Mechatronics, Electronic, Industrial and Control Engineering*. doi: 10.2991/meic-15.2015.61
- Li, L., Manier, H., & Manier, M.-A. (2019). Hydrogen supply chain network design: An optimization-oriented review. *Renewable and Sustainable Energy Reviews*, 103, 342-360. doi: 10.1016/j.rser.2018.12.060
- MacKenzie, B. R., & Schiedek, D. (2007). Long-term sea surface temperature baselines—time series, spatial covariation and implications for biological processes. *Journal of Marine Systems*, 68(3-4), 405-420. doi: 10.1016/j.jmarsys.2007.01.003
- Maggio, G., Nicita, A., & Squadrito, G. (2019). How the hydrogen production from res could change energy and fuel markets: A review of recent

- literature. *International Journal of Hydrogen Energy*, 44(23), 11371–11384. doi: 10.1016/j.ijhydene.2019.03.121
- Mankiw, N. G. (2018). *Principles of economics*. Cengage.
- Maryam, S. (2017). Review of modelling approaches used in the hsc context for the uk. *International Journal of Hydrogen Energy*, 42(39), 24927–24938. doi: 10.1016/j.ijhydene.2017.04.303
- Mcdonagh, S., Ahmed, S., Desmond, C., & Murphy, J. D. (2020). Hydrogen from offshore wind: Investor perspective on the profitability of a hybrid system including for curtailment. *Applied Energy*, 265, 114732. doi: 10.1016/j.apenergy.2020.114732
- McKinsey&Company. (2010). *Transformation of europe's power system until 2050 - including specific consideration for germany*. McKinsey&Company.
- Miao, B., Giordano, L., & Chan, S. H. (2021). Long-distance renewable hydrogen transmission via cables and pipelines. *International Journal of Hydrogen Energy*, 46(36), 18699–18718. doi: 10.1016/j.ijhydene.2021.03.067
- Moreno-Benito, M., Agnolucci, P., & Papageorgiou, L. G. (2017). Towards a sustainable hydrogen economy: Optimisation-based framework for hydrogen infrastructure development. *Computers Chemical Engineering*, 102, 110–127. (Sustainability Energy Systems) doi: 10.1016/j.compchemeng.2016.08.005
- Nadaleti, W. C., Borges dos Santos, G., & Lourenco, V. A. (2020). The potential and economic viability of hydrogen production from the use of hydroelectric and wind farms surplus energy in brazil: A national and pioneering analysis. *International Journal of Hydrogen Energy*, 45(3), 1373–1384. doi: 10.1016/j.ijhydene.2019.08.199
- National Research Council and National Academy of Engineering. (2004). *The hydrogen economy: Opportunities, costs, barriers, and ramp;d needs*. Washington, DC: The National Academies Press. Retrieved from <https://nap.nationalacademies.org/catalog/10922/the-hydrogen-economy-opportunities-costs-barriers-and-rd-needs> doi: 10.17226/10922
- Nayar, K. G., Sharqawy, M. H., Banchik, L. D., & Lienhard V, J. H. (2016). Thermophysical properties of seawater: A review and new correlations that include pressure dependence. *Desalination*, 390, 1–24. doi: 10.1016/j.desal.2016.02.024
- Nord Stream. (2009). *Nord stream environmental impact assessment (eia) documentation for consultation under the espoo convention*. Retrieved from <https://www.nord-stream.com/press-info/library/?q=espoo&category=&type=&country=>
- NSE, HINT, & TNO. (2020). *Energy transport and energy carriers*. North Sea Energy. Retrieved from <https://north-sea-energy.eu/static/13128f408ffceaf0d8281be5275b63c3/6.-FINAL-NSE3-D3.2-D3.3-D3.4-D3.5-D3.6-Inventory-of-power-to-X-integration-options.pdf>

- NSWPH. (2021). *Towards the first hub-and-spoke project — progress of the north sea wind power hub consortium*. North Sea Wind Power Hub. Retrieved from https://northseawindpowerhub.eu/sites/northseawindpowerhub.eu/files/media/document/NSWPH_Concept%20Paper_05_2021_v2.pdf
- NSWPH. (2022). *Grid integred offshore power-to-gas: A feasibility review and discussion of power grid-integrated offshore power-to-gas*. North Sea Wind Power Hub. Retrieved from https://northseawindpowerhub.eu/sites/northseawindpowerhub.eu/files/media/document/NSWPH_Grid-integrated%20offshore%20Power-to-Gas_Discussion%20paper%20%231.pdf
- Oliveira, A. M., Beswick, R. R., & Yan, Y. (2021). A green hydrogen economy for a renewable energy society. *Current Opinion in Chemical Engineering*, 33, 100701. doi: 10.1016/j.coche.2021.100701
- Papapetrou, M., & Kosmadakis, G. (2022). Resource, environmental, and economic aspects of sghe. *Salinity Gradient Heat Engines*, 319–353. doi: 10.1016/b978-0-08-102847-6.00006-1
- PBL. (2018). *The future of the north sea*. PBL Netherlands environmental assessment agency. Retrieved from <https://www.pbl.nl/sites/default/files/downloads/pbl-2018-the-future-of-the-north-sea-3193.pdf>
- Peters, M. C. A. M., Vaessen, J., & Van der Meer, R. (2020). *Offshore hydrogen production in the north sea enables far offshore wind development*. Retrieved from <https://repository.tno.nl//islandora/object/uuid:1b137052-0c82-466f-9e29-fa12fb347d0f>
- PosHYdon. (2021). *Poshydon*. Retrieved from <https://poshydon.com/en/home-en/process/>
- Procainsa SA. (2016). Retrieved from https://www.procainsa.com/wp-content/uploads/2017/03/EN_Case_study_Pipeline_LE.pdf
- Quintel Intelligence. (n.d.). *Energy transition model*. Retrieved from <https://pro.energytransitionmodel.com/>
- Rahman, M. S. (2017). *Basic graph theory*. Springer International Publishing.
- Reidmiller, D., Avery, C., Easterling, D., Kunkel, K., Lewis, K., Maycock, T., & Stewart, B. (2018). *Impacts, risks, and adaptation in the united states: Fourth national climate assessment, volume ii*. U.S. Global Change Research Program. doi: <https://nca2018.globalchange.gov/>
- Rijksoverheid. (2022). *The esbjerg declaration on the north sea as a green power plant of europe*. Ministerie van Algemene Zaken. Retrieved from <https://www.rijksoverheid.nl/documenten/publicaties/2022/05/18/the-esbjerg-declaration-on-the-north-sea-as-a-green-power-plant-of-europe>
- Ruth, M., Jadun, P., Gilroy, N., Connelly, E., Boardman, R., Simon, A., ... Zuboy, J. (2020). *The technical and economic potential of the h2@scale concept within the united states*. Retrieved from <https://www.nrel.gov/docs/fy21osti/77610.pdf>

- Schmitt, A. (2022). *Eu energy outlook 2050: How will the european electricity market develop over the next 30 years?* Retrieved from <https://blog.energybrainpool.com/en/eu-energy-outlook-2050-how-will-the-european-electricity-market-develop-over-the-next-30-years/>
- Schrum, C., Lowe, J., Meier, H. E. M., Grabemann, I., Holt, J., Mathis, M., ... Wakelin, S. (2016). Projected change—north sea. In *North sea region climate change assessment* (pp. 175–217). Cham: Springer International Publishing.
- Sedaghat, A., Mostafaeipour, A., Rezaei, M., Jahangiri, M., & Mehrabi, A. (2020). A new semi-empirical wind turbine capacity factor for maximizing annual electricity and hydrogen production. *International Journal of Hydrogen Energy*, 45(32), 15888-15903. doi: 10.1016/j.ijhydene.2020.04.028
- Sens, L., Neuling, U., & Kaltschmitt, M. (2022). Capital expenditure and levelized cost of electricity of photovoltaic plants and wind turbines – development by 2050. *Renewable Energy*, 185, 525-537. Retrieved from <https://www.sciencedirect.com/science/article/pii/S0960148121017626> doi: 10.1016/j.renene.2021.12.042
- Seo, S.-K., Yun, D.-Y., & Lee, C.-J. (2020). Design and optimization of a hydrogen supply chain using a centralized storage model. *Applied Energy*, 262, 114452. doi: 10.1016/j.apenergy.2019.114452
- Siemens Gamesa. (2019). *Siemens gamesa launches 10 mw offshore wind turbine; annual energy production (aep) increase of 30% vs. predecessor.* Retrieved from <https://www.siemensgamesa.com/en-int/newsroom/2019/01/new-siemens-gamesa-10-mw-offshore-wind-turbine-sg-10-0-193-dd>
- Singlitico, A., Østergaard, J., & Chatzivasileiadis, S. (2021). Onshore, offshore or in-turbine electrolysis? techno-economic overview of alternative integration designs for green hydrogen production into offshore wind power hubs. *Renewable and Sustainable Energy Transition*, 1, 100005. doi: 10.1016/j.rset.2021.100005
- Staurland, G., & Aamodt, M. (2004). *Designing Offshore Pipeline Systems Divided Into Sections of Different Design Pressures* (Vols. 2004 International Pipeline Conference, Volumes 1, 2, and 3). doi: 10.1115/IPC2004-0217
- Stehly, T., Beiter, P., & Duffy, P. (2020). *2019 cost of wind energy review*. Golden, CO: National Renewable Energy Laboratory. NREL/TP-5000-78471. Retrieved from <https://www.nrel.gov/docs/fy21osti/78471.pdf>
- Stichting New Energy Coalition. (2019). *Deliverable wp1: Offshore reuse potential for existing gas infrastructure in a hydrogen supply chain as part of the project “gas infrastructure opportunities for a hydrogen supply chain”.* Retrieved from <https://www.newenergycoalition.org/custom/uploads/2020/07/Offshore-Reuse-Potential-for-Existing-Gas-Infrastructure-in-a-Hydrogen-Supply-Chain.pdf>
- Strbac, G., Papadaskalopoulos, D., Chrysanthopoulos, N., Estanqueiro, A., Algarvio, H., Lopes, F., ... et al. (2021). Decarbonization of electricity systems in europe: Market design challenges. *IEEE Power and Energy Magazine*, 19(1), 53–63. doi: 10.1109/mpe.2020.3033397

- Stuurgroep Extra Opgave. (2022). *Alles uit de kast - een verkenning naar de opgaven voor het nederlandse elektriciteitssysteem van 2030*. Ministry of Economic Affairs and Climate Policy. Retrieved from <https://www.rijksoverheid.nl/documenten/rapporten/2022/04/22/rapport-alles-uit-de-kast-eindrapportage-werkgroep-extra-opgave>
- Tesfahunegn, S., Ulleberg, Ø., Vie, P., & Undeland, T. (2011). Pv fluctuation balancing using hydrogen storage – a smoothing method for integration of pv generation into the utility grid. *Energy Procedia*, *12*, 1015-1022. doi: 10.1016/j.egypro.2011.10.133
- TNO, NEC, Boskalis, RoyalHaskoningDHV, DEME, Tebodin, B., & RUG. (2020). *Offshore energy islands*. North Sea Energy. Retrieved from https://north-sea-energy.eu/static/0856dd12a36d1f321aaf757706bd5913/8a.-FINAL-NSE3_D3.8-Final-report-on-the-techno-economic-environmental-and-legal-assessment-of-offshore-energy-islands.pdf
- Topham, E., Gonzalez, E., McMillan, D., & João, E. (2019). Challenges of decommissioning offshore wind farms: Overview of the european experience. *Journal of Physics: Conference Series*, *1222*(1), 012035. doi: 10.1088/1742-6596/1222/1/012035
- Topham, E., & McMillan, D. (2017). Sustainable decommissioning of an offshore wind farm. *Renewable Energy*, *102*, 470–480. doi: 10.1016/j.renene.2016.10.066
- UN General Assembly. (1982). *United nations convention on the law of the sea*. Retrieved from https://www.un.org/depts/los/convention_agreements/texts/unclos/unclos_e.pdf
- Urbanucci, L. (2018). Limits and potentials of mixed integer linear programming methods for optimization of polygeneration energy systems. *Energy Procedia*, *148*, 1199–1205. doi: 10.1016/j.egypro.2018.08.021
- Van der Male, P. (2021). *Oe44005 - 2021 - lecture notes part ii - offshore wind*. TU Delft. Retrieved from <https://brightspace.tudelft.nl/d21/le/content/401347/viewContent/2373533/View>
- Voloshin, V. I. (2009). *Introduction to graph theory*. Nova Science Publishers.
- Wang, A., Jens, J., Mavins, D., Moultak, M., Schimmel, M., Van Der Leun, K., ... Buseman, M. (2021). *European hydrogen backbone: Analysing future demand, supply, and transport of hydrogen*. Retrieved from https://gasforclimate2050.eu/wp-content/uploads/2021/06/EHB_Analysing-the-future-demand-supply-and-transport-of-hydrogen_June-2021_v3.pdf
- Wang, A., Van Der Leun, K., Peters, D., & Buseman, M. (2020). *European hydrogen backbone*. Retrieved from https://gasforclimate2050.eu/wp-content/uploads/2020/07/2020_European-Hydrogen-Backbone_Report.pdf
- WRADC. (2011). *Overview of desalination plant intake alternatives*. WateReuse Association Desalination Committee. Retrieved from https://watereuse.org/wp-content/uploads/2015/10/Intake_White_Paper.pdf

- Xiao, P., Hu, W., Xu, X., Liu, W., Huang, Q., & Chen, Z. (2020). Optimal operation of a wind-electrolytic hydrogen storage system in the electricity/hydrogen markets. *International Journal of Hydrogen Energy*, 45(46), 24412–24423. doi: 10.1016/j.ijhydene.2020.06.302
- Xuemei, L. (2013). The value of holding scarce wind resource—a cause of overinvestment in wind power capacity in china. *Energy Policy*, 63, 97-100. doi: 10.1016/j.enpol.2013.08.044
- Yang, X.-S., & Karamanoglu, M. (2020). Nature-inspired computation and swarm intelligence: A state-of-the-art overview. *Nature-Inspired Computation and Swarm Intelligence*, 3–18. doi: 10.1016/b978-0-12-819714-1.00010-5
- Yue, M., Lambert, H., Pahon, E., Roche, R., Jemei, S., & Hissel, D. (2021). Hydrogen energy systems: A critical review of technologies, applications, trends and challenges. *Renewable and Sustainable Energy Reviews*, 146, 111180. doi: 10.1016/j.rser.2021.111180
- Zhou, J., Peng, J., Liang, G., & Deng, T. (2019). Layout optimization of tree-tree gas pipeline network. *Journal of Petroleum Science and Engineering*, 173, 666–680. doi: 10.1016/j.petrol.2018.10.067

A

OFFSHORE WIND FARM CHARACTERISTICS

In this appendix, the incumbent and new wind farms presented by [EMODnet \(2021\)](#) are shown. These wind farms form the basis of the hydrogen system in the North Sea.

Table A.1: Overview of all the offshore wind farms within the system, data derived from [EMODnet \(2021\)](#).

ID	Country	Name	Capacity MW	Status	Year
BEL1	Belgium	Rentel	309	Production	2018
BEL2	Belgium	Norther	370	Production	2018
BEL3	Belgium	Seastar	252	Production	2020
BEL4	Belgium	Mermaid	235,2	Production	2020
BEL5	Belgium	C-Power (Zone A)	141,15	Production	2013
BEL6	Belgium	C-Power (Zone B)	184,5	Production	2013
BEL7	Belgium	Northwind	216	Production	2014
BEL8	Belgium	Belwind phase 1	165	Production	2010
BEL9	Belgium	Northwester 2	219	Production	2020
BEL10	Belgium	Belwind phase 2 (Nobelwind) (Zone 2)	165	Production	2017
BEL11	Belgium	Belwind phase 2 (Nobelwind) (Zone 1)	165	Production	N/A
DEU1	Germany	BARD Offshore 1	400	Production	2013
DEU2	Germany	Deutsche Bucht	252	Production	2019
DEU3	Germany	Veja Mate	402	Production	2017
DEU4	Germany	alpha ventus	60	Production	2009
DEU5	Germany	DanTysk	302,4	Production	2014
DEU6	Germany	Borkum Riffgrund West	900	Approved	N/A
DEU7	Germany	Borkum Riffgrund 1	312	Production	2015
DEU8	Germany	Amrumbank West	302,4	Production	2015
DEU9	Germany	Nordsee Ost	295	Production	2015
DEU10	Germany	Butendiek	288	Production	2015
DEU11	Germany	GlobalTech I	400	Production	2015
DEU12	Germany	EnBW Hohe See	497	Production	2019
DEU13	Germany	Sandbank	124	Production	2017
DEU14	Germany	Sandbank	164	Production	2017
DEU15	Germany	Gode Wind 01	344,52	Production	2017
DEU16	Germany	EnBW He dreiht	900	Approved	N/A
DEU17	Germany	Nordergruende	111	Production	2017
DEU18	Germany	Riffgat	113,4	Production	2014
DEU19	Germany	Merkur Offshore (MEG Offshore I)	396	Production	2019
DEU20	Germany	Trianel Windpark Borkum Phase 1	200	Production	2015
DEU21	Germany	Trianel Windpark Borkum Phase 2	95	Production	2020
DEU22	Germany	Trianel Windpark Borkum Phase 2	107	Production	2020
DEU23	Germany	Nordsee One	332	Production	2017

DEU24	Germany	Borkum Riffgrund 2	416	Production	2018
DEU25	Germany	Borkum Riffgrund 2	32	Production	2018
DEU26	Germany	OWP West	240	Approved	N/A
DEU27	Germany	Borkum Riffgrund West II	204	Planned	N/A
DEU28	Germany	Borkum Riffgrund West II	54	Planned	N/A
DEU29	Germany	Kaskasi II	342	Approved	N/A
DEU30	Germany	Gode Wind 02	263,1	Production	2017
DEU31	Germany	Meerwind Sued/Ost	288	Production	2015
DEU32	Germany	Albatros	112	Production	2020
DEU33	Germany	Gode Wind 3	242,75	Approved	N/A
DEU34	Germany	N-3.5	420	Planned	N/A
DEU35	Germany	N-3.6	480	Planned	N/A
DEU36	Germany	N-3.7	225	Planned	N/A
DEU37	Germany	N-3.8	433	Planned	N/A
DEU38	Germany	N-6.6	630	Planned	N/A
DEU39	Germany	N-6.7	270	Planned	N/A
DEU40	Germany	N-7.2	930	Planned	N/A
DEU41	Germany	N-9.1	1000	Planned	N/A
DEU42	Germany	N-9.2	1000	Planned	N/A
DEU43	Germany	N-9.3	1000	Planned	N/A
DEU44	Germany	N-9.4	1000	Planned	N/A
DEU45	Germany	N-10.1	1000	Planned	N/A
DEU46	Germany	N-10.2	1000	Planned	N/A
DNK1	Denmark	Fanm Bugt	N/A	Planned	N/A
DNK2	Denmark	Nordsren II vest	N/A	Planned	N/A
DNK3	Denmark	Vesterhav Syd	168	Approved	N/A
DNK4	Denmark	Nordsren III vest	N/A	Planned	N/A
DNK5	Denmark	Vesterhav Nord	160	Approved	N/A
DNK6	Denmark	Nordsren II	N/A	Planned	N/A
DNK7	Denmark	Jyske Banke	N/A	Planned	N/A
DNK8	Denmark	Nordsren III	N/A	Planned	N/A
DNK9	Denmark	Thor	900	Planned	N/A
DNK10	Denmark	Nordsren I	N/A	Planned	N/A
DNK11	Denmark	Horns Rev I	160	Production	2002
DNK12	Denmark	Nissum Bredning	28	Production	2018
DNK13	Denmark	Horns Rev II	209,3	Production	2009
DNK14	Denmark	Renland	17	Production	2003
DNK15	Denmark	Horns Rev III	407	Production	2019
NLD1	Netherlands	Borssele	1502,5	Planned	N/A
NLD2	Netherlands	Ijmuiden Ver	4000	Planned	N/A
NLD3	Netherlands	Hollandse Kust D	N/A	Planned	N/A
NLD4	Netherlands	Hollandse Kust E	N/A	Planned	N/A
NLD5	Netherlands	Hollandse Kust (Noord)	700	Approved	N/A
NLD6	Netherlands	Hollandse Kust (Zuid)	1649	Planned	N/A
NLD7	Netherlands	Hollandse Kust (West)	1400	Planned	N/A
NLD8	Netherlands	Hollandse Kust F	N/A	Planned	N/A
NLD9	Netherlands	Ten Noorden van de Wadden	700	Planned	N/A
NLD10	Netherlands	Borssele Kavel II	376	Production	2020
NLD11	Netherlands	Borssele Kavel III	352	Production	2020
NLD12	Netherlands	Borssele Kavel IV	353	Production	2020
NLD13	Netherlands	Borssele Kavel V	19	Production	2020
NLD14	Netherlands	NSW Offshore windpark Egmond aan Zee	108	Production	2006
NLD15	Netherlands	Prinses Amalia Windparken	120	Production	2008
NLD16	Netherlands	WP Q10 / Eneco Luchterduinen	129	Production	2015

NLD17	Netherlands	ZeeEnergie / Gemini II	300	Production	2017
NLD18	Netherlands	Buitengaats / Gemini I	300	Production	2017
NLD19	Netherlands	HKZ Kavel IV	700	Construction	N/A
NLD20	Netherlands	HKZ Kavel III	700	Construction	N/A
NLD21	Netherlands	HKZ Kavel II	700	Construction	N/A
NLD22	Netherlands	HKZ Kavel I	700	Construction	N/A
NLD23	Netherlands	Borssele Kavel I	376	Production	2020
NLD24	Netherlands	HKN Kavel V	700	Approved	N/A

B | NATURAL GAS INFRASTRUCTURE CHARACTERISTICS

In this appendix, the incumbent natural gas transmission infrastructure is presented in [Table B.1](#). Within the table, the corresponding hydrogen transmission capacity (C_p) is also indicated.

Table B.1: Overview of all the incumbent gas pipelines and their potential hydrogen capacity, data derived from [EMODnet \(2022\)](#).

ID	Status	Size <i>in</i>	C_p <i>MW</i>
PL0226_PR	Active	8	399,5
PL0218_PR	Active	10	624,2
PL0061_PR	Active	10,7	714,6
PL0125_PR	Abandoned	10	624,2
PL0126_PR	Abandoned	6	224,7
PL1024_PR	Active	36	8089,7
PL1025_PR	Active	40	9987,2
PL1026_PR	Active	40	9987,2
PL0080_PR	Active	10	624,2
PL0111_PR	Active	10	624,2
PL1011_PR	Active	N/A	N/A
PL0008_PR	Active	24	3595,4
PL0187_PR	Active	42	11010,9
PL0186_PR	Active	40	9987,2
PL0224_PR	Active	14	1223,4
PL0104_PR	Active	4	99,9
PL0105_PR	Active	4	99,9
PL0099_PR	Active	26	4219,6
PL0150_PR	Active	6	224,7
PL0151_PR	Active	12	898,9
PL1014_PR	Active	N/A	N/A
PL1015_PR	Active	8	399,5
PL0097_PR	Active	12	898,9
PL0098_PR	Active	24	3595,4
PL0068_PR	Abandoned	6	224,7
PL0069_PR	Active	14	1223,4
PL0070_PR	Active	10	624,2
PL0071_PR	Active	8	399,5
PL0020_PR	Active	10	624,2
PL0122_PR	Active	12	898,9
PL0123_PR	Active	12	898,9
PL0010_PR	Active	12,75	1014,7
PL0100_PR	Active	10	624,2
PL0101_PR	Active	12	898,9
PL0006_PR	Active	10	624,2
PL0007_PR	Active	24	3595,4
PL0102_PR	Active	12	898,9
PL0103_PR	Active	4	99,9
PL0117_PR	Active	8	399,5

PL0119_PR	Active	14	1223,4
PL0062_PR	Active	18	2022,4
PL0063_PR	Active	18	2022,4
PL0049_PR	Active	10	624,2
PL0112_PR	Abandoned	10	624,2
PL0120_PR	Active	7	274,0
PL0043_PR	Abandoned	4	99,9
PL0127_PR	Active	6	224,7
PL0017_PR	Abandoned	10	624,2
PL0090_PR	Active	24	3595,4
PL0091_PR	Active	24	3595,4
PL0129_PR	Active	6	224,7
PL0176_PR	Active	36	8089,7
PL0227_PR	Under construction	8	399,5
PL1182_PR	Proposed	12	898,9
PL1183_PR	Proposed	8	399,5
PL1016_PR	Active	14	1223,4
PL0059_PR	Active	14	1223,4
PL0188_PR	Active	N/A	N/A
PL0189_PR	Active	N/A	N/A
PL0086_PR	Abandoned	6	224,7
PL0145_PR	Active	10	624,2
PL0143_PR	Abandoned	8	399,5
PL0142_PR	Active	36	8089,7
PL0019_PR	Abandoned	20	2496,8
PL0096_PR	Active	10	624,2
PL0128_PR	Abandoned	6	224,7
PL0044_PR	Active	10	624,2
PL0023_PR	Active	18	2022,4
PL0045_PR	Active	20	2496,8
PL1017_PR	Active	30	5617,8
PL0121_PR	Abandoned	7,5	351,1
PL0073_PR	Active	8	399,5
PL0170_PR	Active	6	224,7
PL0172_PR	Active	10	624,2
PL0169_PR	Active	12	898,9
PL0016_PR	Active	24	3595,4
PL0072_PR	Active	20	2496,8
PL1001_PR	Active	40	9987,2
PL1002_PR	Active	42	11010,9
PL0035_PR	Active	14	1223,4
PL0037_PR	Active	10	624,2
PL0141_PR	Active	10	624,2
PL0147_PR	Active	10	624,2
PL0148_PR	Active	14	1223,4
PL0053_PR	Active	12	898,9
PL0046_PR	Active	20	2496,8
PL1006_PR	Active	14	1223,4
PL1008_PR	Active	3	56,2
PL0134_PR	Abandoned	10	624,2
PL0136_PR	Active	12	898,9
PL0153_PR	Active	14	1223,4
PL0131_PR	Active	10	624,2
PL0132_PR	Active	24	3595,4
PL0054_PR	Abandoned	12	898,9
PL0173_PR	Active	8	399,5
PL0175_PR	Active	6	224,7
PL0108_PR	Active	12	898,9
PL0058_PR	Active	12	898,9
PL0149_PR	Active	20	2496,8

PL0194_PR	Active	12	898,9
PL0081_PR	Active	11	755,3
PL0082_PR	Active	10	624,2
PL0133_PR	Active	4	99,9
PL0195_PR	Active	14	1223,4
PL0196_PR	Active	10	624,2
PL0197_PR	Active	10	624,2
PL0198_PR	Active	10	624,2
PL0083_PR	Abandoned	10	624,2
PL0084_PR	Abandoned	8	399,5
PL0085_PR	Active	12	898,9
PL1013_PR	Active	N/A	N/A
PL0191_PR	Active	N/A	N/A
PL0192_PR	Active	6	224,7
PL0193_PR	Active	8	399,5
PL0167_PR	Abandoned	8	399,5
PL0168_PR	Active	24	3595,4
PL0156_PR	Active	10	624,2
PL0157_PR	Active	12	898,9
PL0158_PR	Active	6	224,7
PL0159_PR	Active	10	624,2
PL0161_PR	Active	6	224,7
PL0162_PR	Active	26	4219,6
PL0163_PR	Active	12	898,9
PL0164_PR	Active	10	624,2
PL0165_PR	Active	10	624,2
PL0166_PR	Active	10	624,2
PL0155_PR	Active	10	624,2
PL0029_PR	Active	14	1223,4
PL0030_PR	Active	24	3595,4
PL0076_PR	Active	10	624,2
PL0077_PR	Active	10	624,2
PL0032_PR	Active	20	2496,8
PL0033_PR	Active	10	624,2
PL0113_PR	Active	12	898,9
PL0114_PR	Active	12	898,9
PL0115_PR	Abandoned	8	399,5
PL0140_PR	Active	10	624,2
PL1021_PR	Active	8	399,5
PL1023_PR	Active	10,75	721,3
PL0177_PR	Active	N/A	N/A
PL0178_PR	Active	N/A	N/A
PL0137_PR	Active	24	3595,4
PL0138_PR	Active	8	399,5
PL0139_PR	Active	12	898,9
PL0207_PR	Active	8	399,5
PL0208_PR	Active	10	624,2
PL0209_PR	Active	10	624,2
PL0034_PR	Abandoned	10	624,2
PL0021_PR	Active	12	898,9
PL1004_PR	Active	8,5	451,0
PL0154_PR	Active	18	2022,4
PL0003_PR	Active	36	8089,7
PL0204_PR	Active	10	624,2
PL0027_PR	Abandoned	10	624,2
PL0075_PR	Active	10	624,2
PL0213_PR	Active	8	399,5
PL0160_PR	Active	6	224,7
PL0018_PR	Abandoned	20	2496,8
PL0207_UM	Active	2	25,0

PL0171.PR	Active	12	898,9
PL1009.PR	Active	N/A	N/A
PL0200.PR	Active	8	399,5
PL0206.PR	Active	10	624,2
PL0001.PR	Abandoned	10	624,2
PL0214.PR	Abandoned	12	898,9
PL0221.PR	Proposed	8	399,5
PL0211.PR	Active	12	898,9
PL0066.PR	Active	10	624,2
PL0036.PR	Active	10	624,2
PL1186.PR	Active	14	1223,4
PL1187.PR	Active	10	624,2
PL0056.PR	Abandoned	10	624,2
PL0057.PR	Active	10	624,2
PL0065.PR	Active	20	2496,8
PL0013.PR	Abandoned	10	624,2
PL0014.PR	Abandoned	7	274,0
PL0028.PR	Abandoned	20	2496,8
PL0210.PR	Active	6	224,7
PL0088.PR	Active	6	224,7
PL0089.PR	Active	10,5	688,2
PL0203.PR	Abandoned	9,5	563,3
PL0015.PR	Active	10,75	721,3
PL0110.PR	Abandoned	10	624,2
PL0215.PR	Active	8	399,5
PL0216.PR	Active	6	224,7
PL0217.PR	Active	10	624,2
PL0233.PR	Proposed	10	624,2
PL0219.PR	Under construction	6	224,7
PL0222.PR	Proposed	10	624,2
PL0079.PR	Abandoned	6	224,7
PL0067.PR	Active	10	624,2
PL1020.PR	Active	12	898,9
PL0002.PR	Abandoned	10	624,2
PL0004.PR	Active	36	8089,7
PL0005.PR	Abandoned	10	624,2
PL0047.PR	Active	10	624,2
PL0223.PR	Proposed	8	399,5
327394	Active	40	9987,2
310326	Active	40	9987,2
326340	Active	40	9987,2
319166	Active	36	8089,7
323212	Active	42	11010,9
326374	Active	42	11010,9
321002	Active	40	9987,2
324844	Active	36	8089,7
321784	Active	36	8089,7
500007694	Abandoned	6	224,7
500006834	Active	10	624,2
500003715	Active	N/A	N/A
500007026	Active	8	399,5
500005952	Abandoned	12	898,9
500006832	Active	10	624,2
500006952	Active	N/A	N/A



Within this appendix, a more detailed derivation of the different techno-economic parameters is given. In [Section C.1](#), offshore wind farms are analysed. In [Section C.2](#), the transmission infrastructure is analysed. And in [Section C.3](#), the electrolyzers and other components acquainted with hydrogen production are elaborated on.

C.1 OFFSHORE WIND ENERGY

On average, the Capital Expenditures ([CapEx](#)) of offshore wind energy (based on offshore fixed-bottom wind turbines) result in 2000 *EUR/kW* ([Sens et al., 2022](#)); these costs include the turbine [CapEx](#) and Balance Of System ([BOS](#)) [CapEx](#). The [BOS](#) encompasses all the components of the system other than the turbine itself; a more specified overview of the all the different [CapEx](#) of an offshore wind turbine can be found in [Figure C.1](#). Moreover, a wind turbine is subject to Operational Expenditures ([OpEx](#)) during its operational life. The averaged [OpEx](#) are 118 *EUR/kW/yr* ([Stehly et al., 2020](#)).

For the H₂-in-Turbine wind farms, the [BOS CapEx](#) is reduced with 11%. This is because no array cables or substations need to be installed. Moreover, the wind turbines are assumed to have a capacity of 10 MW ([Assumption 10](#)) and a diameter of 193 m ([Siemens Gamesa, 2019](#)). Following the rule of thumb that wind farms should be distanced 5 times the diameter from each other ([Grady et al., 2005](#)), the distancing becomes 965 m.

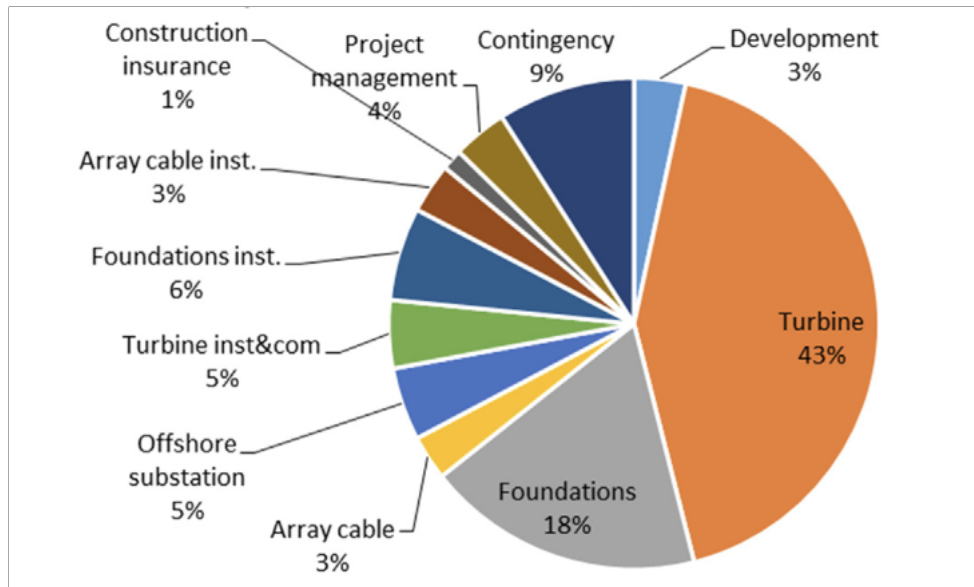


Figure C.1: Estimated breakdown of the CapEx of a baseline offshore wind farm in 2015 (Lacal-Arántegui et al., 2018).

When the operational life of an offshore wind farm has been concluded, decommissioning starts. The costs of decommissioning for offshore wind farms are on average 4% of the CapEx (Topham & McMillan, 2017; Kaiser & Snyder, 2012).

C.2 TRANSMISSION INFRASTRUCTURE

The energy locked within hydrogen can be transported via natural gas pipelines. However, the energy density of hydrogen is low compared to natural gas. Therefore, it is important to determine the new capacity of the pipelines.

The new capacity is based on the pipeline size, operating pressure, temperature, flow speed, and the Low Heating Value (LHV) of hydrogen (González Díez et al., 2020). From these parameters, only the pipeline size is not considered to be the same for all pipelines within this thesis: The pipeline sizes vary from 2 to 42 in; each pipeline is therefore assigned to a new hydrogen capacity.

Typically, the operation pressure of subsea pipeline is upstream 150 to 250 bar, and downstream 60 to 80 bar (Staurland & Aamodt, 2004). In this thesis, a value of 80 bar is assumed for all new and incumbent subsea gas pipelines. This low value is used because higher pressure might increase the chance of pipeline leakages and embrittlement (Breunis, 2021). The temperature¹ of the subsea pipeline is assumed to be 10 °C, which is the annual average temperature in the North Sea (MacKenzie & Schiedek, 2007). Moreover, a flow speed of 20 m/s is assumed as this is safe value (González Díez et al., 2020). And finally, the LHV of hydrogen is 120,1 MJ or 33,3 kWh (National Research Council and National Academy of Engineering, 2004). The maximum technical capacity \dot{C}_p MW for each pipeline can now be calculated using Equation C.1:

¹ It is assumed that the reference point is in thermal equilibrium with the ambient temperature.

$$\dot{C}_p = \dot{n} \cdot M_{H_2} \cdot LHV_{H_2} \quad (C.1)$$

in which

$$\dot{n} = \frac{P\dot{V}}{RT} = \frac{Pv_p A_p}{RT} \quad (C.2)$$

where M_{H_2} is the molar mass of H_2 ; LHV_{H_2} is the low heating value of H_2 ; P is the pressure inside the pipe; v_p is the flow speed; A_p is the area of the pipe; R is the gas constant; and, T is the temperature of the reference point.

The **CapEx** of natural gas pipelines is considered to be 110.000 *EUR/in – km* (ICF International, 2014). Hydrogen pipelines are considered to be 10% more expensive than natural gas pipelines (Maggio et al., 2019), hence the final **CapEx** of the hydrogen pipelines is 121.000 *EUR/in – km*.

Aside from installing new pipelines within the system, pipelines can also be repurposed. Repurposing natural gas pipelines to transport hydrogen has additional costs affiliated with it. These costs are set at 10% of the **CapEx** of a newly build hydrogen pipeline (Wang et al., 2020). Aside from the **CapEx**, the offshore pipeline infrastructure also faces **OpEx**. The **OpEx** of the offshore pipeline infrastructure is assumed to be 7% of the **CapEx**, as proposed by the CEER (2019).

A final remark regarding the offshore infrastructure are splitting points within the pipeline. There exists the possibility to split a pipeline into two (or more) new pipelines; however, after consultation with industry experts by Brosschot (2022), the decision is made that no additional costs are acquainted with splitting a pipeline.

C.3 ELECTROLYSER

According to Calado & Castro (2021), the so-called PEM electrolyser is most suitable for offshore hydrogen systems due to the smaller footprint and easier maintenance. A PEM electrolyser has an averaged **CapEx** (during 2030, 2040, and 2050) of roughly 600 *EUR/kW*. Here, the costs are linked to the electricity input of the offshore wind farm(s) (Danish Energy Agency, 2021; NSE et al., 2020), and not to the capacity of the offshore wind farm(s) to which the electrolyser is connected. The yearly **OpEx** of such an electrolyser set-up is established at 4% of the **CapEx** and the electrolyser has an estimated operational life of 20 years (IRENA, 2020).

As water is used as an input for the electrolyser, a desalination plant is also needed. The amount of water for an electrolyser is set at 0,18 *kg/kWh_e* (Danish Energy Agency, 2021). Here, the megawatts hour reflect to the amount of electricity input in the electrolyser. The needed energy for electrolysis per volume of water is determined to be 2,99 *kWh/m³* (TNO et al., 2020). Combining this with the density of sea water (1023,6 *kg/m³* (Nayar et al., 2016)) and with the costs of an offshore desalination plant (3500 *EUR/kW* (NSE et al., 2020)), the **CapEx** becomes 1883,7 *EUR/MW_e*. The **OpEx** are considered so remarkably low for the plant, that they are neglected (NSE et al., 2020).

The desalination plants are estimated to have an operational life of 30 years (WRADC, 2011).

The output of the electrolyser is 30 *bar*. However, as the pipeline pressure is set at 80 *bar*, an compressor is needed. The costs of a compressor are defined by the power used (González Díez et al., 2020). Hence:

$$\text{CapEx}_{\text{compressor}} = 2665,04 \cdot \dot{W} \quad (\text{C.3})$$

where

$$\dot{W} = \dot{m} \cdot \frac{RT}{M_W} \cdot \frac{\gamma}{\gamma - 1} \cdot \frac{Z_1 + Z_2}{2} \cdot \frac{1}{\eta_s \eta_m} \left[\left(\frac{P_2}{P_1} \right)^{\frac{\gamma-1}{\gamma}} - 1 \right] \quad (\text{C.4})$$

\dot{m} the mass flow rate in *kg/s*; P is the inlet (1) and outlet (2) pressure in *bar*, which are 30 (González Díez et al., 2020) and 80 *bar* respectively; Z is the compressibility factor of hydrogen at the inlet (1) and outlet (2), these are roughly 1,005 and 1,03 respectively (Elberry et al., 2021); T is the inled temperature in *K* of the compressor, which is set at 333,15 *K* (González Díez et al., 2020); γ is the specific heat ratio of hydrogen, which is 1,41; M_W is the molar mass in *kg/kmol* of hydrogen, which is 2,016 *kg/kmol*; η_s is the compressor efficiency in %, which is 80% (González Díez et al., 2020); η_m is the mechanical efficiency in %, which is 98% (González Díez et al., 2020); and finally, R is the ideal gas constant of 8314 in *J/K kmol*.

The yearly *OpEx* of the compressor are estimated to be 8% of the *CapEx* (NSE et al., 2020) and an estimated operational life of 20 years (EPA, 2006).

D | ELECTROLYSERS

This appendix presents the different electrolyser hubs and compressor stations. In [Table D.1](#), [D.2](#), [D.3](#), and [D.4](#), these are presented per country and to what wind farms they are connected for 2030, 2040 and 2050. And additionally, in [Table D.5](#) the coordinates of the different electrolyser hubs/compressor stations are presented.

Table D.1: Electrolyser hubs and their respective assigned wind farms in Belgium. '(N)' is a new wind farm.

Electrolyser hub	2030	2040	2050
E-BEL1	BEL2	BEL2	BEL2
E-BEL2	BEL5, BEL6	BEL5, BEL6	BEL5, BEL6
E-BEL3	BEL1, BEL3, BEL4, BEL9	BEL1, BEL3, BEL4, BEL9	BEL1, BEL3, BEL4, BEL9
E-BEL4	BEL8, BEL10, BEL11	BEL8, BEL10, BEL11	BEL8, BEL10, BEL11
E-BEL5	BEL7	BEL7	BEL7
E-BEL6	BEL12(N)	BEL12(N)	BEL12(N)
E-BEL7	-	BEL13(N)	BEL13(N), BEL14(N)

Table D.2: Electrolyser hubs and their respective assigned wind farms in Denmark. '(N)' is a new wind farm. The H₂-in-Turbine wind farms are connected to a compressor hub, not an electrolyser hub.

Electrolyser hub	2030	2040	2050
E-DNK1	DNK13	DNK13	DNK13
E-DNK2	DNK15	DNK15	DNK15
E-DNK3	DNK3	DNK3	DNK3
E-DNK4	DNK5, DNK14, DNK12	DNK5, DNK14, DNK12	DNK5, DNK14, DNK12
E-DNK5	DNK10	DNK10	DNK10
E-DNK6	DNK9	DNK9	DNK9
E-DNK7	DNK6	DNK6	DNK6
E-DNK8	-	DNK15(N)	DNK15(N)
E-DNK9	-	DNK16(N)	DNK16(N)
E-DNK10	-	DNK17(N)	DNK17(N)
E-DNK11	-	DNK18(N)	DNK18(N)

E-DNK12	-	DNK19(N)	DNK19(N)
E-DNK13	-	DNK20(N)	DNK20(N)
E-DNK14	-	-	DNK21(N)
H2inTurb-DNK1	-	-	DNK22(N)
H2inTurb-DNK2	-	-	DNK23(N)

Table D.3: Electrolyser hubs and their respective assigned wind farms in Germany. '(N)' is a new wind farm. The H₂-in-Turbine wind farms are connected to a compressor hub, not an electrolyser hub.

Electrolyser hub	2030	2040	2050
E-DEU1	DEU18	DEU18	DEU18
E-DEU2	DEU24, DEU25, DEU7, DEU4, DEU19, DEU20, DEU21, DEU22	DEU24, DEU25, DEU7, DEU4, DEU19, DEU20, DEU21, DEU22	DEU24, DEU25, DEU7, DEU4, DEU19, DEU20, DEU21, DEU22
E-DEU3	DEU27, DEU28, DEU26, DEU6	DEU27, DEU28, DEU26, DEU6	DEU27, DEU28, DEU26, DEU6
E-DEU4	DEU35, DEU34, DEU37, DEU23, DEU15, DEU30, DEU33, DEU36	DEU35, DEU34, DEU37, DEU23, DEU15, DEU30, DEU33, DEU36	DEU35, DEU34, DEU37, DEU23, DEU15, DEU30, DEU33, DEU36
E-DEU5	DEU38, DEU2, DEU3, DEU1, DEU39	DEU38, DEU2, DEU3, DEU1, DEU39	DEU38, DEU2, DEU3, DEU1, DEU39
E-DEU6	DEU40, DEU16	DEU40, DEU16	DEU40, DEU16
E-DEU7	DEU41, DEU42, DEU43, DEU44	DEU41, DEU42, DEU43, DEU44	DEU41, DEU42, DEU43, DEU44
E-DEU8	DEU31, DEU9, DEU29, DEU8	DEU31, DEU9, DEU29, DEU8	DEU31, DEU9, DEU29, DEU8
E-DEU9	-	DEU13, DEU14, DEU5	DEU13, DEU14, DEU5
E-DEU10	-	DEU45, DEU46	DEU45, DEU46
E-DEU11	-	DEU32, DEU11, DEU12	DEU32, DEU11, DEU12
H2inTurb-DEU1	-	DEU47(N), DEU48(N)	DEU47(N), DEU48(N)
H2inTurb-DEU2	-	-	DEU49(N)
H2inTurb-DEU3	-	-	DEU50(N)
H2inTurb-DEU4	-	-	DEU51(N), DEU52(N), DEU53(N)

Table D.4: Electrolyser hubs and their respective assigned wind farms in the Netherlands. '(N)' is a new wind farm. The H₂-in-Turbine wind farms are connected to a compressor hub, not an electrolyser hub.

Electrolyser hub	2030	2040	2050
E-NLD1	NLD23, NLD10	NLD23, NLD10	NLD23, NLD10
E-NLD2	NLD11, NLD12, NLD13	NLD11, NLD12, NLD13	NLD11, NLD12, NLD13
E-NLD3	NLD7	NLD7	NLD7
E-NLD4	NLD19, NLD20	NLD19, NLD20	NLD19, NLD20
E-NLD5	NLD21, NLD22	NLD21, NLD22	NLD21, NLD22
E-NLD6	NLD15	NLD15	NLD15
E-NLD7	NLD2	NLD2	NLD2
E-NLD8	NL5, NLD24	NL5, NLD24	NL5, NLD24
E-NLD9	NLD15	NLD15	NLD15
E-NLD10	NLD14	NLD14	NLD14
E-NLD11	NLD9	NLD9	NLD9
E-NLD12	NLD17	NLD17	NLD17
E-NLD13	NLD18	NLD18	NLD18
E-NLD14	-	NLD3	NLD3
E-NLD15	-	NLD4	NLD4
E-NLD16	-	NLD25(N)	NLD25(N)
E-NLD17	-	NLD26(N)	NLD26(N)
E-NLD18	-	NLD27(N)	NLD27(N)
E-NLD19	-	NLD28(N)	NLD28(N)
E-NLD20	-	NLD29(N)	NLD29(N)
E-NLD21	-	NLD30(N)	NLD30(N)
H2inTurb-NLD1	-	-	NLD31(N)
H2inTurb-NLD2	-	-	NLD32(N)

Table D.5: Spatial coordinates of the electrolyzers. Coordinate reference system: "WGS 84 / UTM zone 31N". Authority ID: "EPSG:32631"

Electrolyser	X-coordinate	Y-coordinate
E-BEL1	499950	5707103
E-BEL2	497102	5710262
E-BEL3	491975	5712697
E-BEL4	487366	5726058
E-BEL5	494349	5718719
E-BEL6	471637	5715304
E-BEL7	469520	5707303
E-DEU1	729705	5954732
E-DEU2	725053	5988541
E-DEU3	707567	5994231
E-DEU4	757748	5988127
E-DEU5	696964	6026455
E-DEU6	716346	6022697
E-DEU7	680044	6044568
E-DEU8	807558	6043777

E-DEU9	756645	6120886
E-DEU10	700353	6059643
E-DEU11	718920	6031808
H2inTurb-DEU1	710479	6076027
H2inTurb-DEU2	707132	6088630
H2inTurb-DEU3	718784	6080788
H2inTurb-DEU4	716439	6101748
E-DNK1	791365	6170142
E-DNK2	793814	6181642
E-DNK3	810808	6226591
E-DNK4	811810	6287512
E-DNK5	777018	6206939
E-DNK6	789650	6255946
E-DNK7	731511	6232203
E-DNK8	719531	6212991
E-DNK9	705871	6189574
E-DNK10	751729	6272509
E-DNK11	758559	6333003
E-DNK12	720507	6276900
E-DNK13	695139	6220309
E-DNK14	711347	6252378
H2inTurb-DNK1	676128	6195874
H2inTurb-DNK2	684743	6259327
E-NLD1	503206	5728405
E-NLD2	499445	5730168
E-NLD3	550832	5797938
E-NLD4	571108	5797938
E-NLD5	571676	5793201
E-NLD6	579412	5807017
E-NLD7	535241	5855881
E-NLD8	588660	5837286
E-NLD9	582976	5826749
E-NLD10	598684	5825968
E-NLD11	676816	5989593
E-NLD12	689152	5991213
E-NLD13	699284	5991619
E-NLD14	552916	5836804
E-NLD15	575831	5862215
E-NLD16	567234	5894732
E-NLD17	518878	5911579
E-NLD18	596904	5922265
E-NLD19	546929	5968099
E-NLD20	672005	5969203
E-NLD21	667587	6014484
H2inTurb-NLD1	582866	5994959
H2inTurb-NLD2	554822	5991497

COLOPHON

